THE UNIVERSITY OF CHICAGO

MECHANISMS MITIGATING OPIOID-INDUCED RESPIRATORY DEPRESSION AFTER REPEAT FENTANYL USE

A DISSERTATION SUBMITTED TO

THE FACULTY OF THE DIVISION OF THE BIOLOGICAL SCIENCES

AND THE PRITZKER SCHOOL OF MEDICINE

IN CANDIDACY FOR THE DEGREE OF

DOCTOR OF PHILOSOPHY

COMMITTEE ON NEUROBIOLOGY

BY

CAROLINE SZUJEWSKI

CHICAGO, ILLINOIS

DECEMBER 2024

Abstract

Opioid-induced respiratory depression (ORID) is the hallmark of opioid overdose and a major risk factor for death due to fentanyl. While repeat opioid use (ROU) elevates the risk of death, understanding its influence over breathing and its control has been poorly resolved. We developed a mouse model of ROU involving daily fentanyl use (5 days). We examined how ROU impacted breathing and activity from the preBötzinger complex (preBötC), a brainstem network critical to inspiratory rhythmogenesis. Acute fentanyl use caused a profound metabolic crisis during ORID involving a mismatch between ventilation and oxygen consumption. Our findings also revealed a crucial distinction in respiratory responses to ROU. Most mice (77%) had an adaptive ventilatory response, indicative of the development of tolerance to OIRD following ROU, and the relationship between ventilation and oxygen consumption improved during OIRD. However, in 23% of mice, the adaptive response failed to emerge, underscoring the heterogeneity in ventilatory and metabolic outcomes. Following ROU, rhythmogenesis in the preBötzinger complex was less sensitive to μ-opioid receptor agonism, indicating that adaptation to ROU involves centrally-mediated changes in the inspiratory medullary network. These findings reveal a series of physiological changes following ROU, typically resulting in improved ventilation and oxygenation during ORID. Such changes—or lack thereof—may contribute to the unpredictable nature of overdose susceptibility among opioid users.

It has been well documented in the literature that one factor that can alter opioid overdose susceptibility in repeat users is the context of drug administration. Despite ROU increasing tolerance to opioid effects, taking opioids in an environmental context where they have not previously been administered the drug results in a loss of tolerance and an increase in opioid overdose susceptibility. While Context-Dependent Tolerance to overdose susceptibility and

analgesia has been well described in the literature, Context-Dependent Tolerance to OIRD, and the neural mechanisms that support it have not been investigated. The Locus Coeruleus (LC) is a principal source of noradrenergic neuromodulation that can influence breathing responses to blood gas deviations. It is also involved with cue-reward associative relationships, Opioid Use Disorder, and opioid withdrawal. Using fiber photometry and simultaneous whole-body plethysmography in a mouse model of repeat fentanyl administration, we tested the hypothesis that ROU leads to context-based tolerance to OIRD supported by LC activity. The development of tolerance to OIRD coincided with enhanced LC activity coupled with transient increases in breathing. Changing the context of fentanyl use to a context not previously associated with the drug altered LC activity and its correlation with transient increases in breathing and reduced the tolerance to OIRD that developed with ROU. Optogenetic activation of the LC minimized OIRD magnitude in fentanyl-naïve subjects. These findings underscore the importance of the LC in facilitating OIRD tolerance from learned associations during ROU. Failure to establish such associations and the corresponding LC activity may increase susceptibility to overdose and death among chronic opioid users.

This thesis is dedicated to my parents, who pushed me toward achieving my academic goals and provided me with every opportunity to reach them. Thank you for always believing in my potential, even when I didn't believe in myself.

.

Table of Contents

List of Figures

List of Supplemental Figures

List of Tables

List of Supplemental Tables

Acknowledgments

I have many people to thank who helped me throughout this long journey. First, I would like to thank my mentor Fred Garcia. I remember when I first met Fred. Never had I met someone so enthusiastic and excited about science. Studying the respiratory network was not anything I would have pictured for myself when starting out grad school, but I'm glad that I ended up where I did. Lab really did end up feeling like a home away from home and one thing I can say about being in your lab is that it has been a lot of fun, filled with tons of laughs. I was never afraid or intimidated to discuss something with you, or ask what might be a stupid question. No matter what it was, you always gave me your attention. I will be forever grateful for your help and willingness to go over a talk with me or discuss something, even outside of normal work hours. I have learned so much from you over the past 5 years and I've thoroughly enjoyed all of our conversations and speculations about what could be going on. It will be weird to have a normal job following this experience, but I will always remember these formative years fondly and I appreciate you for mentoring me through the ups and downs of being a scientist.

I also want to thank the rest of the members of the lab. Without the support from all of you, everything would have been harder. A special shout out to Brigitte for reading parts of this dissertation document and helping me workshop ideas. Thank you, Andrew for always being so attentive at my practice talks and giving me your feedback. Carolina and Alejandra, even though we did not work on the same project, you both always brought so much light into the lab and I loved being able to procrastinate for a bit by chatting with you. Matt, you were instrumental in this thesis work. I was so lucky to have found such a diligent, hard-working, and intelligent undergraduate to help with this project. I wish you all of the best in medical school. To all of my grad school friends, Stas, Nelson, Shivang, Ezra, Edgar, Carolina, and Ross, I am so grateful to

have made your friendship during this time. Getting your PhD is not something that most people can understand, and I am so lucky to have had the support of all of you as I went through this process. Nelson and Shivang, thank you for your constant peer mentorship. From the start of my first year, you both were always there to guide and support me, no matter what. Thank you for being so generous with your time and always so kind to me.

A special thank you to Jo Gogola for helping me with all of the immunohistochemistry verifications, Rachel Donka for helping me with the ROC analyses, and Ali Alamri for helping me write matlab code. A HUGE thank you to Shivang for being so involved in not only helping me write the fiber photometry analysis code, but thinking about how best to go about analyzing my data. You never had to help me, but I always knew I could count on you and you were always so generous of your time. It is rare to come across people who truly enjoy helping others as much as you do. You are one of the brightest, kindest people and I know you are going to do truly amazing things in your life. There will undoubtedly be some huge scientific accomplishments in your future.

A huge thank you to my committee, Dan McGehee, Mitch Roitman, and Mark Sheffield. I know we had a lot of committee meetings at the end, and I so appreciate you putting in the time and effort to help me get across the finish line. While committee meetings could be intense at times, there was always some levity with you three around. Dan, thank you for your constant mentorship and for reminding me to have confidence in myself and in my abilities. From the start, you have been an excellent teacher to me. You continually challenged me to do better and to get out of my comfort zone. Those challenges have trained me to be a better scientist and critical thinker. Mitch, while I didn't end up attending UIC, I am so happy that we got to work together in some capacity. It is evident from visiting your lab how much your trainees admire

and look up to you, and it is because you inspire excitement and joy in your lab and in the science that you do. And you did that with me after every committee meeting when you took the time to write out a thorough follow-up email, and always ending it by encouraging me and reminding me what an interesting project this was. Mark, thank you for all of your input on how to analyze my data during the committee meetings. You were the very much-needed signal processing guru as my project started expanding far beyond my knowledge base. Thank you for being so supportive in the committee meetings and for being friends with Fred.

To my Chicago/Latin friends. By now, we are all family. And even though I know that you never had any idea what I was doing in lab, you guys always supported me. There are way too many of you to mention by name, but a special thank you to my best friend Eleanor who always had time the time for me when I needed her.

To my parents, thank you for not letting me switch my major at USC from neuroscience to music industry. You always knew what I wanted before I did, and I am so grateful that you had the forethought that I did not when I was an undergraduate. I am so indebted to you both for taking care of me and molding me into the person I am today. I know that it is my work that allowed me to complete the PhD, but I always had you both there with me every step of the way, so I knew that I was never really alone in this. Mom, thank you for always listening to me as I went on about what I was stressed about and all the work I had to do, and for somehow caring about all of the little things in my life as much as I did. No one cares like you do. Perhaps that's why all of the animals always are attached to your hip. Dad, I will never forget your saying, "Be cool baby, be cool". Forever and always, I will strive to just be cool. To not get too into my head, to remind myself that everything is good and will be ok. To my brother Peter, thank you being a calming presence always. You're so cool and I will always look up to you!

Finally, to my husband Henry, thank you for being so patient as I went through this journey. I know it took a little longer than we wanted, but you always stuck by my side and supported me. You're my motivational coach constantly reminding me to have confidence in what I do and to not give up. Thanks for sending me daily motivational Michael Jordan and Kobe Bryant photos so that I can dominate, just like them. This whole experience has taught me that you are a partner for life. Even if you don't fully understand why I am doing what I'm doing, you trust my judgment and you help me through it. You keep me positive, and most importantly, you always make me smile, remind me to have a little fun, and to not take everything too seriously. This adventure will be over and I am so excited for the next adventure with you.

Introduction

An overview of breathing

Breathing is perhaps one of the most important behaviors that any animal will do in their lifetime. It is a complex, motor behavior that emerges from central processes, which receive input from peripheral and sensory modalities, as well as other areas of the brain[1,2]. The respiratory network is comprised of several different neuronal populations distributed throughout the brainstem[1,3–5]. Activity between these different neuronal networks is critical to shaping spontaneous breathing and must be continuously coordinated with other areas in the brain to optimize breathing with other physiological processes and behaviors, such as cardiovascular activity[6,7], vocalization[8] and swallowing[9]. Breathing is also intrinsically linked to emotional, cognitive, and physiological state[2]. Imagine being on a plane experiencing extreme turbulence. You're seated, but your breathing has quickened as panic and fear start to arise. As the turbulence subsides and the pilot declares that everyone is out of harm's way, the fear subsides, and with it, so does your rapid, panicked breathing. While breathing is an automatic behavior that can respond to our emotional state, it can also be consciously controlled. For example, consciously slowing breathing down will promote relaxation, bolster mood, and reduce stress. With that being said before you proceed with reading this thesis document, please take three deep breaths.

Breathing is a physiological process

Breathing is an essential behavior. It allows for gas exchange in our lungs. Cellular respiration uses glucose and O_2 to form adenosine triphosphate (ATP) through the electron transport chain, which provides energy for cellular functions. A byproduct of this reaction is the

production of Carbon Dioxide (CO_2)[10]. To maintain proper function, the body needs to consistently maintain blood gas homeostasis and exchange CO_2 for Oxygen (O_2) (Partial Pressure, O_2: 75-100 mmHg, CO_2: 35-45 mmHg). Our breathing must consistently keep up with the metabolic demands of changing behaviors. When we inhale, we breathe O_2-rich air into our lungs, which diffuses down its concentration gradient into the capillaries of the alveoli, the site of gas exchange where arterial blood is oxygenated[2]. During expiration, venous blood arriving to the lungs is low in O_2 and high in CO_2. During inspiration, gas exchange occurs in the pulmonary respiratory zone, where both O_2 and CO_2 diffuse down their respective concentration gradients—O_2 enters the blood while CO_2 exits. During exhalation, CO_2 is expelled from the body[11]. This process of ventilation and gas exchange is critical for maintaining blood gas homeostasis. The amount of gas exchange occurring in the lungs is measured by Minute Ventilation (V_e). V_e is the product of Respiratory Rate (RR, how many breaths are taken per unit time), and Tidal Volume (V_T, the volume of each breath). When blood gas homeostasis deviates from normal conditions, breathing compensates. A decrease in arterial O_2 results in the hypoxic ventilatory response, while an increase in arterial CO_2 results in the hypercapnic ventilatory response. Both ventilatory reflexes aim to correct any imbalance in blood gases and result in increased ventilation. The hypoxic ventilatory response pattern consists of an initial increase in V_e that is primarily driven by an increase in RR. The hypercapnic ventilatory response increases V_e by increasing V_T[12].

Autonomic control of breathing

Breathing represents the integration of three distinct neurobiological aspects: rhythm and pattern generation, sensory input, and motor output. Integration of these modalities allows for the

autonomic control of breathing and occurs in a highly interconnected system of neural networks located largely across the pons and medulla in the brainstem[1]. Various brainstem sites contribute to the proper functioning of the respiratory network and the central control of breathing.

Rhythm and Pattern Generation

The ventral respiratory column in the medulla is comprised of multiple areas that are responsible for respiratory rhythm generation. Perhaps one of the most important areas within the ventral respiratory column is the PreBötzinger Complex (preBötC), the site of inspiratory rhythmogenesis. The preBötC can be isolated in a slice preparation and maintain synchronous, spontaneous inspiratory activity and has been used as a model for studying the neural basis for inspiratory rhyhmogenesis[13]. Thus, much is known about how activity in this network is assembled. PreBötC activity and rhythm generation rely on glutamatergic signaling and α-amino-3-hydroxy-5-methyl-4-isoxazole-propionate receptor (AMPAr) agonism[13,14,15]. Neurons of the preBötC exhibit three distinct firing patterns that are active relative to the inspiratory burst. Together, they drive the generation of a spontaneous inspiratory rhythm. These are inspiratory neurons that burst during inspiration, post-inspiratory neurons that burst immediately after the inspiratory phase, and expiratory neurons that are tonically active and are inhibited during the entire duration of the inspiratory and post-inspiratory phases[13]. Some inspiratory neurons, also referred to as pacemaker neurons, have an intrinsic bursting ability and will continue this activity pattern when synaptically isolated from other excitatory input[13,16,17]. These so-called pacemakers possess a voltage-gated persistent sodium current (I_{NaP}) and a Ca^{2+} gated cation current (I_{CAN}) to enable their intrinsic bursting properties and typically lead the inspiratory network in the inspiratory cycle[13,16,18]. Blockage of these currents leads to the abolishment of intrinsic bursting

in pacemaker neurons[16]. Inhibition is equally as important in maintaining a stable inspiratory rhythm[19]. PreBötC neurons have a refractory period due to after-hyperpolarization in which excitation will not elicit a subsequent burst but will rather prolong the time to the next burst. Furthermore, increasing inhibition during the inspiratory phase will increase the frequency of bursting[19].

The Kolliker-Fuse nucleus (KF) is another area critical for maintaining the normal pattern of breathing. It is important for expiration and upper airway control and lesions in the KF lead to apneustic breathing, or sustained inspiration, and a square breath waveform[5,20,21,22]. The KF has glutamatergic projections throughout the respiratory network, which modulates the rate and pattern of breathing[5,20]. Glutamatergic input to the KF is crucial to its function and modulation. Agonism of the N-methyl-D-aspartate receptor (NMDAr) in KF will stimulate respiratory rate, while antagonizing KF NMDAr results in decreased respiratory rate and cessation of the post-inspiratory phase of breathing[20]. Reciprocal glutamatergic connections exist between the KF and preBötC, further demonstrating the importance of feedback between this pattern-generating network and the inspiratory network for maintaining synchronized and stable breathing[20].

Sensory Input

Sensory inputs to areas of rhythm generation are essential to modulate activity to adapt to changing behavioral and metabolic demands. Different modalities of sensation that the respiratory network responds to are mechano-, thermo-, and chemosensation[5]. The vagus nerve relays information to respiratory brainstem sites from thermoreceptors in the lungs and larynx and mechanoreceptors that monitor pressure in the larynx and stretch in the lungs[5,23]. Chemoreception is the sensing of changes in O_2 and CO_2 in the blood. Maintaining homeostasis

of blood gases is a necessary responsibility of breathing, and homeostatic deviations are sensed by the respiratory network, which modulates activity accordingly[5,24].

The canonical area of chemosensation in the respiratory network is the retrotrapezoid nucleus (RTN), which is critical for sensing increases in CO_2, which will increase its activity in response to CO_2[5,25,26]. The RTN modulates activity in the respiratory network with glutamatergic projections in response to changes in blood gases[27]. The RTN reciprocally connects to the nucleus of the solitary tract (NTS). In addition to being glutamatergic, the NTS releases norepinephrine (NE)[28] and receives afferent projections of the carotid bodies, which are the primary O_2 sensors in the body[29]. The NTS is also important for the hypercapnic ventilatory response, or an increase in breathing in response to an increase in CO_2[30]. The NTS has widespread projections and input throughout the respiratory network that are involved with various roles in the central control of breathing, including modulatory, motor, premotor, chemosensory, and pattern generators, and acts as a relay center of sensory information. Both the KF and preBötC receive input from and project to the NTS, which again supports the importance of the integration of sensory information with rhythmogenic activity[5].

Neuromodulatory brainstem areas alter their activity in response to deviations in blood gases. Both the raphe nuclei, which is the primary source of serotonergic modulation in the brainstem respiratory network, and the Locus Coeruleus (LC), the primary source of adrenergic drive, are chemosensitive[5]. Enhanced LC activity during hypercapnia is primarily mediated through gap junction signaling, and ablating the LC significantly attenuates the Hypercapnic Ventilatory Response[31,32]. Without peripheral chemosensory input, inhibiting LC decreases both inspiratory and active expiratory activity that occurs during hypercapnia. LC firing rates will increase in response to hypoxia and contribute to hypoxia-induced sighs[33]. Distinct areas of

chemosensation play different roles in the central control of breathing with diverse connections throughout the respiratory network and brain to aid in widespread modulation of breathing to maintain blood gas homeostasis.

Motor Output

Finally, integrating motor output with inspiratory drive and sensory information is critical to the physical behavior of breathing. The ventral respiratory group contains premotor neurons that project to the phrenic nerve, which controls the contraction of the diaphragm muscle[34]. The NTS has direct projection to the phrenic nerve, aiding in the direct modulation of breathing based on chemosensory input[5,34]. Increasing CO_2 will result in increased peak phrenic activity and corresponding increased respiratory rate[35]. Another important motor output of the respiratory network is the coordination of the hypoglossal (XII) cranial nerve, which innervates the tongue muscles. Phasic XII activation results in movement of the tongue to open the upper airways, allowing for proper inhalation of air during inspiration[36]. XII activity directly precedes phrenic activity, suggesting the initiation of tongue movement needs to occur before inhalation and lung expansion[35]. PreBötC projects to a premotor area, which then projects directly to XII, demonstrating the importance of coordination between motor output and inspiratory rhythmogenesis[37]. Obstructive Sleep Apnea occurs when there is a loss of upper airway muscle tone, which is controlled by the XII[38,39].

Coordination of breathing with other behaviors and physiological processes

Cardiorespiratory Coupling

Breathing is a neurobiological process that requires coordination between these respiratory modalities and other brain centers to modulate breathing for behaviors and physiological processes. To increase efficiency in the maintenance of blood gas homeostasis, respiratory activity should be coordinated with cardiovascular activity to optimize blood flow so that gas exchange during inspiration occurs with deoxygenated blood, which supplies a concentration gradient for O_2 to diffuse down so that oxygenated blood can then flow throughout the rest of the body. Respiratory and cardiovascular areas are anatomically close to one another in the medulla, aiding in their functional coupling[7]. Respiratory sinus arrhythmia is a normal change in heart rate that coordinates with breathing phase. During inhalation, heart rate is increased, and during exhalation, heart rate is decreased[5,7]. Coordination between the two systems is in part driven by preBötC activity. Inhibiting preBötC activity will lead to apneas. These apneas are accompanied by inhibition of thoracic sympathetic nerve activity and a decrease in heart rate[7]. Furthermore, inhibition of preBötC results in a loss of coupling seen between inspiration and heart rate in respiratory sinus arrhythmia. The muscarinic receptor antagonist atropine, which blocks parasympathetic activity, will stop respiratory sinus arrhythmia and lead to an increase in heart rate. These results suggest an effect of preBötC activity on parasympathetic and sympathetic drive[7]. Disease states, such as Rett Syndrome, demonstrate the importance of cardiorespiratory coupling. Patient's with Rett Syndrome exhibit a characteristic breath-hold at the peak of an inspiration. Normally breath-holds correspond to decreases in heart rate; however in Rett Syndrome, there is an initial, short decrease in heart rate, followed by an

increase, which then results in a mismatch between breathing and heart rate and a termination of respiratory sinus arrhythmia[6].

Changes in blood gases further exhibit the coordination between breathing and the cardiovascular system. The hypoxic ventilatory response, an increase in breathing that is stimulated by a decrease in circulating O_2, results in an initial increase in both breathing and heart rate, which is then followed by a subsequent decrease in both. Hypotheses suggest that the initial increase is driven by a sympathetic drive, while the subsequent decrease is driven by a parasympathetic drive[6].

Coordination of breathing and swallowing

Another critical behavior that needs to be coordinated with breathing is swallowing. Swallowing is a complicated bilateral motor behavior, and failure in its synchronization with breathing can lead to aspiration while eating. People with neurodegenerative diseases often develop a swallowing disorder from a lack of coordination with breathing and swallowing, and aspiration pneumonia is a leading cause of death for this population[40]. Swallowing is an oral behavior that occurs during post-inspiration, a phase of breathing where other oral behaviors, such as vocalization and cough, also occur. The phase of breathing is controlled by an area in the respiratory network called the Postinspiratory complex (PiCo)[41,42]. Neurons in PiCo co-express glutamate and acetylcholine and project to the preBötC. Optogenetic stimulation of glutamatergic/cholinergic PiCo neurons during the post-inspiratory phase of respiration resulted in swallow behavior. PiCo induced swallowing led to inhibition of inspiration during swallow. Furthermore, the respiratory cycle was reset depending on where in the respiratory cycle (e.g. how far from inspiration) the swallow was elicited[41]. This study further emphasizes the central

mechanisms behind the coordination of breathing with other oral behaviors and how activation of those behaviors can modulate the respiratory rhythm.

Dynamic network states

PreBötC reconfiguration generates distinct network states

Network state is also a determinant of the pattern of breathing. The preBötC can generate three distinct forms of fictive breathing: eupnea (normal breathing), sigh, and gasp. Sighs and gasps are attempts at autoresuscitation and to increase ventilation, however, gasps typically occur as a final attempt to breathe, while sighs can be more emotional based[43]. Both sighs and eupnea occur in normoxia[43,44]. Sighs occur in rhythm with inspiratory preBötC activity, are biphasic, and are cadmium-sensitive, indicating their dependence on I_{CAN}. In hypoxic and anoxic conditions, gasps occur. Gasps have shorter rise times and durations as compared to eupneic burst waveforms[43]. Unlike sighs, gasping is dependent on I_{NaP} as opposed to I_{CAN}, and overall inhibition on inspiratory drive is decreased as compared to eupnea. The switch to I_{NaP} during hypoxia-induced gasping indicates that bursting becomes dependent on the intrinsic properties of the neuron as opposed to synaptic[45]. Thus, the network state of preBötC shifts by the amount of O_2 available in the air. Furthermore, while eupnea depends on both I_{CAN} and I_{NaP}, there are shifts in network state during sighs and gasps that reconfigure the network to be dependent on a distinct pacemaker current.

Neuromodulation influences the state of the respiratory network

Neuromodulation is an important component that allows the respiratory network to be plastic and adapt rapidly based on metabolic and behavioral demands. These modulatory

chemicals interact with chemosensory, rhythm generation, and motor aspects of the network to appropriately configure network output. This can lead to changes in the frequency and amplitude of breathing and have fluctuating effects depending on the network state. There are multiple sources of neuromodulation originating in the brainstem. The raphe nucleus and LC are the primary sources of serotonin and norepinephrine (NE) in the brain, respectively[46]. Both project to the inspiratory rhythm generator, the preBötC[4]. Substance P is another prolific neuromodulator in the respiratory network that facilitates the inspiratory rhythm through neurokinin-1 receptor (NK1r) activation[44]. It is released in the preBötC from raphe and NTS. Both of these centers also release endogenous opioids onto preBötC[44]. Anatomical studies demonstrate that the preBötC and the ventral respiratory column receive input from many other brainstem sources that release additional neuromodulators suggesting the importance of neuromodulation on the inspiratory rhythm generator[44].

Viemari & Ramirez investigated how NE changes the network configuration of the preBötC. Application of NE onto the isolated preBötC network in slice results in an increase in population-level inspiratory activity in the frequency of the inspiratory rhythm as well as the duration and area of bursts. This effect was blocked by the α_1 receptor antagonist prazosin, suggesting that the stimulation of inspiratory activity by NE is α_1 mediated. Rhythmic population-level activity is killed by synapitcally isolating the slice. Despite the loss of the loss of the population activity, pacemaker neurons in the preBötC remain rhythmic, while non-pacemaker neurons lose their rhythmicity but still fire action potentials. Application of NE to synaptically isolated non-pacemaker neurons converts them into pacemaker neurons, suggesting that NE leads to the generation of a more robust inspiratory rhythm by converting non-pacemakers into pacemakers. There are cadmium-sensitive pacemaker neurons (dependent on

I_{CAN}, the Ca^{2+} activated cation current) and cadmium-insensitive pacemaker neurons (dependent on I_{NaP}, the persistent Na^{+} current). Converted non-pacemaker neurons became cadmium-sensitive pacemakers[17]. This increase in the number of inspiratory neurons contributing intrinsically to the generation of spontaneous population-level activity in the preBötC would lead to stronger excitatory output to other respiratory areas and increased resilience from perturbations to the inspiratory network. However, in the slice prep, this modulation by NE on preBötC activity induces irregularities during exposure to acute intermittent hypoxia by increasing inhibition on inspiratory cells, due to α_2 agonism[47]. This indicates the delicate nature of neuromodulation on rhythm generation and how adaptive processes can become maladaptive when combined with a perturbation, such as a diseased state.

While this study investigates how NE on its own affects preBötC activity, many neuromodulatory inputs release co-localized neuromodulators[44]. Thus, the interaction of multiple neuromodulators on inspiratory rhythmogenesis is important to understand. Doi & Ramirez investigated the extent of neuromodulatory effect dependent on network state (e.g. network leaning towards facilitation or inhibition). Blocking facilitating α_1 NE and serotonergic 5-hydroxytryptamine receptor 2 (5-HT_2) followed by blocking Substance P facilitating NK1r signaling results in a greater depression of frequency of respiratory activity (measured at the intercostal muscle, the muscles between our ribs that contract during inhalation), as compared to blocking NK1r alone. However, inhibiting NK1r and subsequently stimulating either the LC or raphe to increase the release of NE and serotonin, respectively, in the respiratory network resulted in a rebound of respiratory frequency above control levels[46]. These experiments show that a respiratory network tilted toward inhibition is more susceptible to further inhibition in a non-linear manner. Furthermore, it demonstrates that the inhibition of the NK1 system can still

result in an excitatory network state when there is excitatory neuromodulatory input from other brainstem areas (LC and raphe).

The effect of opioids on the central control of breathing

While some neuromodulators facilitate inspiratory rhythmogenesis, others inhibit it. Enkephalins and endorphins are endogenous opioids that bind to opioid receptors in the body (mu (μ), delta (δ), and kappa (κ))[48]. The μ-opioid receptor (μ-OR) is prolifically expressed throughout the respiratory network and agonism of the μ-OR by opioids is primarily responsible for Opioid-Induced Respiratory Depression (OIRD), which is the primary cause of opioid overdose[49,50]. Canonical μ-OR signaling decreases both intrinsic and synaptic excitability of the cell by activating G-protein-gated inwardly rectifying K^+ currents (GIRK) and inhibiting voltage-gated Ca^{2+} currents, respectively (**Fig 1**)[3, 51]. Stable breathing relies on rhythm generation, modulatory mechanisms, sensory feedback and motor output. Opioids suppress all four of these systems, leading to OIRD[3,52,53]. One area critical to the central control of breathing that contain μ-ORs is the PreBotzinger Complex (preBötC). Suppression of preBötC by opioids is critical for OIRD[54]. However, the suppression of preBötC by μ-OR agonists and its subsequent effects on respiratory activity and breathing can be highly variable and state-dependent[46,55,56,57,]. Hypotheses behind this variability include compensatory interactions between neuromodulator and neurotransmitter systems to maintain stable breathing[46,55]. These studies suggest that the degree of OIRD is dependent on the neuromodulatory state of the respiratory network at the time of drug intake.

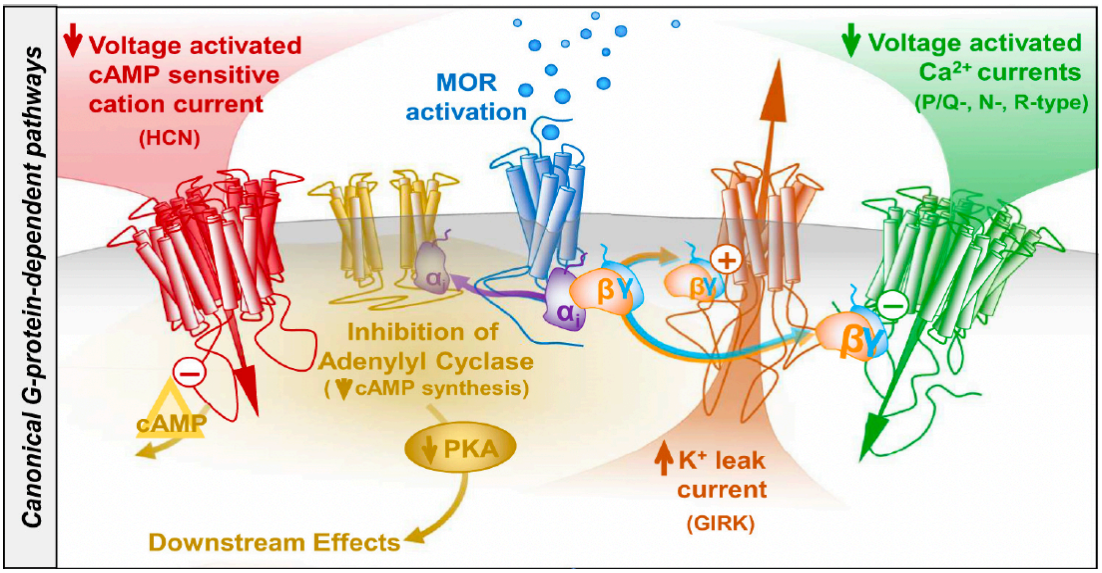

Figure 1. Schematic of canonical μ-Opioid Receptors

This figure is adapted from reference 49. Gβγ subunit activates GIRK channels and K^+ currents, while inhibiting voltage-gated Ca^{2+} currents to decrease intrinsic and synaptic excitability, respectively.

The KF is another brainstem area critical for the regulation of breathing that contains μ-ORs. While preBötC generates an inspiratory rhythm, the KF is critical for modulation of preBötC and other respiratory areas to contribute to breathing regularity and pattern[58]. At clinically relevant doses of morphine (10-20 mg/kg), deletion of μ-OR from either the preBötC or KF, as well as deletion of μ-OR from both areas, results in a reduction in OIRD[50,59]. However, at higher doses of morphine (30 & 100 mg/kg), deletion of μ-OR from the preBötC results in more OIRD as compared to deletion from the KF[59]. Thus, in addition to neuromodulatory state contributing to the degree of OIRD, there is a differential dose-dependent response to opioids in the suppression of KF and preBötC that contributes to the degree of OIRD and overall instability of the respiratory network. Injection of the opioid fentanyl directly into KF results in apneustic breathing patterns (longer duration of exhalation). Simultaneous injection of fentanyl and

antagonism of μ-ORs in the KF increases the rate of respiratory activity but does not reverse the apneustic pattern of breathing[60]. This result in conjunction with the successful reduction in OIRD with conditional deletion of μ-OR from KF indicates that there are network interactions throughout these respiratory centers that contribute to OIRD and allow for its reversal.

While μ-ORs are expressed throughout the respiratory network, inhibition by opioids of the preBötC and the KF have been shown to be essential for OIRD to occur. Deleting the μ-OR from either or both areas attenuates the degree of OIRD after low and high doses of opioids[50,59]. These two areas are critical for rhythm generation and inspiratory drive. Thus, the majority of research has focused on how μ-OR activation in these areas leads to OIRD. This research has primarily focused on how acute doses of opioids affect the KF and preBötC to lead to OIRD. However, how repeated OIRD, which results in hypoxia and hypercapnia, changes the state of the respiratory network and how this may lead to variability in opioid-induced responses is not well understood.

The Opioid Epidemic

History of The Epidemic

The United States is in the midst of an Opioid Epidemic. Since the end of the 20th century, there has been a continued surge in the number of overdose deaths due to opioids[61,62]. In 2021, 220 people died every day from an opioid overdose, and while the number of deaths leveled off from 2021 to 2022, it still remains at an all-time high[62]. Increased dependence and usage of opioid drugs began in the 1990's as the management of pain symptoms became increasingly important to physicians[63]. During this time, Purdue Pharma released the narcotic oxycodone, a partial derivative of the opium plant under the trade name OxyContin[64,65]. This

new pain medication exploded without patients fully realizing the high abuse potential that came with taking the drug. This surge in opioid usage led to the first phase of the opioid epidemic, which primarily involved the use and abuse of prescription opioids (**Fig 2**)[62,66]. Increased dependency and addiction to prescription opioids then led to the second phase of the epidemic, which involved patients becoming addicted and dependent on opioids and switching their use to Heroin, a Schedule I drug (**Fig 2**)[62]. A sharp uptick in overdose deaths after 2013, the beginning of phase three, is due to the introduction and proliferation of the use of synthetic opioids such as fentanyl (**Fig 2**)[62,67]. The use of fentanyl and synthetic opioids is particularly dangerous because of the increased potency of the drug, leading to a rapid onset of effects [68,69]. Furthermore, because fentanyl is so potent, only a small amount is needed to feel the effects. As a result, it is being mixed into other illicit substances such as cocaine, heroin, and counterfeit prescription pills, resulting in accidental exposure to fentanyl and users unknowingly taking large quantities of the drug[62,70].

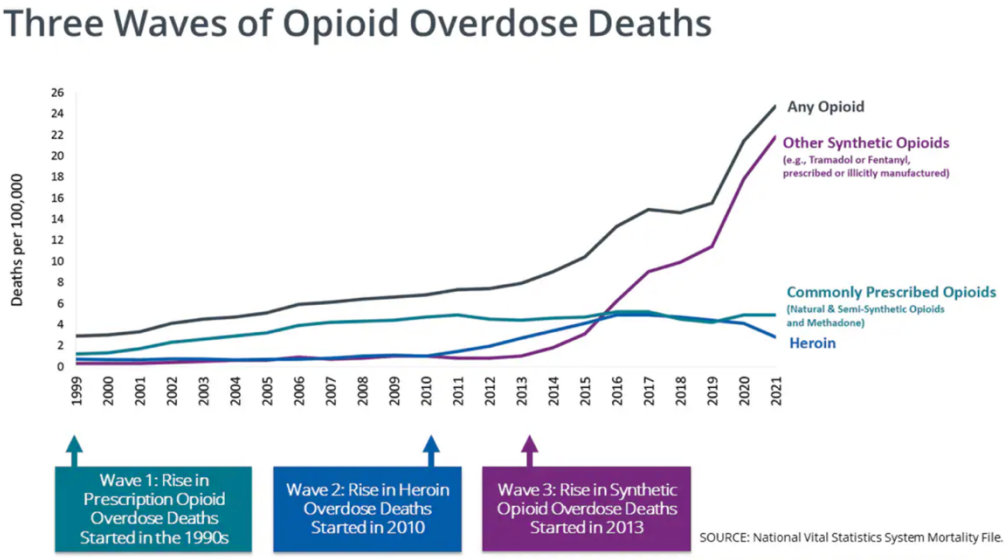

Figure 2. The Opioid Epidemic is made up of three distinct phases

This figure is adapted from reference 62.

Opioid Overdose

Respiratory depression is a hallmark of opioid overdose, and it occurs as a result of opioids binding to the μ-OR[49,71]. Our lab has proposed a model of the progression of opioid overdose, from the initiation step of respiratory depression, through death (**Fig 3**). Respiratory depression leads to elevated CO_2 levels (hypercapnia) and subsequent decreases in O_2 levels (hypoxia). Severe hypoxia leads to metabolic dysfunction, which is followed by cardio-respiratory collapse. However, there are common complications that arise after resuscitation from cardio-respiratory collapse, such as pulmonary edema and neuronal cell death that could result in eventual death. As patients progress through these stages, we propose that the likelihood of survival also decreases. The first step of OIRD is crucial in the cascade to overdose. Knocking out the μ-OR in the preBötC and KF results in the ablation of morphine-induced respiratory depression and protection from subsequent hypoxia[50], demonstrating how focusing on this first step of OIRD is crucial in understanding how to prevent opioid overdose and death.

The goal standard of care to reverse opioid overdose is the administration of the μ-OR antagonist naloxone[72]. Naloxone is not as effective at reversing fentanyl-induced respiratory depression as compared to morphine-induced respiratory depression for two primary reasons[69]. First, the potency and resulting rapid onset of depression from fentanyl allows for less intervention time with naloxone prior to cardio-respiratory collapse[69,71]. After arrest, chest compressions are necessary to maintain circulation to the brain to enable naloxone to act on respiratory centers contributing to overdose[71]. The rate of onset for respiratory depression is much faster after fentanyl administration as compared to heroin or morphine (**Fig 4**), which correlates with fentanyl having the greatest lipophilicity of the three opioids.[69] Because fentanyl is more potent, a lower dose is needed to elicit the same effects as less potent opioids[69]. In Hill

et al., mice were administered fentanyl (0.112 mg/kg), heroin (7.5 mg/kg), or morphine (7.5 mg/kg) in doses that resulted in equivalent depression of Minute Ventilation (V_e). The second reason naloxone is not as effective in reversing fentanyl-induced overdose is that, unlike morphine and other naturally derived opioids, fentanyl, which is currently driving overdose deaths, binds to receptors outside of the μ-OR, including α_{1A} and α_{1B} adrenergic receptors and cholinergic receptor subtypes[73,52]. In addition to respiratory depression, fentanyl inhibits breathing through respiratory muscle rigidity and wooden chest syndrome. Fentanyl interactions with the adrenergic receptors are hypothesized to be involved in these fentanyl-specific symptoms. Fentanyl has similar binding affinities as norepinephrine (NE) at α_{1A} and α_{1B} receptor subtypes, but not α_{1D}. Less competition of NE binding at α_{1D} receptors could be involved in muscle rigidity and wooden chest syndrome[52]. Antagonizing the α_1 receptor in the LC with prazosin prior to fentanyl administration reduces muscle rigidity, indicating LC and α_1 in this fentanyl-specific phenomenon[53]. Thus, the high potency and rapid onset time of fentanyl, plus its action on α_1 receptors contribute to naloxone's lack of effectiveness in reversing overdose due to fentanyl.

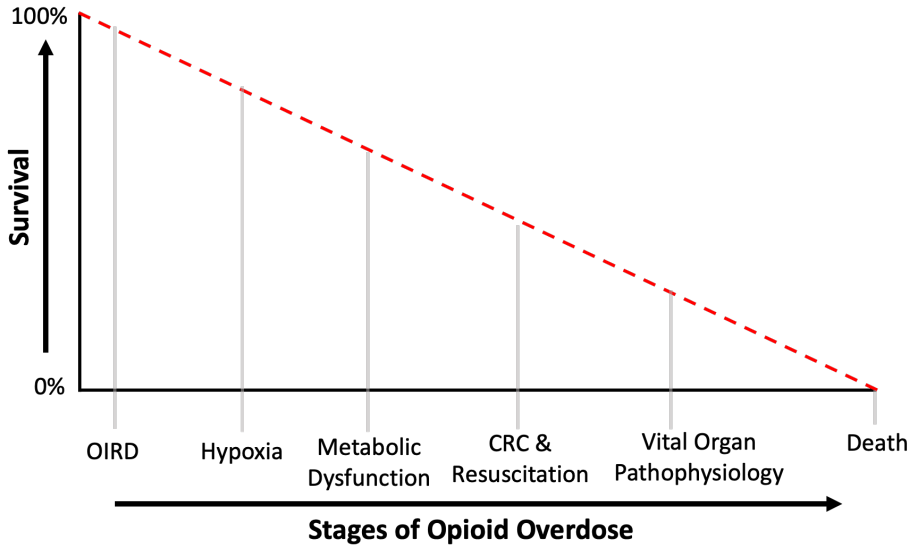

Figure 3. Proposed model describing the stages of opioid overdose beyond respiratory complications

OIRD rapidly causes systemic hypoxia. Hypoxia leads to metabolic dysfunction, followed by cardiorespiratory collapse (CRC), where resuscitation is attempted with naloxone. Vital organ pathophysiology (e.g. pulmonary edema) during CRC and upon resuscitation is a common complication that decreases survival following fentanyl overdose.

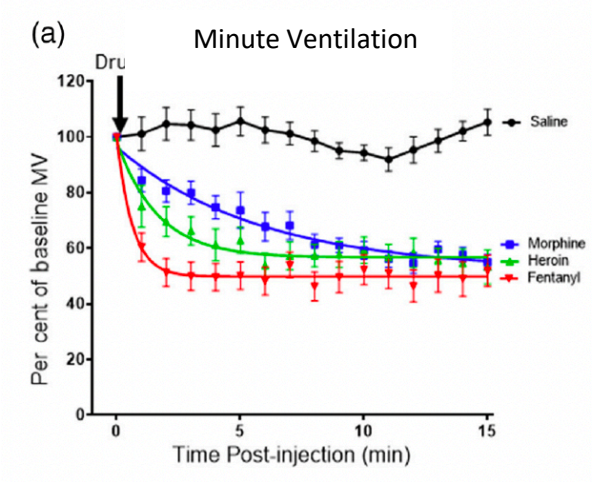

Figure 4. Rate of onset for maximum respiratory depression with fentanyl, morphine, and heroin

This figure is adapted from reference 69. Fentanyl (0.112 mg/kg), heroin (7.5 mg/kg), or morphine (7.5 mg/kg) were administered to mice. These doses eventually reach an equivalent depression in Minute Ventilation; however, fentanyl has the fastest onset of the three opioids.

Opioid Use Disorder

The Diagnostic and Statistical Manual of Mental Disorders Fifth Edition (DSM-5) from the American Psychiatric Association defines mild, moderate, and severe Opioid Use Disorder (OUD) with the Diagnostic Criteria in Figure 5[74]. These DSM-5 criteria incorporate qualifications of the dependency-forming aspect of the drug, such as tolerance and withdrawal, as well as criteria that focus on drug abuse and how it interferes with one's life, such as inability to fulfill obligations at home or work. The National Institute of Drug Abuse estimates that in 2021, 2.5 million U.S. adults suffered from OUD in 2021[75]. OUD is chronic and habitual in its nature, with the majority of users participating in repeat drug use[66]. Overdose deaths are driven by those who use the drug in a chronic and repeated fashion, not early users[76]. Opioids are highly dependency-forming, and developing OUD following the use of opioids is higher as compared with other drugs[66]. Relapse rates can be as high as 60% during the initial 3 months after first attempt of drug cessation[77]. Early use is reinforced by activation of reward-circuitry in the Ventral Tegmental Area (VTA) and Nucleus Accumbens (NAc) (**Fig 6**); however, with repeated use, withdrawal symptoms and negative effects become the driving force behind using, switching from positive reinforcement of drug use to avoidance behavior of adverse effects[66,78,79]. Acute opioid administration leads to plasticity changes in VTA Dopaminergic (DA) neurons that result in enhanced postsynaptic excitatory responses to presynaptic input, and while explored less, chronic exposure has been shown to increase VTA^{DA} activity, leading to increased excitability of this neuronal population[80].

DSM-5 Criteria for Diagnosis of Opioid Use Disorder

Diagnostic Criteria*
These criteria not considered to be met for those individuals taking opioids solely under appropriate medical supervision.

Check all that apply

	Opioids are often taken in larger amounts or over a longer period of time than intended.
	There is a persistent desire or unsuccessful efforts to cut down or control opioid use.
	A great deal of time is spent in activities necessary to obtain the opioid, use the opioid, or recover from its effects.
	Craving, or a strong desire to use opioids.
	Recurrent opioid use resulting in failure to fulfill major role obligations at work, school or home.
	Continued opioid use despite having persistent or recurrent social or interpersonal problems caused or exacerbated by the effects of opioids.
	Important social, occupational or recreational activities are given up or reduced because of opioid use.
	Recurrent opioid use in situations in which it is physically hazardous
	Continued use despite knowledge of having a persistent or recurrent physical or psychological problem that is likely to have been caused or exacerbated by opioids.
	*Tolerance, as defined by either of the following: (a) a need for markedly increased amounts of opioids to achieve intoxication or desired effect (b) markedly diminished effect with continued use of the same amount of an opioid
	*Withdrawal, as manifested by either of the following: (a) the characteristic opioid withdrawal syndrome (b) the same (or a closely related) substance are taken to relieve or avoid withdrawal symptoms

Total Number Boxes Checked: _____

Severity: **Mild**: 2-3 symptoms. **Moderate**: 4-5 symptoms. **Severe**: 6 or more symptoms

Figure 5. Diagnostic Criteria for Opioid Use Disorder (OUD)

This figure is adapted from reference 74. OUD can range from mild (2-3 symptoms), to moderate (4-5 symptoms), to severe (6 or more) disease.

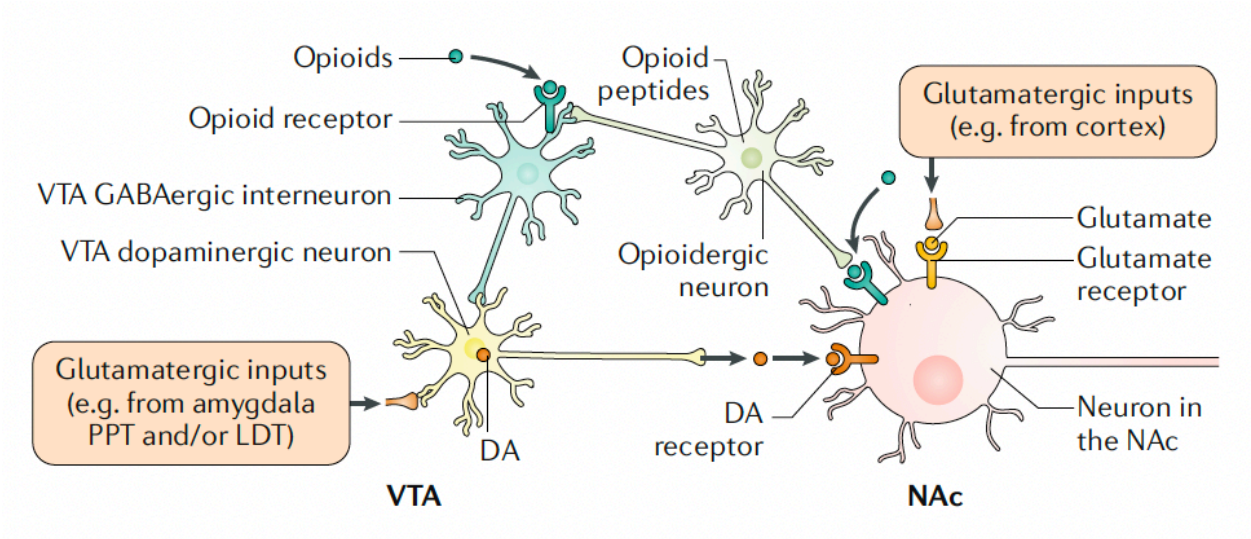

Figure 6. Opioid receptor expression in the reward pathway

This figure was adapted from reference 66. Opioids inhibit VTA GABAergic interneurons primarily through μ-OR, resulting in the disinhibition of Dopaminergic VTA neurons and increased dopamine release from the VTA to bind to post-synaptic NAc binding sites.

Tolerance to Opioids

Canonical mechanisms of opioid tolerance

Drugs of abuse lead to disturbances in homeostasis, and mechanisms of tolerance develop to combat these drug-induced perturbations and return the system to a baseline state[81]. Tolerance is defined as a "diminished response to a substance that occurs with frequent use[61]", which requires escalating dosages to achieve the desired effect[77]. This is demonstrated by a shift of the dose-response curve to the right (**Fig 7**) and is a result of compensatory responses to combat the drug effects [82]. Known compensatory responses are both pharmacodynamic and pharmacokinetic. Pharmacokinetics describes what the body does to the drug in four basic stages: absorption, distribution, metabolism, and excretion[83]. Pharmacodynamics describes what the drug does to the body, and can involve tolerance at the receptor, cellular, system, and synaptic levels[77]. Receptor level tolerance due to receptor desensitization (uncoupling from G-

protein signaling) and internalization contribute to opioid tolerance from acute and repeat use[84]. Cellular mechanisms, such as enhanced cAMP rebound activity after opioid inhibition, contribute to withdrawal[77]. System adaptations from repeat opioid use on opioid-sensitive neurons leads to indirect changes in excitability elsewhere[77]. Finally, repeat opioid use will lead to synaptic plasticity at synapses altered by opioid signaling[77]. These findings indicate that repeat opioid use can lead to a tolerance that alters the drug's effectiveness and to the remodeling of neural connections.

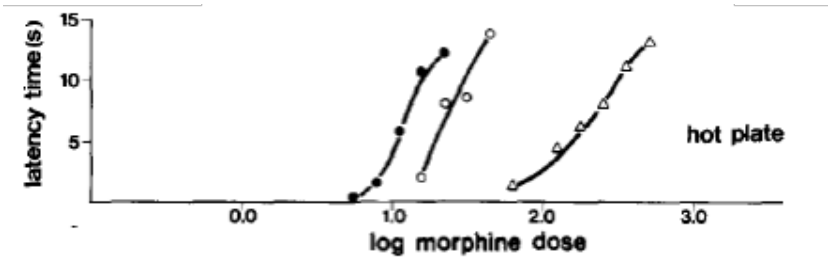

Figure 7. Analgesic dose-response curves to morphine

This figure is adapted from reference 81. After acute morphine administration (left), 16 mg/kg for 20 days (middle), and 32 mg/kg for 20 days (right). Hot plate assay for analgesia was used. Latency for the animal to lick or remove their paws was measured.

While these ubiquitous mechanisms of tolerance exist, the extent and speed of its development are not equal for all effects of opioids[81,85]. The primary effects of opioids are analgesia, euphoria, constipation, and respiratory depression, and while literature supports the development of tolerance to the euphoric and analgesic effects[86,87], the degree and linearity in which tolerance develops to the respiratory depressive effects is less understood and even thought to not develop[81,85,88,89,90,91]. The KF, critical for eupnea and the central control of breathing, does not display significant cellular and receptor (desensitization) level tolerance to morphine[88], perhaps contributing to the belief that tolerance to opioid-induced respiratory

depression does not develop or develops so slowly in comparison to the other effects (analgesia and euphoria) that it is not relevant. However, a recent small study in humans showed that chronic opioid patients needed larger doses of fentanyl to cause a 50% reduction in breathing as compared to opioid naïve patients[92], indicating that tolerance to OIRD does develop with repeat use and that the neural circuitry behind this adaptation should be further investigated.

Context-Dependent Tolerance

Rewards are inherent to the learning process. The relationship between rewards and the cues associated with them has been thoroughly investigated, and the neural mechanisms behind this relationship are well-established[93–95]. Both classical and operant conditioning are forms of learning that link a cue to a subsequent reward. In drug abuse, the rewarding aspects of the drug become coupled with drug-associated cues, and this learning is strengthened with repeat drug use. Rewarding stimuli cause increased Dopamine (DA) release from the VTA to the NAc[66,96]. If the reward is continuously paired with a preceding cue, then DA release will occur at cue presentation, prior to any reward receipt[95]. This relationship between cues and rewards can induce drug-seeking behavior and craving[66]. In drug abuse, users typically administer the drug in the same locations. Thus, a common cue paired with drug reward is the environmental context of drug administration.

In addition to perpetuating the cycle of addiction, drug-associated cues have been implicated in the development of tolerance[82,86,97–100]. Because a commonly associated drug cue is the environmental context of drug administration, this phenomenon was termed Context-Dependent Tolerance. It demonstrates that the development of tolerance to the effects of a drug is a conditioned process and can result in variable levels of tolerance that are dependent upon

exteroceptive stimuli. Simply moving the location of drug administration can alter the effectiveness of the drug. Context-dependent tolerance has been observed in opioids, nicotine, and alcohol[100–102]. The development of context-dependent tolerance to the analgesic effects of opioids has been well studied. Investigations have found that the degree of tolerance to drug-induced mortality and the analgesic effects to opioids is dependent on the location of drug administration[100,103,104], but that this form of tolerance can be extinguished through paradigms that decouple the reward from the contextual cue[97,98]. Studies also indicate that context-dependent tolerance can be diminished by inhibiting learning, further demonstrating how learning is essential in the production of tolerance with repeated drug use[82].

Shepard Siegel, a forefather in the research surrounding Context-Dependent Tolerance, likened the development of this tolerance to Pavlovian conditioning. Siegel hypothesized that the administration of opioids leads to drug effects (euphoria, analgesia, respiratory depression, mortality, etc.), which serve as an unconditioned stimulus, which in turn elicits an unconditioned response that mediates acute tolerance to the drug effects. Repeatedly pairing opioid administration and its subsequent effects with distinctive environmental cues results in those environmental cues becoming a conditioned stimulus. Thus, the environmental cues on their own should elicit a conditioned response, that will also mediate tolerance. Siegel referred to this conditioned response as a compensatory conditioned responses (CCR), because it opposes and attenuates the drug effects[82]. Furthermore, being in the previously drug-paired environmental context without subsequent opioid administration should still elicit CCRs to combat the drug effects, resulting in withdrawal symptoms[82]. This hypothesis agrees with the observation that drug-paired cues often send users into drug-seeking behavior.

Siegel used this Pavlovian-based hypothesis of Context-Dependent Tolerance to investigate increased opioid overdose deaths that were occurring among chronic users. The term "overdose" is commonly a misnomer for the reasoning behind why there is a death associated with opioid use[76,105]. Rather, a common theme of opioid-induced deaths is that they often occur when the user takes the drug in an unknown place[106,107]. Thus, the cause of opioid-associated death is rarely due to an increased dosage of the drug[76,105,108] but could be the result of a loss of context-dependent tolerance[109]. Siegel was able to replicate the context-dependent risk of opioid-induced mortality experimentally in rats. He showed that simply changing the environmental context of drug administration from one that had previously been associated with the drug to one that had no previous drug association resulted in 50% more deaths[105]. This demonstrated that opioid overdose risk is in part based on the location of drug administration.

While context-dependent tolerance has been thoroughly investigated in terms of the analgesic and lethality aspects of opioids, how context-dependent tolerance develops to Opioid-Induced Respiratory Depression (OIRD) and the central mechanisms behind tolerance to OIRD remain unknown. Central mechanisms of opioid-induced CCRs have been discussed in the literature[110]. Cholecystokinin (CCK), a peptide hormone made in neurons[111] has been implicated in context-dependent tolerance to the analgesic effects of opioids[110]. By interacting with the μ-OR in the dorsal-root ganglion, it decreases μ-OR activity, resulting in subdued analgesic effects of opioids[112]. However, there has been a paucity of studies continuing this investigation as it pertains to OIRD and its contribution to context-dependent induced mortality to opioids.

The function of the Locus Coeruleus

Functional organization

The Locus Coeruleus (LC) is the primary source of noradrenergic drive in the brain. The LC has many functions, but one overarching hypothesis about its role in brain function is that it broadcasts salient information throughout the brain and promotes reconfiguration of functional networks, behavioral flexibility, and adaptation, depending on an animal's needs at any given moment[113]. Vigilance, arousal, stress response, orientation of attention to novel or salient stimuli, cue-reward relationships, memory, and stimulation of autonomic processes like breathing and heart rate all involve the LC[93,113,93,113–116]. The involvement of the LC in such a diverse and distinct set of behaviors and functions can be attributed to the widespread projections of LC neurons throughout the brain[117]. The organization of LC inputs is not as well studied as outputs but multiple theories of organization have been hypothesized that similarly to LC outputs, LC receives inputs from a wide variety of areas from the brainstem and forebrain[114]. Recent anatomical and electrophysiological studies suggest that LC neurons could be a part of distinct functional modules[118] and that LC functional organization is made up of 1) distinct inputs that send specific projections to modify specific behaviors, and 2) broad inputs that have broad or discrete outputs[119]. The LC had previously been thought to consist of a homogeneous population of noradrenergic (NE) neurons. Recent studies have shown that the LC is a heterogeneous population of cells with distinct co-transmitter expression[114,120]. These distinct populations of cell types also have differing electrophysiological properties associated with them[114]. Furthermore, the firing patterns of LC neurons have been associated with distinct functional outputs. Phasic firing (10 Hz) is associated with the facilitation of learning and positive valence, while tonic activation at 25 Hz was associated with a fear response. While not fully understood, it is

hypothesized that distinct firing patterns preferentially activate certain ensembles within the LC, leading to different behavioral responses[121,122]. For example, LC activity will change from tonic to phasic bursting with the presentation of threatening, unexpected, or other salient stimuli to initiate reorientation of attention [113,123,124]. Thus, within the rather small nucleus of the LC, the literature supports the idea that there are distinct ensembles of neurons that contribute to the wide variety of behaviors known to involve the LC[114].

Arousal

LC activity and ensembles involved varies based on the desired behavioral output. Perhaps the behavior that the LC is most well-known to contribute to is arousal[123]. NE activity is associated with sympathetic drive, and the release of NE in the cortex has been shown to promote arousal[124,125]. Arousal state, such as sleep and wake, correlate with different types of LC activity[117]. Lower frequency activity is loosely associated with lower levels of arousal (such as slow-wave sleep), and there is a cessation of activity during REM sleep[125]. Manipulating LC activity by either inhibition or excitation reduces wakefulness and promotes wakefulness, respectively[123]. The cortex, which has reciprocal connections to the LC, exhibits slow oscillations during slow-wave sleep and anesthesia. During these unaroused states, LC activity becomes synchronous and burst-like[118].

Breathing

Arousal mechanisms and LC activity are linked to breathing[126]. Yackel et al. found a specific subset of neurons in the preBötC that project to the Locus Coeruleus and promote arousal behaviors. When ablated, mice no longer exhibit behaviors indicative of an increased

arousal state, such as sniffing, and increased behaviors indicative of a decreased arousal state, such as sitting and grooming[127]. The LC is chemosensitive and will increase its activity to stimulate breathing in response to hypercapnia[32,32,128,129]. Hypercapnia occurs with Opioid-Induced Respiratory Depression (OIRD). However, acute opioid administration suppresses this ventilatory response[130,131]. Unlike the canonical opioid-sensitive respiratory center, the KF, the LC is known to develop cellular and receptor level tolerance with repeat morphine administration[84]. This suggests that with continued opioid use, LC develops tolerance to μ-OR agonism and suppression of activity by opioids, allowing for the LC to stimulate breathing in response to hypercapnia due to OIRD. Immunohistochemistry studies show that μ-OR trafficking and internalization in the LC after precipitated withdrawal with the μ-OR antagonist naloxone is distinct in rats chronically treated with morphine as compared to those given an acute dose[132]. Furthermore, co-treatment of fentanyl with the α_1 antagonist yohimbine, which blocks inhibition of LC neurons by NE, results in less respiratory depression. NE application to the preBötC, which is suppressed by opioids, increases rhythmic activity in preBötC and breathing output, indicating the ability of NE neuromodulation to reconfigure the inspiratory network[17,46]. These findings suggest a possible role of LC activity and NE in maintaining breathing during OIRD.

Opioid Use and Withdrawal

The LC and NE have been previously implicated in the development of drug abuse and opioid withdrawal. While the literature has primarily focused on the role of DA in drug abuse, there are studies that implicate the role of NE in the self-administration of opioids, opioid-induced locomotion, and the development of opioid-conditioned place preference, further suggesting its role in the development of Opioid Use Disorder[133]. LC activity, similarly to

VTA^{DA} signaling, will initially increase with a reward, but with repeated pairing of a reward with a cue, activity shifts and increases with the presentation of the cue and preceding the behavioral response to obtain the reward[93]. Protocols to extinguish the coupling between cue and reward result in a cessation of increased LC activity with the cue. Subsequent pairing of the cue with the reward again shifts the LC response to the presentation of the cue, signaling the adaptability of the LC response in dynamic cue-reward relationships[93]. A circuit involving both LC and VTA to piriform cortex has been implicated in learning the valence of sensory cues[121]. LC activity is increased during opioid withdrawal[134], and enhancement of sympathetic activation leading to sympathetic syndrome is common after naloxone-precipitated withdrawal[135]. These findings suggest the importance of the LC^{NE} system in opioid reward processing and drug withdrawal.

Salient information processing and memory consolidation

The complex and dynamic world we live in requires continued learning, sensory processing, and tuning of attention toward important and new stimuli and the LC plays a critical role in these processes[115,116,114]. Survival necessitates quick behavioral adaptation to a changing environment. It is hypothesized that global LC^{NE} projections position it to act as a broadcaster of salient, unexpected, rewarding, or otherwise relevant information to the rest of the brain. The brain then responds by reconfiguring functional networks, allowing for adaptable behavioral responses to an ever-changing world[113]. For example, novel or unexpected stimuli result in phasic burst-like firing within the LC that quickly habituates with repeated exposure[136]. Likewise, the initiation of task-related behaviors is associated with phasic LC activation[93,137].

The LC is also important in encoding this information into memory. LC^{NE} input to hippocampal CA3 facilitates novel context memory encoding[138,139] and silencing LC inputs to

the hippocampus inhibits the hippocampus from forming a contextual map of a novel environment[140]. The LC is involved with emotional memory encoding, which depends on amygdala activation of LC[141]. Furthermore, the LC^{NE} system is involved in long-term potentiation (LTP). A new hypothesis proposes a positive feedback loop between glutamate and NE release to enhance synaptic plasticity at glutamatergic synapses. LC^{NE} is released and interacts with glutamatergic transmission on postsynaptic glutamate neurons that contain adrenergic receptors. It is hypothesized that this co-release occurs with phasic activation of LC neurons[121]. In turn, ionotropic and metabotropic glutamatergic receptors that are located on NE terminals increase NE release. This reciprocal mechanism supports the dynamic potentiation of salient information processing and encoding[114].

Summary of Thesis Work

The increased amount of deaths due to opioid overdose combined with the gold standard of overdose reversal, naloxone, not being as effective in the treatment of fentanyl-induced overdose has resulted in The Opioid Epidemic remaining a continued health crisis, despite numerous efforts to combat it. These overdose deaths are driven by people who repeatedly use opioids, however, despite this repeat use, their susceptibility to opioid overdose changes between drug-using experiences. To better understand why opioid overdose occurs, the field of respiratory neurophysiology has focused its efforts on studying how acute opioid administration affects the respiratory network to lead to Opioid-Induced Respiratory Depression (OIRD), a hallmark of opioid overdose. It is well understood that suppression of activity in the preBötC and KF by opioids is critical for OIRD to occur. However, the field has largely overlooked how repeat opioid use alters the central control of breathing and the respiratory network's susceptibility to

opioid neuromodulation. This was due to a belief that Repeat Opioid Use (ROU) does not alter susceptibility or increase tolerance to OIRD, however, Shepard Siegel's work identifies that ROU does have effects on opioid overdose susceptibility, a hallmark of which is OIRD, and that tolerance developed with ROU is learned and can be lost depending on the conditions of the user's drug taking, e.g. the context of drug administration. The goal of this thesis work aims to fill this knowledge gap by answering three main questions:

1) How does ROU affect the central control of breathing (e.g. does tolerance to OIRD develop with ROU)?
2) What central mechanisms support the development of tolerance?
3) How are these mechanisms altered based on the location of drug administration to change the degree of OIRD and subsequent opioid overdose susceptibility?

This work will allow us to begin to understand how the state-dependent nature of the respiratory network modulates the degree of OIRD and how this s altered with ROU, which contributes to labile susceptibility of opioid overdose. We hypothesize that ROU results in areas of the respiratory network critical to eupnea developing tolerance to opioid neuromodulation. One aspect of this central tolerance is due to a shift in network state due to enhanced LC^{NE} drive, leading to decreased OIRD after fentanyl administration. Furthermore, we hypothesize that this tolerance is conditional on exteroceptive factors, such as the location of drug administration.

References

1. Alheid GF, McCrimmon DR. The chemical neuroanatomy of breathing. Respir Physiol Neurobiol. 2008;164(1-2):3-11. doi:10.1016/j.resp.2008.07.0141. Alheid, G. F. & McCrimmon, D. R. The chemical neuroanatomy of breathing. Respir. Physiol. Neurobiol. 164, 3–11 (2008).

2. West, J. B. Respiratory Physiology: The Essentials. (Lippincott Williams & Wilkins, 2008).
3. Ikeda, K. et al. The respiratory control mechanisms in the brainstem and spinal cord: integrative views of the neuroanatomy and neurophysiology. J. Physiol. Sci. JPS 67, 45–62 (2016).
4. Bianchi, A. L., Denavit-Saubié, M. & Champagnat, J. Central control of breathing in mammals: neuronal circuitry, membrane properties, and neurotransmitters. Physiol. Rev. 75, 1–45 (1995).
5. Krohn, F. et al. The integrated brain network that controls respiration. eLife 12, e83654 (2023).
6. Garcia, A. J., Koschnitzky, J. E., Dashevskiy, T. & Ramirez, J.-M. Cardiorespiratory Coupling in Health and Disease. Auton. Neurosci. Basic Clin. 175, 26–37 (2013).
7. Menuet, C. et al. PreBötzinger complex neurons drive respiratory modulation of blood pressure and heart rate. eLife 9, e57288 (2020).
8. Park, J. et al. Brainstem control of vocalization and its coordination with respiration. Science 383, eadi8081 (2024).
9. Ashhad, S., Kam, K., Del Negro, C. A. & Feldman, J. L. Breathing Rhythm and Pattern and Their Influence on Emotion. Annu. Rev. Neurosci. 45, 223–247 (2022).
10. Patel, S., Miao, J. H., Yetiskul, E., Anokhin, A. & Majmundar, S. H. Physiology, Carbon Dioxide Retention. in StatPearls (StatPearls Publishing, Treasure Island (FL), 2024).
11. Wagner, P. D. The physiological basis of pulmonary gas exchange: implications for clinical interpretation of arterial blood gases. Eur. Respir. J. 45, 227–243 (2015).
12. Brinkman, J. E., Toro, F. & Sharma, S. Physiology, Respiratory Drive. in StatPearls (StatPearls Publishing, Treasure Island (FL), 2024).
13. Ramirez, J.-M. & Baertsch, N. A. The Dynamic Basis of Respiratory Rhythm Generation: One Breath at a Time. Annu. Rev. Neurosci. 41, 475–499 (2018).
14. Shao, X. M., Ge, Q. & Feldman, J. L. Modulation of AMPA receptors by cAMP-dependent protein kinase in PreBötzinger complex inspiratory neurons regulates respiratory rhythm in the rat. J. Physiol. 547, 543–553 (2003).
15. Tryba, A. K., Peña, F. & Ramirez, J.-M. Stabilization of bursting in respiratory pacemaker neurons. J. Neurosci. Off. J. Soc. Neurosci. 23, 3538–3546 (2003).
16. Ramirez, J.-M. & Viemari, J.-C. Determinants of inspiratory activity. Respir. Physiol. Neurobiol. 147, 145–157 (2005).
17. Viemari, J.-C. & Ramirez, J.-M. Norepinephrine Differentially Modulates Different Types of Respiratory Pacemaker and Nonpacemaker Neurons. J. Neurophysiol. 95, 2070–2082 (2006).
18. Smith, J., Koshiya, N., Negro, C. D., Butera, R. & Wilson, C. Mechanisms of respiratory rhythm generation in vitro. I. Pacemaker neurons and networks in the pre-Bötzinger complex (pre-BötC). Respir. Res. 2, 2.5 (2001).
19. Baertsch, N. A., Baertsch, H. C. & Ramirez, J. M. The interdependence of excitation and inhibition for the control of dynamic breathing rhythms. Nat. Commun. 9, 843 (2018).
20. Varga, A. G., Maletz, S. N., Bateman, J. T., Reid, B. T. & Levitt, E. S. Neurochemistry of the Kölliker-Fuse nucleus from a respiratory perspective. J. Neurochem. 156, 16–37 (2021).
21. Dutschmann, M. & Herbert, H. The Kölliker-Fuse nucleus gates the postinspiratory phase of the respiratory cycle to control inspiratory off-switch and upper airway resistance in rat. Eur. J. Neurosci. 24, 1071–1084 (2006).
22. Fung, M. L. & St John, W. M. The functional expression of a pontine pneumotaxic centre in neonatal rats. J. Physiol. 489 (Pt 2), 579–591 (1995).

23. Kaufman, M. P., Iwamoto, G. A., Ashton, J. H. & Cassidy, S. S. Responses to inflation of vagal afferents with endings in the lung of dogs. Circ. Res. 51, 525–531 (1982).
24. Cummins, E. P., Strowitzki, M. J. & Taylor, C. T. Mechanisms and Consequences of Oxygen and Carbon Dioxide Sensing in Mammals. Physiol. Rev. (2019) doi:10.1152/physrev.00003.2019.
25. Marina, N. et al. Essential Role of Phox2b-Expressing Ventrolateral Brainstem Neurons in the Chemosensory Control of Inspiration and Expiration. J. Neurosci. 30, 12466–12473 (2010).
26. Mulkey, D. K. et al. Respiratory control by ventral surface chemoreceptor neurons in rats. Nat. Neurosci. 7, 1360–1369 (2004).
27. Rosin, D. L., Chang, D. A. & Guyenet, P. G. Afferent and efferent connections of the rat retrotrapezoid nucleus. J. Comp. Neurol. 499, 64–89 (2006).
28. García-Medina, N. E. & Miranda, M. I. Nucleus of the solitary tract chemical stimulation induces extracellular norepinephrine release in the lateral and basolateral amygdala. Brain Stimulat. 6, 198–201 (2013).
29. Zera, T., Moraes, D. J. A., da Silva, M. P., Fisher, J. P. & Paton, J. F. R. The Logic of Carotid Body Connectivity to the Brain. Physiology 34, 264–282 (2019).
30. Nattie, E. & Li, A. Muscimol dialysis into the caudal aspect of the Nucleus tractus solitarii of conscious rats inhibits chemoreception. Respir. Physiol. Neurobiol. 164, 394–400 (2008).
31. de Carvalho, D. et al. Neurochemical and electrical modulation of the locus coeruleus: contribution to CO2drive to breathe. Front. Physiol. 5, 288 (2014).
32. Patrone, L. G. A., Bícego, K. C., Hartzler, L. K., Putnam, R. W. & Gargaglioni, L. H. Cardiorespiratory effects of gap junction blockade in the locus coeruleus in unanesthetized adult rats. Respir. Physiol. Neurobiol. 190, 86–95 (2014).
33. Magalhães, K. S. et al. Locus Coeruleus as a vigilance centre for active inspiration and expiration in rats. Sci. Rep. 8, 15654 (2018).
34. Dobbins, E. G. & Feldman, J. L. Brainstem network controlling descending drive to phrenic motoneurons in rat. J. Comp. Neurol. 347, 64–86 (1994).
35. Fukuda, Y. & Honda, Y. Differences in respiratory neural activities between vagal (superior laryngeal), hypoglossal, and phrenic nerves in the anesthetized rat. Jpn. J. Physiol. 32, 387–398 (1982).
36. Gestreau, C., Dutschmann, M., Obled, S. & Bianchi, A. L. Activation of XII motoneurons and premotor neurons during various oropharyngeal behaviors. Respir. Physiol. Neurobiol. 147, 159–176 (2005).
37. Fregosi, R. F. Respiratory related control of hypoglossal motoneurons—knowing what we don't know. Respir. Physiol. Neurobiol. 179, 43–47 (2011).
38. Ramirez, J.-M. et al. Central and Peripheral factors contributing to Obstructive Sleep Apneas. Respir. Physiol. Neurobiol. 189, 344–353 (2013).
39. Browe, B. M., Peng, Y.-J., Nanduri, J., Prabhakar, N. R. & Garcia, A. J. Gasotransmitter modulation of hypoglossal motoneuron activity. eLife 12, e81978 (2023).
40. Heemskerk, A.-W. & Roos, R. A. C. Aspiration pneumonia and death in Huntington's disease. PLoS Curr. 4, RRN1293 (2012).
41. Huff, A., Karlen-Amarante, M., Oliveira, L. M. & Ramirez, J.-M. Role of the postinspiratory complex in regulating swallow–breathing coordination and other laryngeal behaviors. eLife 12, e86103 (2023).
42. Anderson, T. M. et al. A novel excitatory network for the control of breathing. Nature 536, 76–80 (2016).

43. Lieske, S. P., Thoby-Brisson, M., Telgkamp, P. & Ramirez, J. M. Reconfiguration of the neural network controlling multiple breathing patterns: eupnea, sighs and gasps. Nat. Neurosci. 3, 600–607 (2000).
44. Doi, A. & Ramirez, J.-M. NEUROMODULATION AND THE ORCHESTRATION OF THE RESPIRATORY RHYTHM. Respir. Physiol. Neurobiol. 164, 96–104 (2008).
45. Paton, J. F. R., Abdala, A. P. L., Koizumi, H., Smith, J. C. & St-John, W. M. Respiratory rhythm generation during gasping depends on persistent sodium current. Nat. Neurosci. 9, 311–313 (2006).
46. Doi, A. & Ramirez, J.-M. State-Dependent Interactions between Excitatory Neuromodulators in the Neuronal Control of Breathing. J. Neurosci. 30, 8251–8262 (2010).
47. Zanella, S. et al. When Norepinephrine Becomes a Driver of Breathing Irregularities: How Intermittent Hypoxia Fundamentally Alters the Modulatory Response of the Respiratory Network. J. Neurosci. 34, 36–50 (2014).
48. Zagon, I. S. & McLaughlin, P. J. Endogenous Opioids in the Etiology and Treatment of Multiple Sclerosis. in Multiple Sclerosis: Perspectives in Treatment and Pathogenesis (eds. Zagon, I. S. & McLaughlin, P. J.) (Codon Publications, Brisbane (AU), 2017).
49. Ramirez, J.-M. et al. Neuronal mechanisms underlying opioid-induced respiratory depression: our current understanding. J. Neurophysiol. 125, 1899–1919 (2021).
50. Bachmutsky, I., Wei, X. P., Kish, E. & Yackle, K. Opioids depress breathing through two small brainstem sites. eLife 9, e52694 (2020).
51. Al-Hasani, R. & Bruchas, M. R. Molecular Mechanisms of Opioid Receptor-Dependent Signaling and Behavior. Anesthesiology 115, 1363–1381 (2011).
52. Torralva, R. & Janowsky, A. Noradrenergic Mechanisms in Fentanyl-Mediated Rapid Death Explain Failure of Naloxone in the Opioid Crisis. J. Pharmacol. Exp. Ther. 371, 453–475 (2019).
53. Lui, P. W., Lee, T. Y. & Chan, S. H. Involvement of locus coeruleus and noradrenergic neurotransmission in fentanyl-induced muscular rigidity in the rat. Neurosci. Lett. 96, 114–119 (1989).
54. Montandon, G. & Horner, R. CrossTalk proposal: The preBötzinger complex is essential for the respiratory depression following systemic administration of opioid analgesics. J. Physiol. 592, 1159–1162 (2014).
55. Langer, T. M. et al. Effects on breathing of agonists to μ-opioid or GABAA receptors dialyzed into the ventral respiratory column of awake and sleeping goats. Respir. Physiol. Neurobiol. 239, 10–25 (2017).
56. Krause, K. L. et al. μ-Opioid receptor agonist injections into the presumed pre-Bötzinger complex and the surrounding region of awake goats do not alter eupneic breathing. J. Appl. Physiol. 107, 1591–1599 (2009).
57. Burgraff, N. J., Bush, N. E., Ramirez, J. M. & Baertsch, N. A. Dynamic Rhythmogenic Network States Drive Differential Opioid Responses in the In Vitro Respiratory Network.
58. Navarrete-Opazo, A. A. et al. Endogenous glutamatergic inputs to the Parabrachial Nucleus/Kölliker-Fuse Complex determine respiratory rate. Respir. Physiol. Neurobiol. 277, 103401 (2020).
59. Varga, A. G., Reid, B. T., Kieffer, B. L. & Levitt, E. S. Differential impact of two critical respiratory centres in opioid-induced respiratory depression in awake mice. J. Physiol. 598, 189–205 (2020).

60. Saunders, S. E. & Levitt, E. S. Kölliker-Fuse/Parabrachial complex mu opioid receptors contribute to fentanyl-induced apnea and respiratory rate depression. Respir. Physiol. Neurobiol. 275, 103388 (2020).
61. Lyden, J. & Binswanger, I. A. The United States opioid epidemic. Semin. Perinatol. 43, 123 (2019).
62. CDC. Understanding the Opioid Overdose Epidemic. Overdose Prevention https://www.cdc.gov/overdose-prevention/about/understanding-the-opioid-overdose-epidemic.html (2024).
63. Scher, C., Meador, L., Van Cleave, J. H. & Reid, M. C. Moving Beyond Pain as the Fifth Vital Sign and Patient Satisfaction Scores to Improve Pain Care in the 21st Century. Pain Manag. Nurs. Off. J. Am. Soc. Pain Manag. Nurses 19, 125–129 (2018).
64. Opium Poppy. https://museum.dea.gov/exhibits/online-exhibits/cannabis-coca-and-poppy-natures-addictive-plants/opium-poppy.
65. Alcohol and Drug Policy Commission : Opiates or Opioids — What's the difference? : State of Oregon. https://www.oregon.gov/adpc/pages/opiate-opioid.aspx.
66. Strang, J. et al. Opioid use disorder. Nat. Rev. Dis. Primer 6, 1–28 (2020).
67. O'Donnell, J. K. Deaths Involving Fentanyl, Fentanyl Analogs, and U-47700 — 10 States, July–December 2016. MMWR Morb. Mortal. Wkly. Rep. 66, (2017).
68. Burns, S. M., Cunningham, C. W. & Mercer, S. L. DARK Classics in Chemical Neuroscience: Fentanyl. ACS Chem. Neurosci. 9, 2428–2437 (2018).
69. Hill, R., Santhakumar, R., Dewey, W., Kelly, E. & Henderson, G. Fentanyl depression of respiration: Comparison with heroin and morphine. Br. J. Pharmacol. 177, 254–265 (2020).
70. Pergolizzi, J., Magnusson, P., LeQuang, J. A. K. & Breve, F. Illicitly Manufactured Fentanyl Entering the United States. Cureus 13, e17496 (2021).
71. van Lemmen, M. et al. Opioid Overdose: Limitations in Naloxone Reversal of Respiratory Depression and Prevention of Cardiac Arrest. Anesthesiology 139, 342–353 (2023).
73. Torralva, R. et al. Fentanyl but not Morphine Interacts with Nonopioid Recombinant Human Neurotransmitter Receptors and Transporters. J. Pharmacol. Exp. Ther. 374, 376–391 (2020).
74. Hasin, D. S. et al. DSM-5 Criteria for Substance Use Disorders: Recommendations and Rationale. Am. J. Psychiatry 170, 834–851 (2013).
75. Jones, C. M., Han, B., Baldwin, G. T., Einstein, E. B. & Compton, W. M. Use of Medication for Opioid Use Disorder Among Adults With Past-Year Opioid Use Disorder in the US, 2021. JAMA Netw. Open 6, e2327488 (2023).
76. Darke, S. Opioid overdose and the power of old myths: What we thought we knew, what we do know and why it matters. Drug Alcohol Rev. 33, 109–114 (2014).
77. Christie, M. J. Cellular neuroadaptations to chronic opioids: tolerance, withdrawal and addiction. Br. J. Pharmacol. 154, 384–396 (2008).
78. Goldstein, R. Z. & Volkow, N. D. Drug addiction and its underlying neurobiological basis: neuroimaging evidence for the involvement of the frontal cortex. Am. J. Psychiatry 159, 1642–1652 (2002).
79. Chaudun, F. et al. Distinct μ-opioid ensembles trigger positive and negative fentanyl reinforcement. Nature 630, 141–148 (2024).
80. Doyle, M. A. & Mazei-Robison, M. S. Opioid-Induced Molecular and Cellular Plasticity of Ventral Tegmental Area Dopamine Neurons. Cold Spring Harb. Perspect. Med. 11, a039362 (2021).

81. Fernandes, M., Kluwe, S. & Coper, H. Development and loss of tolerance to morphine in the rat. Psychopharmacology (Berl.) 78, 234–238 (1982).
82. Siegel, S., Baptista, M. A. S., Kim, J. A., McDonald, R. V. & Weise-Kelly, L. Pavlovian psychopharmacology: The associative basis of tolerance. Exp. Clin. Psychopharmacol. 8, 276–293 (2000).
83. Rn), O. R. for N. (Open, Ernstmeyer, K. & Christman, E. Chapter 1 Pharmacokinetics & Pharmacodynamics. in Nursing Pharmacology [Internet]. 2nd edition (Chippewa Valley Technical College, 2023).
84. Levitt, E. S. & Williams, J. T. Morphine Desensitization and Cellular Tolerance Are Distinguished in Rat Locus Ceruleus Neurons. Mol. Pharmacol. 82, 983–992 (2012).
85. Palkovic, B., Marchenko, V., Zuperku, E. J., Stuth, E. A. E. & Stucke, A. G. Multi-Level Regulation of Opioid-Induced Respiratory Depression. Physiology 35, 391–404 (2020).
86. Tiffany, S. T. & Maude-Griffin, P. M. Tolerance to Morphine in the Rat: Associative and Nonassociative Effects.
87. Gardner, E. L. Introduction: Addiction and Brain Reward and Anti-Reward Pathways. Adv. Psychosom. Med. 30, 22–60 (2011).
88. Levitt, E. S. & Williams, J. T. Desensitization and Tolerance of Mu Opioid Receptors on Pontine Kölliker-Fuse Neurons. Mol. Pharmacol. 93, 8–13 (2018).
89. Hill, R. et al. Ethanol Reversal of Tolerance to the Respiratory Depressant Effects of Morphine. Neuropsychopharmacology 41, 762–773 (2016).
90. Emery, M. J., Groves, C. C., Kruse, T. N., Shi, C. & Terman, G. W. Ventilation and the Response to Hypercapnia after Morphine in Opioid-naive and Opioid-tolerant Rats. Anesthesiology 124, 945–957 (2016).
91. Hayhurst, C. J. Differential Opioid Tolerance and Opioid-induced Hyperalgesia.
92. Algera, M. H. et al. Tolerance to Opioid-Induced Respiratory Depression in Chronic High-Dose Opioid Users: A Model-Based Comparison With Opioid-Naïve Individuals. Clin. Pharmacol. Ther. 109, 637–645 (2021).
93. Bouret, S. & Sara, S. J. Reward expectation, orientation of attention and locus coeruleus-medial frontal cortex interplay during learning. Eur. J. Neurosci. 20, 791–802 (2004).
94. Rehman, I., Mahabadi, N., Sanvictores, T. & Rehman, C. I. Classical Conditioning. in StatPearls (StatPearls Publishing, Treasure Island (FL), 2024).
95. Schultz, W. Dopamine reward prediction error coding. Dialogues Clin. Neurosci. 18, 23–32 (2016).
96. Volkow, N. D. et al. Addiction: Decreased reward sensitivity and increased expectation sensitivity conspire to overwhelm the brain's control circuit. BioEssays 32, 748–755 (2010).
97. Siegel, S. Evidence from Rats That Morphine Tolerance Is a Learned Response.
98. Siegel, S., Hinson, R. E. & Krank, M. D. Modulation of tolerance to the lethal effect of morphine by extinction. Behav. Neural Biol. 25, 257–262 (1979).
99. Baker, T. B. & Tiffany, S. T. Morphine Tolerance as Habituation.
100. Tiffany, S. T., Maude-Griffin, P. M. & Drobes, D. J. Effect of Interdose Interval on the Development of Associative Tolerance to Morphine in the Rat: A Dose-Response Analysis.
101. Cepeda-Benito, A., Davis, K. W., Reynoso, J. T. & Harraid, J. H. Associative and behavioral tolerance to the analgesic effects of nicotine in rats: tail-flick and paw-lick assays. Psychopharmacology (Berl.) 180, 224–233 (2005).
102. Crowell, C. R., Hinson, R. E. & Siegel, S. The role of conditional drug responses in tolerance to the hypothermic effects of ethanol. Psychopharmacology (Berl.) 73, 51–54 (1981).

103. Tiffany, S. T., Drobes, D. J. & Cepeda-Benito, A. Contribution of associative and nonassociative processes to the development of morphine tolerance. Psychopharmacology (Berl.) 109, 185–190 (1992).
104. Cepeda-Benito, A. & Tiffany, S. T. Effect of number of conditioning trials on the development of associative tolerance to morphine. Psychopharmacology (Berl.) 109, 172–176 (1992).
105. Siegel, S. The Heroin Overdose Mystery.
106. Gerevich, J., Bácskai, E., Farkas, L. & Danics, Z. A case report: Pavlovian conditioning as a risk factor of heroin 'overdose' death. Harm. Reduct. J. 2, 11 (2005).
107. Siegel, S. Pavlovian conditioning and heroin overdose: Reports by overdose victims. Bull. Psychon. Soc. 22, 428–430 (1984).
108. Becker, C. E. LICIT AND ILLICIT DRUGS. West. J. Med. 120, 180 (1974).
109. Siegel, S. Pavlovian conditioning and drug overdose: When tolerance fails. Addict. Res. Theory 9, 503–513 (2001).
110. Kim, J. A. & Siegel, S. The Role of Cholecystokinin in Conditional Compensatory Responding and Morphine Tolerance in Rats.
111. Rehfeld, J. F. Cholecystokinin—From Local Gut Hormone to Ubiquitous Messenger. Front. Endocrinol. 8, (2017).
112. Yang, Y. et al. Heteromerization of μ-opioid receptor and cholecystokinin B receptor through the third transmembrane domain of the μ-opioid receptor contributes to the anti-opioid effects of cholecystokinin octapeptide. Exp. Mol. Med. 50, 1–16 (2018).
113. Bouret, S. & Sara, S. J. Network reset: a simplified overarching theory of locus coeruleus noradrenaline function. Trends Neurosci. 28, 574–582 (2005).
114. Poe, G. R. et al. Locus coeruleus: a new look at the blue spot. Nat. Rev. Neurosci. 21, 644–659 (2020).
115. Hayat, H. et al. Locus coeruleus norepinephrine activity mediates sensory-evoked awakenings from sleep. Sci. Adv. (2020) doi:10.1126/sciadv.aaz4232.
116. Melnychuk, M. C., Robertson, I. H., Plini, E. R. G. & Dockree, P. M. A Bridge between the Breath and the Brain: Synchronization of Respiration, a Pupillometric Marker of the Locus Coeruleus, and an EEG Marker of Attentional Control State. Brain Sci. 11, 1324 (2021).
117. Sara, S. J. & Bouret, S. Orienting and Reorienting: The Locus Coeruleus Mediates Cognition through Arousal. Neuron 76, 130–141 (2012).
118. Totah, N. K., Neves, R. M., Panzeri, S., Logothetis, N. K. & Eschenko, O. The Locus Coeruleus Is a Complex and Differentiated Neuromodulatory System. Neuron 99, 1055-1068.e6 (2018).
119. Uematsu, A. et al. Modular organization of the brainstem noradrenaline system coordinates opposing learning states. Nat. Neurosci. 20, 1602–1611 (2017).
120. Devoto, P., Flore, G., Saba, P., Fà, M. & Gessa, G. L. Co-release of noradrenaline and dopamine in the cerebral cortex elicited by single train and repeated train stimulation of the locus coeruleus. BMC Neurosci. 6, 31 (2005).
121. Ghosh, A. et al. Locus Coeruleus Activation Patterns Differentially Modulate Odor Discrimination Learning and Odor Valence in Rats. Cereb. Cortex Commun. 2, tgab026 (2021).
122. Noei, S., Zouridis, I. S., Logothetis, N. K., Panzeri, S. & Totah, N. K. Distinct ensembles in the noradrenergic locus coeruleus are associated with diverse cortical states. Proc. Natl. Acad. Sci. 119, e2116507119 (2022).

123. Carter, M. E. et al. Tuning arousal with optogenetic modulation of locus coeruleus neurons. Nat. Neurosci. 13, 1526–1533 (2010).
124. Aston-Jones, G., Chiang, C. & Alexinsky, T. Discharge of noradrenergic locus coeruleus neurons in behaving rats and monkeys suggests a role in vigilance. Prog. Brain Res. 88, 501–520 (1991).
125. Kjaerby, C. et al. Memory-enhancing properties of sleep depend on the oscillatory amplitude of norepinephrine. Nat. Neurosci. 25, 1059–1070 (2022).
126. Liu, N. et al. Respiratory Control by Phox2b-expressing Neurons in a Locus Coeruleus–preBötzinger Complex Circuit. Neurosci. Bull. 37, 31–44 (2021).
127. Yackle, K. et al. Breathing control center neurons that promote arousal in mice. Science 355, 1411–1415 (2017).
128. Gargaglioni, L. H., Hartzler, L. K. & Putnam, R. W. The locus coeruleus and central chemosensitivity. Respir. Physiol. Neurobiol. 173, 264–273 (2010).
129. Biancardi, V., Bícego, K. C., Almeida, M. C. & Gargaglioni, L. H. Locus coeruleus noradrenergic neurons and CO2 drive to breathing. Pflüg. Arch. - Eur. J. Physiol. 455, 1119–1128 (2008).
130. Dahan, A. & Nieuwenhuijs, D. Anesthetic Potency and Influence of Morphine and Sevoflurane on Respiration in □-Opioid Receptor Knockout Mice. 94, (2001).
131. Pattinson, K. T. S. Opioids and the control of respiration. Br. J. Anaesth. 100, 747–758 (2008).
132. Scavone, J. L. & Van Bockstaele, E. J. μ-Opioid Receptor Redistribution in the Locus Coeruleus Upon Precipitation of Withdrawal in Opiate-Dependent Rats. Anat. Rec. 292, 401–411 (2009).
133. Weinshenker, D. & Schroeder, J. P. There and Back Again: A Tale of Norepinephrine and Drug Addiction. Neuropsychopharmacology 32, 1433–1451 (2007).
134. Abercrombie, E. D. & Jacobs, B. L. Systemic naloxone administration potentiates locus coeruleus noradrenergic neuronal activity under stressful but not non-stressful conditions. Brain Res. 441, 362–366 (1988).
135. Baraban, S. C., Stornetta, R. L. & Guyenet, P. G. Respiratory control of sympathetic nerve activity during naloxone-precipitated morphine withdrawal in rats. J. Pharmacol. Exp. Ther. 265, 89–95 (1993).
136. Vankov, A., Hervé-Minvielle, A. & Sara, S. J. Response to novelty and its rapid habituation in locus coeruleus neurons of the freely exploring rat. Eur. J. Neurosci. 7, 1180–1187 (1995).
137. Xiang, L. et al. Behavioral correlates of activity of optogenetically identified locus coeruleus noradrenergic neurons in rats performing T-maze tasks. Sci. Rep. 9, 1361 (2019).
138. Wagatsuma, A. et al. Locus coeruleus input to hippocampal CA3 drives single-trial learning of a novel context. Proc. Natl. Acad. Sci. U. S. A. 115, E310–E316 (2018).
139. Takeuchi, T. et al. Locus coeruleus and dopaminergic consolidation of everyday memory. Nature 537, 357–362 (2016).
140. Grella, S. L. et al. Locus Coeruleus Phasic, But Not Tonic, Activation Initiates Global Remapping in a Familiar Environment. J. Neurosci. 39, 445–455 (2019).
141. Jacobs, H. I. et al. Dynamic behavior of the locus coeruleus during arousal-related memory processing in a multi-modal 7T fMRI paradigm. eLife 9, e52059.

Chapter 1

Introduction

Opioid-induced respiratory depression (OIRD) is a hallmark trait of opioid overdose [1-3]. When left unmitigated, opioid-overdose typically follows a pattern of hypoventilation, subsequent cessation of breathing, cardiorespiratory arrest and ultimately death. Opioids act acutely via μ-opioid receptor (μ-OR) signaling in the brainstem to suppress the ability to generate and maintain inspiratory activity[4,5]. Despite the advancements being made toward understanding the cellular basis of OIRD, the effects of repeated opioid use (ROU) on breathing remain poorly understood. As OIRD remains a leading cause of overdose-related death in the context of the ongoing opioid epidemic[6,7], understanding the occurrence or absence of physiological adaptations in response to ROU is critical. This study explores how ROU leads to changes in ventilation and its control that either minimize or exacerbate OIRD and the risk of respiratory failure.

While persistent opioid use, such as that observed with opioid use disorder, can engender tolerance to both analgesia and euphoria [8-10], the effects of repeat opioid use reach well beyond these phenomena to also impact how one breathes. Sleep apnea, a clinical condition associated with remodeling of the control of breathing[11], is common among chronic opioid users[12,13]. Furthermore, in both humans and animals, chronic opioid use has also been shown to lead to tolerance to OIRD[14-16]. Yet, the lack of understanding into the impact of ROU on breathing significantly impedes the ability to fully address the morbidities and mortalities linked to ORID and overdose.

Here, we investigated how ROU impacts breathing *in vivo* and the impact of ROU on the inspiratory rhythm generator, the preBötC, using the rhythmic medullary brainstem slice preparation. We hypothesized that ROU leads to adaptations in breathing that diminish the action of opioids on breathing and inspiratory rhythmogenesis. Following ROU, two types of respiratory responses emerge. These responses are differentially characterized by the presence or absence of ventilatory adaptation to OIRD following of repeated fentanyl administration. The adaptive ventilatory response is associated with an improvement in for metabolic demand to be met during OIRD. Additionally, inspiratory rhythmogenesis

from the preBötC is less sensitive to opioid neuromodulation following ROU. These data indicate that ROU leads to changes in breathing indicative of opioid tolerance as evidenced by the diminished magnitude of OIRD and the reduced efficacy in μ-OR mediated modulation at level of the inspiratory network.

Methods

Study Approval

All animal protocols were approved by the Institutional of Animal Care and Use Committee at The University of Chicago, in accordance with National Institute of Health guidelines.

Animals

Mice used in this study were housed in AAALAC-approved facilities following a 12/12 h light/dark cycle and were given ad libitum access to food and water. All experiments were performed in the light cycle. Adult mice of both sexes (Postnatal Day: 74 ± 4days, Body mass: 23.78 ± 5.31 g) on a *C57BL/6* background were used for plethysmograph studies. Neonatal mice of both sexes (Postnatal Day 10 ± 1day) on a CD1 background were used for electrophysiological studies. Neonatal mice were housed with their dam, allowing ad libitum access to nutrition.

Repeat Opioid Use (ROU) and fentanyl administration

Two protocols were used for the ROU. Protocol 1: *Adult ROU:* All subjects were acclimatized to handling, being placed into a sham-plethysmography chamber and given *i.p.* injection of saline (0.2-0.3 mL) for five days prior to enrollment into the ROU protocol. The

protocol consisted of five days of fentanyl administration via *i.p.* injection (0.7mg/kg) where breathing was measured via whole-body plethysmography. In a subset of animals, the protocol was extended to six days. Protocol 2: *Neonatal ROU.* A single daily injection of fentanyl (0.70 mg/kg) or saline was delivered *i.p.* for five consecutive days (starting P4 to P6). After approximately 15 minutes following injection, pups were returned to their dam. Approximately twenty-four hours following the end of the protocol, tissue harvest was performed to isolate brain slices for electrophysiology.

Whole Body Plethysmography and Oxygen Measurements

Respiration was measured daily during the ROU protocol using unrestrained flow-through whole-body plethysmography in a custom-constructed chamber (500mL) connected to a strain gauge pressure transducer (DSI, St. Paul MN). Transducer signals were amplified by a Max II amplifier (DSI, St. Paul MN) and recorded using Axoscope (Molecular Devices, San Jose CA) software. Room air (19-21% O_2, balanced N_2) continuously flowed through the system at 0.6 liters per minute. In a subset of subjects, oxygen consumption was measured concurrent with plethysmography. An oxygen sensor (LOX-O2-F: UV Flux 25% Oxygen Flow Through Sensor) (CO2Meter, Ormond Beach, FL) was connected to the outflow and continuously monitored and recorded using GasLab software (GasLab: https://gaslab.com/pages/software-downloads).

Body mass and body temperature for each subject were recorded daily during the study prior to and following fentanyl administration (**Table 1**). Room temperature, chamber temperature and body temperature were recorded each day of the ROU protocol. Barometric pressure was assessed across experimental sessions by using a website that provided the average barometric pressure (timeanddate.com) for the Hyde Park, IL for each experimental day. Baseline breathing

(10 min duration) was recorded after weight and body temperature measurements. At the end of the control period, the mouse was removed from the chamber and administered fentanyl before being promptly returned to record drug-affected breathing (15 min duration). In a subset of experiments, the ventilatory response to a change in blood gas homeostasis was assessed approximately two to three hours following fentanyl administration on Day 1 and Day 5 of ROU. Baseline breathing was initially measured in room air (5 min, FiO_2 = 21%, $FiCO_2$ = 0%, balanced N_2; 5min duration) and then switched to either a hypoxic (i.e., hypoxia, FiO_2 = 10% O_2, $FiCO_2$ = 0%, balanced N_2; 7 min duration) or a hypercapnic gas mixture (i.e., hypercapnia, FiO_2 = 21%, $FiCO_2$ = 5% CO_2, balanced N_2; 7 min duration).

# of Animals (N)	Weight (g)	Age (days)	Body Temp prior to Fentanyl (C)	Body Temp after Fentanyl (C)	Gender
27	23.786 ± 5.319	74 ± 4.526	36.1 ± 0.2	36.9 ± 0.5	M = 17 F = 10

Table 1. Animal subject information used in this study

Post hoc analysis of the plethysmography data was performed using Clampfit 11 (Molecular Devices, San Jose, CA). Respiratory rate (RR, breath•min^{-1}) was calculated by multiplying the average instantaneous frequency by 60 seconds. Tidal volume (V_T, µL•breath^{-1}) was calculated as previously described. [17]. Minute ventilation (V_e = mL•min^{-1}•kg^{-1}) was calculated as the product of tidal volume (V_T, µL*breath^{-1}) and respiratory rate (RR, breaths•min^{-1}) normalized to weight. For experiments involving fentanyl and chemoreflex measurements, breathing was sampled from 10 sec window of quiet breathing (*i.e.*, no movement was evident in the breathing signal) for each minute bin of the experiment. Apneas were assessed in a 300 sec contiguous window of quiet air breathing prior to receipt of fentanyl. An apneic event was

defined as the cessation in breathing that was equal to or greater than twice the mean period of breathing at room air.

In experiments assessing respiratory depression, breathing for the two minutes prior to fentanyl use was used as the reference for baseline ventilation. The lowest V_e measured following fentanyl administration was defined as peak OIRD. Mean inspiratory flow (MIF) was calculated by dividing V_T, by the respective time-to-peak for a given breath. Oxygen consumption (VO_2, $mL \bullet min^{-1}$) was calculated as previously described.[18]

Brain Slice Electrophysiology

Isolated rhythmic brainstem slices were prepared as described.[19] Briefly, mice were anesthetized with inhaled isoflurane and pups were subsequently euthanized by rapid decapitation. Brainstems were dissected, isolated and placed into artificial cerebrospinal fluid (aCSF) (composition in mM: 118 NaCl, 25 $NaHCO_3$, 1 NaH_2PO_4, 1 $MgCl_2$, 3 KCl, 30 Glucose, 1.5 $CaCl_2$, pH = 7.4) equilibrated with 95% O_2, 5% CO_2 at ~4°C. The brainstem was glued to an agar block (dorsal face to agar) with the rostral face upward and submerged in aCSF equilibrated with carbogen. Serial cuts were made through the brainstem until anatomical landmarks such as the narrowing of the fourth ventricle and the hypoglossal axons appeared. The preBötC was isolated in a single transverse brainstem slice (thickness: 650 μm). The slice was transferred into the recording chamber (~6 mL volume), where it was continuously perfused with recirculating aCSF (flow rate: 12–15 mL/min, ~30-34°C). Prior to recording, extracellular KCl was raised to 8 mM, and the spontaneous rhythm was allowed to stabilize before the start of every recording.

Extracellular population activity from the preBötC was recorded with glass suction pipettes filled with aCSF. The recorded signal was sampled at 5 kHz, amplified 10,000 X, with a lowpass

filter of 10 kHz using an A-M instruments (A-M Systems, Sequim, WA) extracellular amplifier. The signal was then rectified and integrated. Recordings of preBötC activity were made under baseline conditions (95% O_2 5% CO_2, 600 sec) followed the addition of the OR agonist, [D-Ala2, NMe-Phe4, Gly-ol5]-enkephalin (DAMGO) and in response to at least two escalating concentrations of DAMGO (25, 300, and 1000 nM; 600 sec per concentration tested). Recordings were stored on a computer for *posthoc* analysis. Burst detection and waveform analysis of the integrated signal from the preBötC was performed using Clampfit 11 (Molecular Devices, San Jose, CA). The mean for all metrics was taken under steady state conditions from the last 120 sec of each experimental condition. Integrated burst amplitude was expressed as a value normalized to baseline burst amplitude. The fictive inspiratory drive of a given integrated burst was determined by dividing burst amplitude by the respective time to peak.

Statistical Analysis

All statistical analyses were performed using Origin (OriginLab Corporation, Northampton, MA). **Supplementary Table 1** provides all statistical tests performed. Statistical significance was defined as p <; 0.05. Unless otherwise stated, values are reported as a mean ± SEM.

Figure	# of Animals (N)	Normality of data set?	Statistical Test	p-value
1a.	27	Yes	Linear regression; r^2= 0.7219; m = 2.65 ± 0.32	< 0.0001
1c.	27	Yes	Two-way ANOVA with means compareision (Day 1 v Day 5)	< 0.0001
1d.	27	No	Wilcoxon Signed Ranks	0.0018

Supplemental Table 1. Summary of statistical analyses in this study

2b.	*21*	*Yes*	*Two-way ANOVA with means compareision (Day 1 v Day 5)*	*<0.0001*
2c.	6	No	Two-way ANOVA with means compareision (Day 1 v Day 5)	0.6338
2d-f (adaptive).	21	Yes	Pair sample t-test (all)	V_e: <0.0001 RR: 0.035 V_T: 0.001
2d-f (non-adaptive).	6	Yes	Pair sample t-test (all)	V_e: 0.062 RR: 0.042 V_T: 0.570
3a.	7	Yes	One-way repeated ANOVA; Dunnett's pairwise comparison, Control = Day 1	V_e: 0.015 RR: 0.453 V_T: 0.011 MIF: 0.001 V_e: Day 2:1 = 1.00; Day 3:1 = 0.505; Day 4:1 = 0.896; Day 5:1 = 0.004*; Day 6:1 = 0.003* RR: Day 2:1 = 0.990; Day 3:1 = 0.895; Day 4:1 = 0.989; Day 5:1 = 0.545; Day 6:1 = 0.998 V_T: Day 2:1 = 0.984; Day 3:1 = 0.382; Day 4:1 = 0.193; Day 5:1 = 0.001*; Day 6:1 ≤ 0.001* MIF: Day 2:1 = 1.00; Day 3:1 = 0.878; Day 4:1 = 0.508; Day 5:1 ≤ 0.001*; Day 6:1 ≤ 0.001*
3b.	4	Yes	One-way repeated ANOVA; Dunnett's pairwise comparison, Control = Day 1	V_e: 1.00 RR: 0.653 V_T: 0.625 MIF:0.632 V_e: Day 2:1 = 0.978; Day 3:1 = 0.997; Day 4:1 = 0.999; Day 5:1 = 0.984; Day 6:1 = 0.999 RR: Day 2:1 = 0.963; Day 3:1 = 0.984; Day 4:1 = 0.998; Day 5:1 = 0.478; Day 6:1 = 0.718 V_T: Day 2:1 = 0.994; Day 3:1 = 1.00; Day 4:1 = 0.999; Day 5:1 = 0.997; Day 6:1 = 982 MIF: Day 2:1 = 1.00; Day 3:1 = 0.912; Day 4:1 = 0.991; Day 5:1 = 0.747; Day 6:1 = 0.924

Supplemental Table 1. Summary of statistical analyses in this study

4a. (adaptive)	*21*	*Yes*	*Pair sample t-test*	*0.12*
4a. (non-adaptive)	6	Yes	Pair sample t-test	0.021
5a.	16	No	Wilcoxon Signed Ranks	0.0016
5b.	16	No	Linear regression; Baseline Day 1: R^2 = 0.371; m = 12.692 ± 4.421 Baseline Day 5: R^2 = 0.267; m = 8.011 ± 3.544; Analysis of covariance (slopes)	0.625
5c.	16	No	Linear regression; OIRD Day 1: R^2 = 0.002; m = -0.371 ± 2.09 OIRD Day 5: R^2 = 0.202; m = 4.161 ± 2.211 Analysis of covariance (slopes)	0.140
5d.	13	No	Linear regression; OIRD Day 1: R^2 = 0.215; m = -2.381 ± 1.373 OIRD Day 5: R^2 = 0.112; m = 4.418 ± 3.754; Analysis of covariance (slopes)	0.045*
5e.	3	No	Linear regression; OIRD Day 1: R^2 = 0.721; m = 10.270 ± 6.387 OIRD Day 5: R^2 = 0.995; m = 3.585 ± 0.246; Analysis of covariance (slopes)	0.317
6b.	17	Yes	Two-way ANOVA with interactions	ROU v. Control: 0.027* [DAMGO]: < 0.001* Interaction between ROU v. Control and Doses: 0.842
6c.	17	Yes	Two-way ANOVA with interactions	ROU v. Control: < 0.001* [DAMGO]: 0.003* Interaction between ROU v. Control and Doses: <0.001*
6d.	17	Yes	Two-way ANOVA with interactions	ROU v. Control: 0.018* [DAMGO]: < 0.001* Interaction between ROU v. Control and Doses: 0.447

Supplemental Table 1. Summary of statistical analyses in this study

6e.	*17*	*Yes*	*Two-way ANOVA with interactions*	*ROU v. Control: < 0.001* [DAMGO]: 0.042* Interaction between ROU v. Control and Doses: 0.001**
6f.	17	Yes	Two-way ANOVA with interactions	ROU v. Control: < 0.001* [DAMGO]: 0.014* Interaction between ROU v. Control and Doses: 0.007*

Supplemental Table 1. Summary of statistical analyses in this study

Results

Effects of repeat opioid use (ROU) on breathing prior to fentanyl use and during Opioid-Induced Respiratory Depression (OIRD)

To determine the impact of repeat fentanyl use on breathing, we assessed quiet breathing prior to (*i.e.*, baseline) and following fentanyl administration in 27 mice on Day 1 and Day 5 of the ROU protocol. No differences were evident in comparisons of baseline tidal volume (V_T) respiratory rate (RR), or minute ventilation (V_e) (**Table 2**). As chronic opioid use has been linked to Biot's breathing and the occurrence of sleep-disordered breathing, we sought to determine whether apneic events during quiet breathing increased despite similarities in ventilatory metrics on Day 1 and Day 5 of the ROU protocol. Regression of the apnea index on Day 5 of ROU versus that on Day 1 suggests that ROU promoted an increase in apneas during air breathing (**Fig 8A**) and that persistent fentanyl use increases the occurrence of apneas. We next sought to examine how ROU impacts opioid-induced respiratory depression (OIRD). Mice naive to fentanyl (*i.e.*, Day 1) exhibited a profound OIRD (**Fig 8B, red**) that was lessened by Day 5 (**Fig 8B, blue**). On Day 1, OIRD occurred rapidly as V_e rapid decreased in the first two minutes following fentanyl administration (**Fig 8C, red**); whereas, the drop in V_e was progressively dropped and plateaued by Day 5 of ROU (**Fig 8C, blue**). Moreover, a comparison of V_e during peak OIRD on Day 1 and Day 5 (**Fig 8D**) inspection of each subject's change in

OIRD by Day 5 of ROU revealed that the impact of ROU on respiratory depression could be broadly categorized into distinct responses (**Fig 9A**). 77% (N=21/27) of mice tested showed an adaptive ventilatory response to ROU (AVR) that was characterized by a positive change in V_e during OIRD on Day 5 relative to Day 1 (**Fig 9A, purple**); whereas, the remaining 23% (N=6/27) of mice showed a non-adaptive ventilatory response to ROU (NVR) characterized by either no change in V_e at Day 5 of fentanyl exposure or an even greater respiratory depression compared to Day 1 (**Fig 9A, yellow**). By Day 5 of ROU, the magnitude of V_e during ORID was greater than that on Day 1 in mice showing the adaptive breathing response following ROU (**Fig 9B**); whereas the magnitude of Ve during OIRD was similar between Day 5 and Day 1 in mice exhibiting the non-adaptive breathing response (**Fig 9C**). Additionally, comparisons of minute ventilation during peak ORID also reveal that Ve (**Fig 9D**), respiratory rate (RR) (**Fig 9E**), and tidal volume (V_T) (**Fig 9E**) markedly improved by Day 5 in AVR mice, yet such improvements were not evident in NVR mice. Furthermore, AVR mice had a greater mean inspiratory flow (MIF) during OIRD when comparing Day 5 to Day 1 of ROU (Day 1: 28.10 ± 6.39 $\mu L \cdot msec^{-1} \cdot g^{-1}$ vs. Day 5: 44.95 ± 6.39 $\mu L \cdot msec^{-1} \cdot g^{-1}$ vs. Day 1 P=0.0317) while MIF in NVR mice were similar during OIRD on Day 1 and Day 5 (Day 1: 39.11 ± 8.25 $\mu L \cdot sec^{-1} \cdot g^{-1}$ vs Day 5: 28.75 ± 3.67 $\mu L \cdot sec^{-1} \cdot g^{-1}$; P=0.22).

Day	V_e (mL/min • g)	RR (breath/min)	V_T(µL/breath • g)	MIF (µL/sec • g)
Day 1	2.101 ± 0.404	349.1 ± 17.3	4.121 ± 0.282	157.9 ± 24.4
Day 5	1.512 ± 0.185	344.3 ± 17.7	4.631 ± 0.424	111.3 ± 11.4
p-value	0.523	0.783	0.359	0.452

Table 2. Ventilation during room air breathing

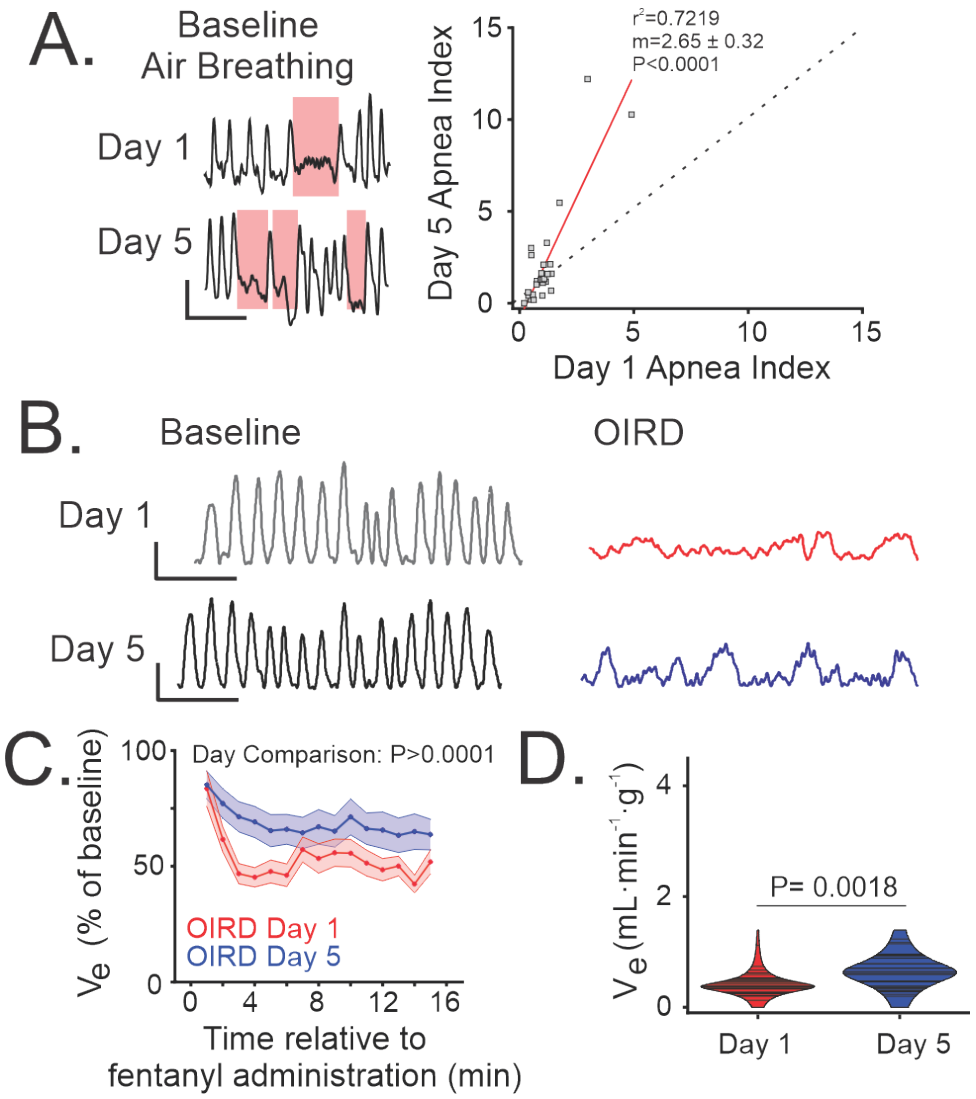

Figure 8. Breathing in response to repeated opioid use

A) (*Left*) Representative breathing trace showing the occurrence of apneas on Day 1 and Day 5 prior to fentanyl administration (*i.e.*, baseline air-breathing). Apneas (highlighted by pink boxes) are increased on Day 5. (*Right*) Linear regression of apnea index on Day 5 versus Day 1 (red line, m=2.65±0.32. Unity line (m = 1, dashed grey line) shown for comparison. Scale bars: 0.5 sec x 2 µL.

B) Representative breathing trace before fentanyl administration (Baseline, Day 1 and Day 5, grey) and during OIRD (Day 1 red, Day 5 blue). Scale bars: 0.5 sec x 2 µL.

C) Time course of V_e over time during OIRD Day 1 (red) and Day 5 (blue); (n=27).

D) Comparison of V_e during OIRD on Day 1 (red) and Day 5 (blue). (n=27).

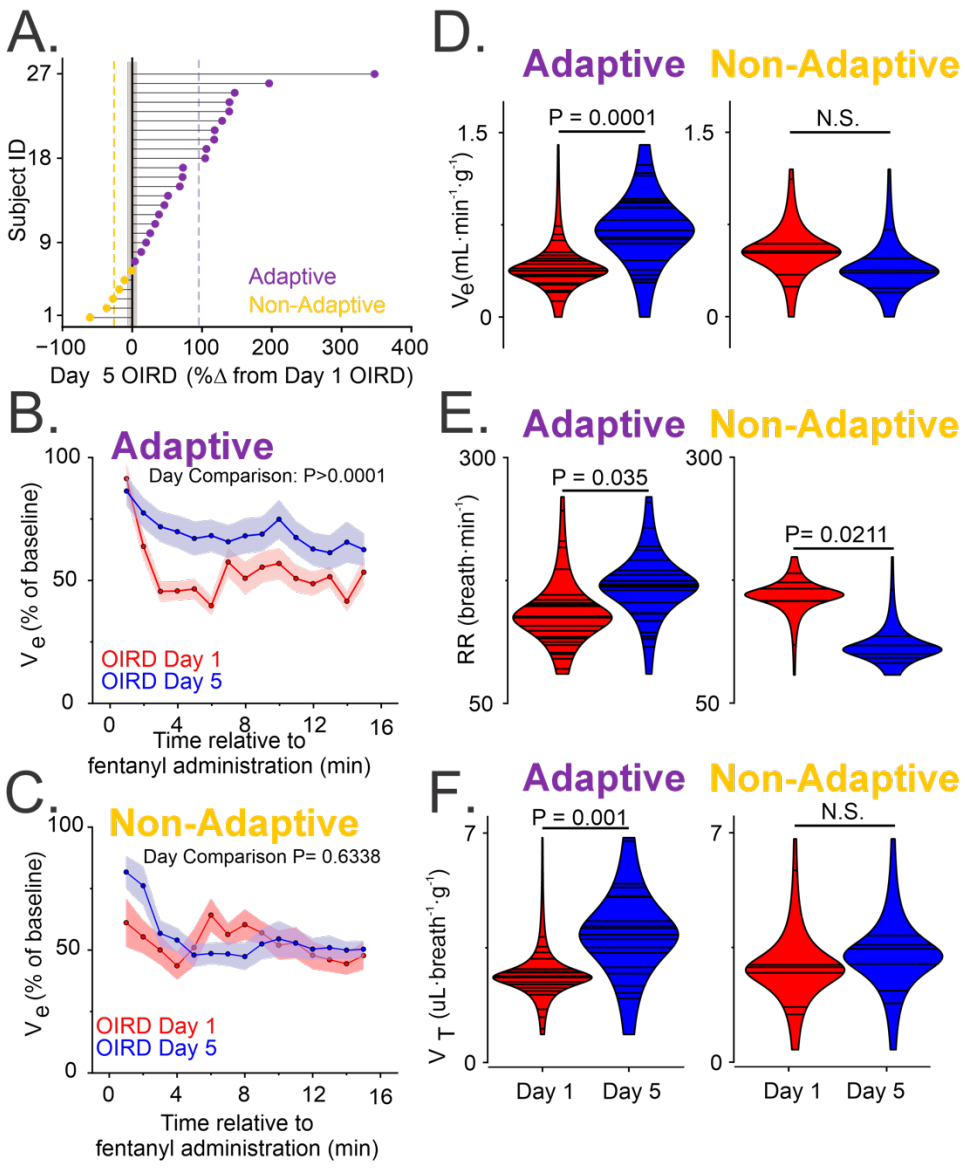

Figure 9. Examining individual Ve reveals divergent responses to ROU

A) The individual percentage change in V_e on Day 5 relative to Day 1 (N=27). Two breathing responses are evident: (1) the adaptive response (purple, N=21/27) where the change in V_e between Day 1 and Day 5 of ROU is greater than 0%; and (2) the non-adaptive response (yellow, N=6/27) where is V_e less than 0%. Dashed vertical lines indicate the mean adaptive (mean=95.1%; purple) and mean non-adaptive (mean=-26.3%; yellow) change in V_e relative to Day 1. For reference, grey box represents the standard deviation (±2.75%) for the change in V_e of saline control animals (N=10) measured on Day 5 relative to Day 1 of saline injections (mean ± S.E.M.: 0.772 ± 0.87) B. Time course of mean V_e during OIRD for adaptive (purple) and non-adaptive response (yellow) on Day 1.

C) Time course of mean V_e during OIRD for adaptive (purple) and non-adaptive response (yellow) on Day 5.
D) Comparison of mean V_e during ORID on Day 1 (red) and Day 5 (blue) in adaptive (left) and non-adaptive (right) individuals.
E) Comparison of mean RR during ORID on Day 1 and Day 5 in adaptive (left) and non-adaptive (right) individuals.
F) Comparison of mean V_T during ORID on Day 1 and Day 5 in adaptive (left) and non-adaptive (right) individuals. N.S.: Not significant ($P>0.05$).

Longitudinal effects of ROU during respiratory depression

In a subset of individuals (N=11), we extended the ROU protocol from five to six days. In these subjects, breathing on each day of the ROU protocol was measured to characterize how it changes daily, before and during OIRD. Mice with the adaptive ventilatory response to ROU (N=7/11) show improvement in V_e (**Fig 10A**), RR (**Fig 10B**), V_T (**Fig 10C**) and MIF (**Fig 10D**) during OIRD through Day 6 of the protocol. In contrast, mice with the non-adaptive response to ROU (N=4/11) do not show consistent improvement in V_e (**Fig 10E**), RR (**Fig 10F**), V_T (**Fig 10G**), or MIF (**Fig 10H**) during OIRD over the course of ROU.

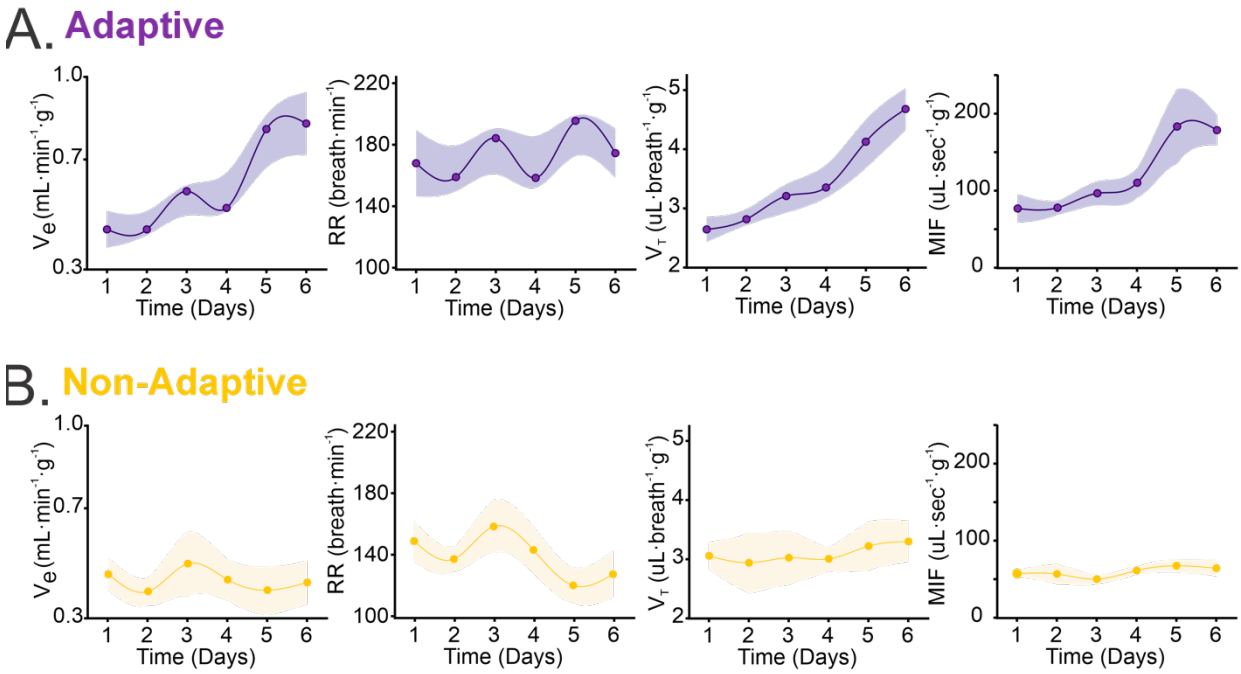

Figure 10. Longitudinal tracking ventilatory metrics during ORID in adaptive and non-adaptive subjects

A) Ve, RR, V_T, and MIF during OIRD over the course of six days of fentanyl administration in mice showing the adaptive response to ROU by Day 5 (N=7/11).
B) Ve, RR, V_T, and MIF during OIRD over the course of six days of fentanyl administration in mice showing the adaptive response to ROU by Day 5 (N=4/11). Values are reported as mean ± S.E.M.

The increased occurrence of apneas is observed in mice with a Non-Adaptive Ventilatory Response

The dichotomy in breathing patterns by Day 5 of ROU did not appear limited to OIRD. While the apnea index during quiet breathing on Day 1 to Day 5 of ROU was not different among the mice with the adaptive breathing response to ROU, the apnea index was larger on Day 5 of ROU in the mice with the non-adaptive breathing response (**Fig 11A**). The apnea index also did not increase over the course of ROU among mice showing the adaptive breathing

response to ROU (**Fig 11B**). However, among mice showing the non-adaptive response to ROU, the apnea index progressively increased over the course of ROU (**Fig 11C**).

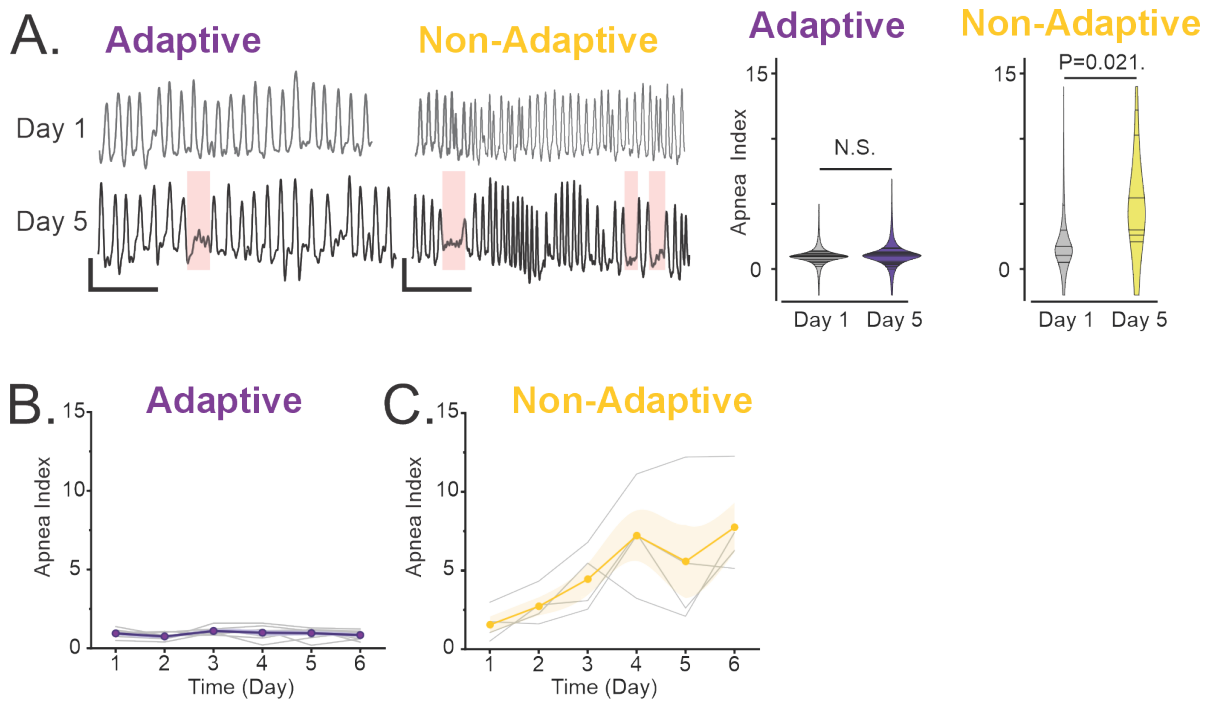

Figure 11. Development of apneas following ROU

A) (*Left*) Representative traces during room-air breathing on Day 1 and Day 5 in an individual from the adaptive response group (purple) and the non-adaptive response group (yellow). Apneas are highlighted by pink boxes. Scale bars: 0.5 sec x 2 µL. (*Right*) Mean apnea index of adaptive animals (N = 21/27; purple) and non-adaptive animals (N= 6/27; yellow) on Day 1 and Day 5.

B) Longitudinal tracking of apnea index during air breathing over the course of ROU in subjects showing the adaptive breathing response (subjects from Figure 3A; N = 7/11). Individual responses in grey, and mean response in purple.

C) Longitudinal tracking of apnea index during air breathing over the course of ROU in subjects showing the non-adaptive breathing response (subjects from Figure 3B; N = 4/11). Individual responses in grey, and mean response in yellow.

The relationship between breathing and O_2 consumption during respiratory depression

Emerging evidence suggest that the state of oxygenation during OIRD influences survival outcomes during fentanyl overdose. [20,21] Therefore, we next set out to determine how ROU

impacts VO_2 and its relationship to breathing. VO_2 was simultaneously assessed with breathing on Day 1 and Day 5 of ROU (N=16). Prior to fentanyl administration, VO_2 was similar on both Day 1 and Day 5 (Day 1: 0.14 vs. Day 5: 0.14, P=0.61). However, ROU led to improved O_2 metabolism during ORID as the change in VO_2 in response to fentanyl was greater on Day 1 relative to Day 5 (**Fig 12A**).

Consistent with previous observations V_e and O_2 metabolism (V_e:VO_2),[22] positive correlations between V_e and VO_2 on were evident Day 1 (r^2 =0.371, m=12.692) and Day 5 (r^2 =0.2670, m=8.011) before fentanyl administration (**Fig 12B**). However, during OIRD on Day 1, the V_e:VO_2 relationship was negative (**Fig 12C** red; r^2 =0.0022, m=-0.3711) indicating an inability for ventilation to adequately support metabolic demand when under the influence of fentanyl. While the relationship between ventilation and O_2 metabolism was still markedly depressed during OIRD on Day 5, the suppressive action of fentanyl on the relationship of V_e:VO_2 appeared to diminish with ROU as the relationship returned to a positive slope (**Fig 12C** blue; r^2=0.2019, m=4.161). The majority of subjects (N=13/16) where VO_2 and breathing were measured showed the adaptive breathing response. The V_e:VO_2 relationship among this group was similar to that observed across the entire population, where the relationship on Day 1 was initially negative during OIRD (**Fig 12D** red; r^2 =0.2146, m=-2.381) and later, on Day 5, appeared to normalize toward a positive correlation during OIRD (**Fig 12D** blue, r^2 =0.1118, m=4.418). In contrast, in non-adaptive subjects, the V_e:VO_2 relationship during OIRD was positive on Day 1 (**Fig 12E** red; r^2 =0.7209, m=10.27) and while still positive on Day 5 (**Fig 12E** blue; r^2 =0.9953, m=3.585) the slope of the correlation appeared to flatten toward a zero.

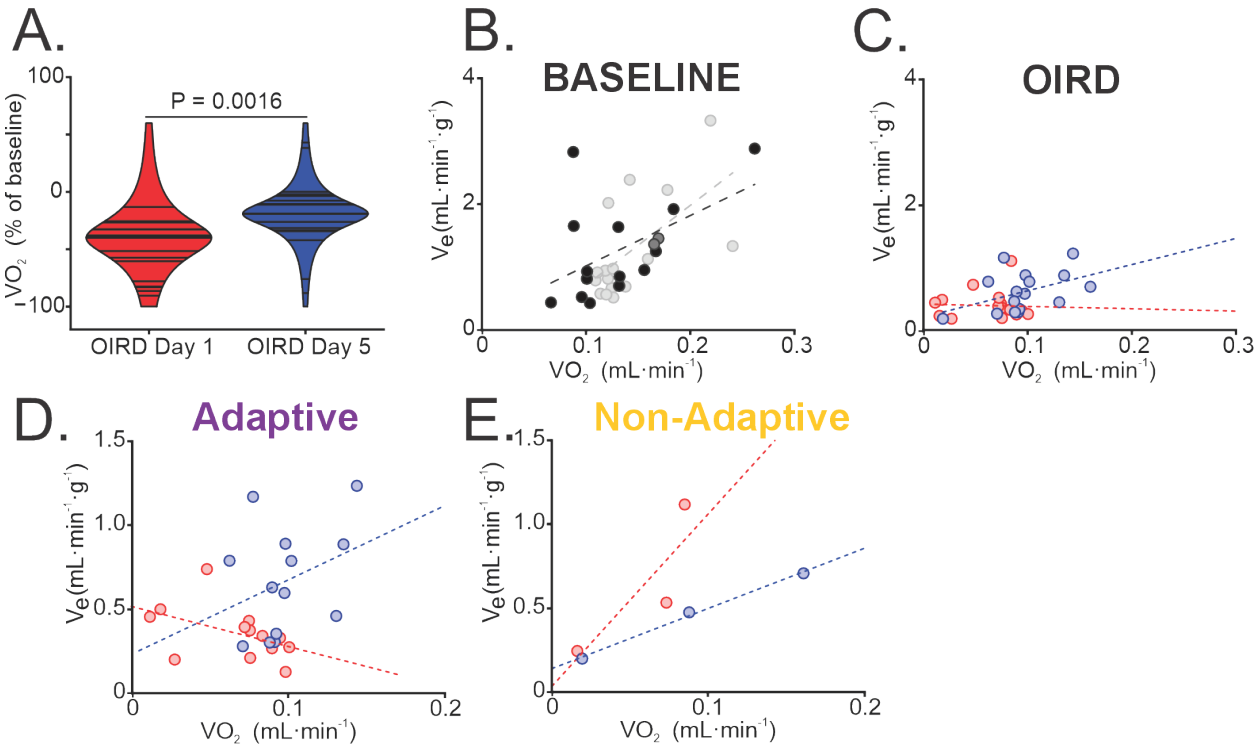

Figure 12. O2 consumption (VO2) and its relationship to breathing changes following ROU

A) VO_2 during OIRD on Day 1 and Day 5 expressed as a percentage of baseline (N=16). While baseline absolute VO_2 was similar between Day 1 and Day 5 (P=0.61, *data not shown*), absolute VO_2 during OIRD was greater on Day 5 (P=0.046, *data not shown*).

B) Comparison of the baseline V_e to VO_2 relationship on Day 1 (grey; Day 1: $r^2 = 0.371$; m = 12.692 ± 4.421) and Day 5 (black; Day 5: $r^2 = 0.267$; m = 8.011 ± 3.544) of ROU.

C) Comparison of the V_e to VO_2 relationship during OIRD on Day 1 (red; Day 1: $r^2 = 0.002$; m = -0.371 ± 2.090) and Day 5 (blue; Day 5: $r^2 = 0.202$; m = ±) of ROU.

D) Comparison of the baseline V_e to VO_2 relationship during OIRD on Day 1 (red; Day 1: $r^2 = 0.215$; m = -2.381 ± 1.373) and Day 5 (blue; Day 5: $r^2 = 0.112$; m = 4.418 ± 3.754) in subjects showing the adaptive response to ROU (N = 13).

E) Comparison of the baseline V_e to VO_2 relationship during OIRD on Day 1 (red; Day 1: $r^2 = 0.721$; m = 10.270 ± 6.387) and Day 5 (blue; Day 5: $r^2 = 0.995$; m = 3.585 ± 0.246) in subjects showing the non-adaptive response to ROU (N=3).

Ventilatory reflexes to hypercapnia and hypoxia are unchanged by ROU

Given the changes in V_e:VO_2 relationship, we next sought to determine how ROU impacts ventilatory responses to hypoxia or hypercapnia on the last day of habituation and on Day 1 and Day 5 of ROU. When compared to the respective measurements made during

habituation, neither the hypoxic ventilatory response (**Table 3)** nor hypercapnic ventilatory response (**Table 4**) were changed following ROU.

	# of Animals (N)	Minute Ventilation (mL/min/g)	Respiratory Rate (Breaths/min)	Tidal Volume (µL/breath/g)	Mean Inspiratory Flow (µL/sec/g)
Day 1 Baseline	10	1.535 ± 0.053	388.34 ± 21.36	3.481 ± 0.376	174.22 ± 30.85
Day 5 Baseline	10	1.554 ± 0.117	393.23 ± 15.24	3.586 ± 0.146	173.21 ± 20.17
p-value[1]	__	0.901	0.718	1.00	0.980
Day 1 HVR	10	1.529 ± 0.081	438.99 ± 36.42	3.411 ± 0.351	164.68 ± 22.44
Day 5 HVR	10	1.613 + 0.065	427.81 ± 22.64	3.924 ± 0.172	184.74 ± 19.34
p-value[2]	__	0.457	0.830	0.109	0.549

Table 3. Respiratory metrics during hypoxic ventilatory response before and after ROU

[1]Comparison of Day 1 vs Day 5 in baseline breathing; [2]Comparison of Day 1 vs Day 5 in HVR.

	# of Animals (N)	Minute Ventilation (mL/min/g)	Respiratory Rate (Breaths/min)	Tidal Volume (µL/breath/g)	Mean Inspiratory Flow (µL/sec/g)
Day 1 Baseline	12	1.372 ± 0.099	191.96 ± 11.88	4.369 ± 0.363	150.72 ± 17.05
Day 5 Baseline	12	1.225 ± 0.127	173.39 ± 12.33	4.025 ± 0.289	146.82 ± 15.62
p-value[1]	__	0.387	0.203	0.370	0.388
Day 1 HCVR	12	1.271 ± 0.069	195.65 ± 13.34	4.899 ± 0.712	168.25 ± 12.36
Day 5 HCVR	12	0.956 + 0.078	190.65 ± 13.90	4.291 ± 0.325	163.75 ± 17.99
p-value[2]	__	0.146	0.821	0.403	0.774

Table 4. Hypercapnic ventilatory response before and after ROU

[1]Comparison of Day 1 vs Day 5 in baseline breathing; [2]Comparison of Day 1 vs Day 5 in HCVR.

ROU desensitizes inspiratory rhythmogenesis to - μ-opioid receptor-dependent neuromodulation

We next sought to determine whether changes in response to ROU could involve alterations from within the preBötzinger Complex (preBötC) inspiratory neural network. To assess this, a series of electrophysiological recordings were performed from the rhythmic preBötC network isolated in brain slices from mice naive to fentanyl use (*i.e.*, control) and mice that underwent repeat fentanyl use (*i.e.*, ROU-treated). Rhythmogenesis from the preBötC of control (N=10) and ROU-treated slices (N=8) were similar (**Fig 13A**) as evidenced by similarities in frequency (control: 0.20 ± 0.03 Hz vs. ROU: 0.26 ± 0.05 Hz; P=0.33), irregularity score of period (control: 0.46 ± 0.08 Hz vs. ROU: 0.55 ± 0.15 Hz; P=0.89) and irregularity score of amplitude (control: 0.20 ± 0.03 Hz vs. ROU: 0.20 ± 0.03; P=0.69). We next compared the dose-response of preBötC activity to μ-OR agonism, using DAMGO (25 to 1000nM, **Fig 6A**). While increasing the concentration of DAMGO in control (**Fig 13B**, grey) and ROU-treated (**Fig 13A,** red) networks suppressed the preBötC activity, a rightward shift in the dose-response curve of the network burst instantaneous frequency was evident in networks that experienced ROU (**Fig 13D**). Additionally, in slices from control mice, both preBötC burst amplitude (**Fig 13E**, grey) and fictive inspiratory drive (**Fig 13F**, grey) diminished with increasing concentrations of DAMGO. However, in the preBötC from ROU treated mice, network burst amplitude (**Fig 13F**, red) and fictive inspiratory drive (**Fig 13F**, grey) were largely insensitive to increasing concentrations of DAMGO.

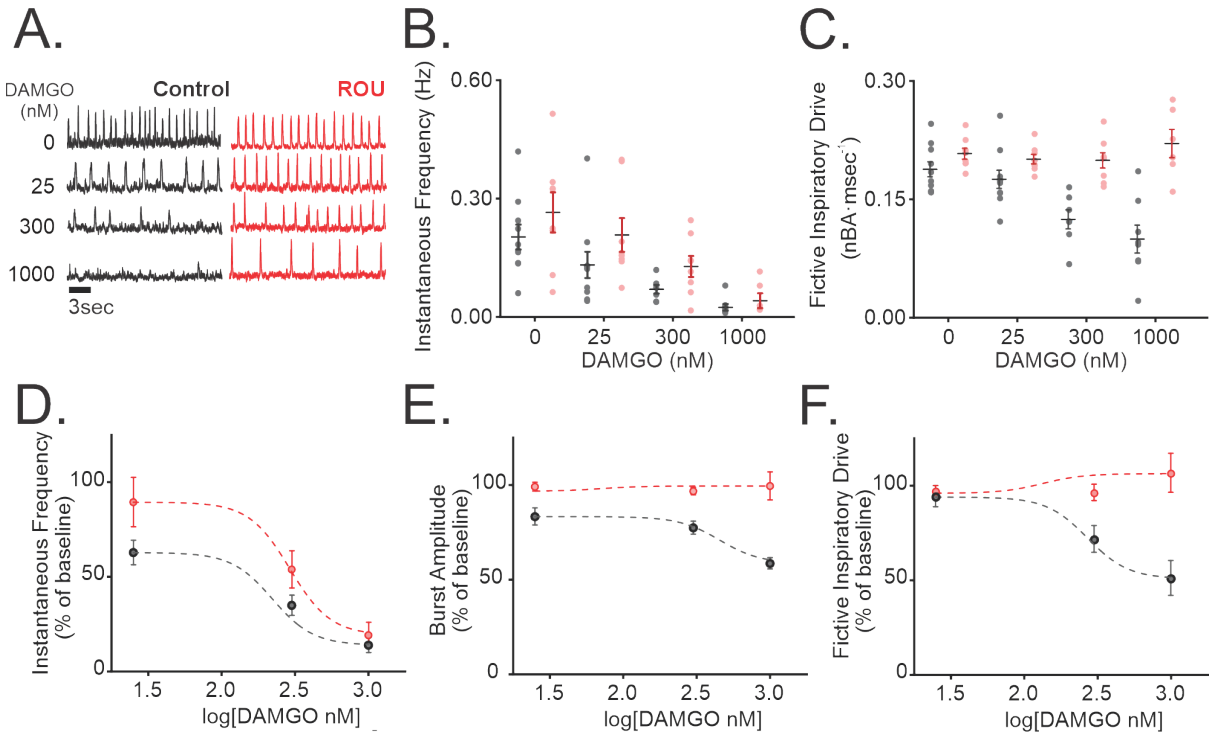

Figure 13. The efficacy of opioid neuromodulation in the in vitro preBötC is reduced following ROU

A) Representative integrated traces from preBötC recordings in response to increasing levels of DAMGO (0 to 1000 uM) in rhythmic slices from control mice (left, black) and mice that underwent ROU (right, red).
B) Comparison of instantaneous frequency of rhythmogenesis in the preBötC between control and ROU.
C) Comparison of fictive inspiratory drive in the preBötC between control and ROU. Fictive inspiratory drive was defined at the normalized Burst amplitude of the preBötC (nBA) divided by time to peak (in msec).
D) Comparison of control and ROU dose response curves of instantaneous frequency.
E) Comparison of control and ROU dose response curves of burst amplitude.
F) Comparison of control and ROU dose response curves of fictive inspiratory drive. Values used in D to E were normalized to baseline values of each respective metric (*i.e.*, 0 nM DAMGO).

Discussion

Repeated fentanyl administration, linked with opioid use disorder, is a recognized risk factor driving fatal opioid overdose.[6,23,24] In this mouse model of ROU, we demonstrate that fentanyl induced respiratory coincides with profound metabolic distress when naïve to fentanyl

use. Following repeated fentanyl use, breathing and its relationship to metabolism during respiratory depression was improved. These changes following ROU coincided with increased inspiratory drive during respiratory depression, and at the level of the preBötC, the sensitivity to opioid neuromodulation was reduced following ROU. Importantly, the adaptive ventilatory response during OIRD was not evident in all subjects—emphasizing the complexity of developing opioid tolerance and its variable impact on respiratory function. These divergent outcomes challenge the notion of uniform outcomes with repeat opioid use. Moreover, our study results also emphasize the importance of repeated opioid use as a factor influencing breathing outcomes and its relationship to metabolism in response to fentanyl exposure. Understanding such underlying factors that cause differences in OIRD following could lead to more effective interventions in opioid use disorder and its treatment.

While fentanyl suppressed breathing both when mice were naïve to fentanyl administration (*i.e.*, Day 1 of ROU) and were experienced with fentanyl administration (*i.e.*, by Day 5 of ROU), the magnitude of respiratory depression was smaller on by Day 5 of when compared to Day 1. The improved ventilation during OIRD after ROU aligns with the definition of respiratory tolerance to opioids previously documented in juvenile and adult rats following repeat fentanyl administration.[25] Our findings also corroborate clinical observations indicating that tolerance to fentanyl-induced respiratory occurs with chronic opioid use[26] while also demonstrating that OIRD tolerance manifests as an integrated response to include changes in metabolism and neuronal activity.

Systemic hypoxia is an expected outcome of opioid overdose and a well-documented phenomenon.[20,27-32] Across species, hypoxic challenges (FiO_2=10%) cause a leftward shift the normally positive relationship between breathing to oxygen metabolism, that is attributed to a

combination of hyperventilation and a reduction of metabolic rate.[33] Our results indicate that fentanyl suppresses the VO_2 to breathing relationship independent of familiarity of use, which emphasizes the potent nature of this opioid to produce conditions where physiological changes in response to repeat use cannot prevent the metabolic distress produced during fentanyl-induced respiratory depression. However, the conversion from a negative to positive V_e to VO_2 relationship following ROU suggests the trajectory of metabolic crisis is altered with experience to repeat fentanyl exposure. As the interaction between fentanyl and hypoxia appears to uniquely affect the susceptibility to opioid-dependent mortality when compared to morphine[20], the improved V_e to VO_2 relationship appears to be an important physiological adaptation that emerges with repeated fentanyl exposure to increase the latency of fentanyl-mediated cardiorespiratory collapse subsequent to respiratory depression.

At the level of the individual, differences between the VO_2 to Ve relationship were evident among mice showing the adaptive and non-adaptive responses. Mice showing the non-adaptive response do not exhibit improved oxygen metabolism during OIRD. Interestingly, among mice with AVR in response to ROU, improved minute ventilation is not necessary for an improved VO_2 to breathing relationship during OIRD among all individuals suggesting that repeat fentanyl exposure drives a constellation of changes in the body beyond breathing. At the systems level, fentanyl-induced muscle rigidity, such as that observed with wooden chest syndrome, has been proposed to produce a hypermetabolic state that promotes the metabolic distress experienced during fentanyl-induced respiratory depression [27 28]. Furthermore, in other cell types of the body, fentanyl has been to shown suppress mitochondrial activity.[34 35 36 37] These opposing actions of fentanyl on metabolism in different systems of the body likely work synergistically to augment the metabolic distress experienced during OIRD when naïve to

fentanyl. Furthermore, compensation to one or both phenomena could occur with ROU and may contribute to the emergence of the adaptive response; whereas failed compensation could contribute to non-adaptive response. These possibilities remain to be investigated and resolved.

With respect to improved breathing, the adaptive response following ROU exhibited an enhancement in inspiratory flow during OIRD. This was not observed among individuals showing the non-adaptive response. Importantly, prior to fentanyl administration (i.e., baseline), no differences in inspiratory flow were detected when comparing adaptive and non-adaptive responders. Furthermore, both the ventilatory hypercapnic chemoreflex and ventilatory hypoxic chemoreflex appeared to be unchanged by ROU. Thus, improved inspiratory flow during OIRD appeared to be a unique response to fentanyl-mediated modulation of breathing rather than related to either a generalized enhancement of inspiratory flow or augmented ventilatory chemoreflexes by ROU.

Analgesic and euphoric tolerance is known to occur with opioid use emerges and stems from genetic, biochemical and neurophysiological changes throughout the brain[38]. Our in vitro brain slice experiments in the preBötC also supports the view that tolerance to opioid-dependent modulation of breathing involves changes in central inspiratory drive. While baseline rhythms from the preBötC were similar between control slices and slices from mice that experienced ROU, the preBötC rhythm was less sensitive to μ-OR based neuromodulation in slices from mice that experienced ROU when compared to control. Reduced sensitivity to μ-OR agonism was prominent in the dose-response of the preBötC network burst amplitude, fictive inspiratory drive and to a lesser degree, instantaneous frequency of the network rhythm. Independent of ROU, the synaptic and intrinsic properties of the preBötC have been shown to be important determinants dictating dynamics and stability in response to μ-OR agonism within the network.[39,40]

Furthermore, genetic elimination of μ-ORs in the preBötC can minimize OIRD[41,42], and our *in vitro* observations support the concept that changes in the preBötC contribute to enhancing inspiratory drive during OIRD after ROU.

While we show that ROU leads to changes in rhythmogenesis from within the preBötC that are consistent with the emergence of respiratory tolerance to OIRD and the adaptive response to ROU, other respiratory networks known to contribute to inspiratory drive and OIRD[43] may also contribute to these phenomena. For example, chronic morphine administration can lead to desensitization in potassium currents activated by μ-OR agonism within neurons of the Kölliker Fuse nucleus[44]. It will be important to further resolve how ROU impacts the properties of the inspiratory network and determine the impact of ROU-mediated changes throughout the respiratory network.

The assessment of the impact of ROU on breathing using whole-body plethysmography was not without its recognized limitations. Notably, the barometric approach to determine V_T and metrics derived from V_T can be confounded in conditions characterized by high flow resistance, resulting in an overestimation of tidal volume[17 45]. As fentanyl can increase airway resistance[27], our calculations of V_e and inspiratory flow could be overestimated during increased airway rigidity. To more effectively assess V_T would require independent measurement of the cycle timing by measuring diaphragmatic activity and or breathing mechanics. Such measurements would require invasive instrumentation and the use of anesthesia. In rats naive to fentanyl use, sedation has been shown to prevent the spontaneous recovery of inspiratory activity during fentanyl-dependent respiratory depression[27]. We sought to avoid potential confounds such as that related to anesthetic use, given the paucity of understanding related to repeat fentanyl use on breathing. Additionally, both our measurements of VO_2 and our

electrophysiological experiments support that ventilation and inspiratory drive are improved with ROU.

In conclusion, our study determined that prolonged, repeated exposure to fentanyl drives a respiratory adaptation that minimizes OIRD. This is, however, subject-dependent as a majority of animals exhibited a respiratory adaptation, while a minority of them did not. Complicating this is the respiration-O_2 metabolism relationship in non-adaptive animals where improvements in V_e and/or V_T are minimal, but O_2 metabolism as a function of Ve is preserved. In adaptive animals, the effect of ROU on improved breathing during OIRD may be attributed to the effect of ROU on inspiratory drive in the whole-animal and at the level of the preBötC. This study offers crucial insights into the varied respiratory adaptations resulting from ROU, with significant implications. Identifying both adaptive and non-adaptive responses not only deepens our foundational understanding into ORID but also opens new avenues for targeted strategies to minimize or mitigate opioid related overdose. Future studies will be essential for exploring how our results may be further advanced and leveraged to reduced mortalities associated with chronic opioid use.

References

1. Dahan, A., Overdyk, F., Smith, T., Aarts, L. & Niesters, M. Pharmacovigilance: a review of opioid-induced respiratory depression in chronic pain patients. *Pain Physician* **16**, E85-94 (2013).
2. Hoffman, J. R., Schriger, D. L. & Luo, J. S. The empiric use of naloxone in patients with altered mental status: a reappraisal. *Ann Emerg Med* **20**, 246-252 (1991).
3. Darke, S. & Zador, D. Fatal heroin 'overdose': a review. *Addiction* **91**, 1765-1772 (1996).
4. Montandon, G. *et al.* PreBotzinger complex neurokinin-1 receptor-expressing neurons mediate opioid-induced respiratory depression. *J Neurosci* **31**, 1292-1301 (2011).
5. Montandon, G. & Horner, R. CrossTalk proposal: The preBotzinger complex is essential for the respiratory depression following systemic administration of opioid analgesics. *J Physiol* **592**, 1159-1162 (2014).

6. Webster, L. R. Risk Factors for Opioid-Use Disorder and Overdose. *Anesth Analg* **125**, 1741-1748 (2017).
7. Park, T. W. *et al.* Understanding Risk Factors for Opioid Overdose in Clinical Populations to Inform Treatment and Policy. *J Addict Med* **10**, 369-381 (2016).
8. Mercadante, S., Arcuri, E. & Santoni, A. Opioid-Induced Tolerance and Hyperalgesia. *CNS Drugs* **33**, 943-955 (2019).
9. Mercadante, S. & Portenoy, R. K. Opioid poorly-responsive cancer pain. Part 2: basic mechanisms that could shift dose response for analgesia. *J Pain Symptom Manage* **21**, 255-264 (2001).
10. Cahill, C. M., Walwyn, W., Taylor, A. M. W., Pradhan, A. A. A. & Evans, C. J. Allostatic Mechanisms of Opioid Tolerance Beyond Desensitization and Downregulation. *Trends Pharmacol Sci* **37**, 963-976 (2016).
11. Ramirez, J. M. *et al.* Central and peripheral factors contributing to obstructive sleep apneas. *Respir Physiol Neurobiol* **189**, 344-353 (2013).
12. Freire, C., Sennes, L. U. & Polotsky, V. Y. Opioids and obstructive sleep apnea. *J Clin Sleep Med* **18**, 647-652 (2022).
13. Walker, J. M. *et al.* Chronic opioid use is a risk factor for the development of central sleep apnea and ataxic breathing. *J Clin Sleep Med* **3**, 455-461 (2007).
14. Paronis, C. A. & Woods, J. H. Ventilation in morphine-maintained rhesus monkeys. II: Tolerance to the antinociceptive but not the ventilatory effects of morphine. *J Pharmacol Exp Ther* **282**, 355-362 (1997).
15. Athanasos, P. *et al.* Methadone maintenance patients are cross-tolerant to the antinociceptive effects of very high plasma morphine concentrations. *Pain* **120**, 267-275 (2006).
16. Hill, R. *et al.* Ethanol Reversal of Tolerance to the Respiratory Depressant Effects of Morphine. *Neuropsychopharmacology* **41**, 762-773 (2016).
17. Lim, R. *et al.* Measuring respiratory function in mice using unrestrained whole-body plethysmography. *J Vis Exp*, e51755 (2014).
18. Mortola, J. P., Rezzonico, R. & Lanthier, C. Ventilation and oxygen consumption during acute hypoxia in newborn mammals: a comparative analysis. *Respir Physiol* **78**, 31-43 (1989).
19. Garcia, A. J., 3rd *et al.* Chronic Intermittent Hypoxia Alters Local Respiratory Circuit Function at the Level of the preBotzinger Complex. *Front Neurosci* **10**, 4 (2016).
20. Burgraff, N. J., Baertsch, N. A. & Ramirez, J. M. A comparative examination of morphine and fentanyl: unravelling the differential impacts on breathing and airway stability. *J Physiol* **601**, 4625-4642 (2023).
21. Haouzi, P. *et al.* Severe Hypoxemia Prevents Spontaneous and Naloxone-induced Breathing Recovery after Fentanyl Overdose in Awake and Sedated Rats. *Anesthesiology* **132**, 1138-1150 (2020).
22. Meyer, L. C., Hetem, R. S., Mitchell, D. & Fuller, A. Hypoxia following etorphine administration in goats (Capra hircus) results more from pulmonary hypertension than from hypoventilation. *BMC Vet Res* **11**, 18 (2015).
23. Kaye, A. D. *et al.* Prescription Opioid Abuse in Chronic Pain: An Updated Review of Opioid Abuse Predictors and Strategies to Curb Opioid Abuse: Part 1. *Pain Physician* **20**, S93-S109 (2017).

24. Springer, S. A., Korthuis, P. T. & Del Rio, C. Integrating Treatment at the Intersection of Opioid Use Disorder and Infectious Disease Epidemics in Medical Settings: A Call for Action After a National Academies of Sciences, Engineering, and Medicine Workshop. *Ann Intern Med* **169**, 335-336 (2018).
25. Laferriere, A., Colin-Durand, J. & Moss, I. R. Ontogeny of respiratory sensitivity and tolerance to the mu-opioid agonist fentanyl in rat. *Brain Res Dev Brain Res* **156**, 210-217 (2005).
26. Algera, M. H. *et al.* Tolerance to Opioid-Induced Respiratory Depression in Chronic High-Dose Opioid Users: A Model-Based Comparison With Opioid-Naive Individuals. *Clin Pharmacol Ther* **109**, 637-645 (2021).
27. Haouzi, P. & Tubbs, N. Effects of fentanyl overdose-induced muscle rigidity and dexmedetomidine on respiratory mechanics and pulmonary gas exchange in sedated rats. *J Appl Physiol (1985)* **132**, 1407-1422 (2022).
28. Neumueller, S. E. *et al.* Effects of sub-lethal doses of fentanyl on vital physiologic functions and withdrawal-like behaviors in adult goats. *Front Physiol* **14**, 1277601 (2023).
29. Baud, F. J. [Mechanisms of opioid-induced overdose: experimental approach to clinical concerns]. *Ann Pharm Fr* **67**, 353-359 (2009).
30. Kiyatkin, E. A. Respiratory depression and brain hypoxia induced by opioid drugs: Morphine, oxycodone, heroin, and fentanyl. *Neuropharmacology* **151**, 219-226 (2019).
31. Solis, E., Jr., Cameron-Burr, K. T. & Kiyatkin, E. A. Rapid Physiological Fluctuations in Nucleus Accumbens Oxygen Levels Induced by Arousing Stimuli: Relationships with Changes in Brain Glucose and Metabolic Neural Activation. *Front Integr Neurosci* **11**, 9 (2017).
32. Solis, E., Jr., Cameron-Burr, K. T., Shaham, Y. & Kiyatkin, E. A. Fentanyl-Induced Brain Hypoxia Triggers Brain Hyperglycemia and Biphasic Changes in Brain Temperature. *Neuropsychopharmacology* **43**, 810-819 (2018).
33. Frappell, P., Lanthier, C., Baudinette, R. V. & Mortola, J. P. Metabolism and ventilation in acute hypoxia: a comparative analysis in small mammalian species. *Am J Physiol* **262**, R1040-1046 (1992).
34. Kirshner, B., Gold, M. & Zimmerman, B. Comparison between the prevalence and treatment of wheezing and coughing in Brampton and Mississauga children. *J Clin Epidemiol* **43**, 765-771 (1990).
35. Djafarzadeh, S., Vuda, M., Jeger, V., Takala, J. & Jakob, S. M. The Effects of Fentanyl on Hepatic Mitochondrial Function. *Anesth Analg* **123**, 311-325 (2016).
36. Zamparelli, M. *et al.* Analgesic doses of fentanyl impair oxidative metabolism of neonatal hepatocytes. *J Pediatr Surg* **34**, 260-263 (1999).
37. Vilela, S. M. *et al.* Are fentanyl and remifentanil safe opioids for rat brain mitochondrial bioenergetics? *Mitochondrion* **9**, 247-253 (2009).
38. Volkow, N. D. & Morales, M. The Brain on Drugs: From Reward to Addiction. *Cell* **162**, 712-725 (2015).
39. Baertsch, N. A., Bush, N. E., Burgraff, N. J. & Ramirez, J. M. Dual mechanisms of opioid-induced respiratory depression in the inspiratory rhythm-generating network. *Elife* **10** (2021).

40. Chou, G. M., Bush, N. E., Phillips, R. S., Baertsch, N. A. & Harris, K. D. Modeling Effects of Variable preBotzinger Complex Network Topology and Cellular Properties on Opioid-Induced Respiratory Depression and Recovery. *eNeuro* **11** (2024).
41. Varga, A. G., Reid, B. T., Kieffer, B. L. & Levitt, E. S. Differential impact of two critical respiratory centres in opioid-induced respiratory depression in awake mice. *J Physiol* **598**, 189-205 (2020).
42. Bachmutsky, I., Wei, X. P., Kish, E. & Yackle, K. Opioids depress breathing through two small brainstem sites. *Elife* **9** (2020).
43. Stucke, A. G., Levitt, E. S. & Montandon, G. Editorial: Opioid-induced respiratory depression: neural circuits and cellular pathways. *Front Physiol* **14**, 1348910 (2023).
44. Levitt, E. S. & Williams, J. T. Desensitization and Tolerance of Mu Opioid Receptors on Pontine Kolliker-Fuse Neurons. *Mol Pharmacol* **93**, 8-13 (2018).
45. Mortola, J. P. & Frappell, P. B. On the barometric method for measurements of ventilation, and its use in small animals. *Can J Physiol Pharmacol* **76**, 937-944 (1998).

Chapter 2

Introduction

Our findings in Chapter 1 reveal that contrary to previously believed, Repeat Opioid Use (ROU) does alter susceptibility to Opioid-Induced Respiratory Depression (OIRD). In the majority of subjects, we found that five days of repeat fentanyl administration resulted in a progressive decline in the effect of fentanyl to suppress breathing. This suggests that with five days of ROU, subjects develop tolerance to OIRD. We demonstrate that the development of tolerance to OIRD is due in part to reduced opioid neuromodulation at the level of the preBötC. The decreased effectiveness of the selective μ-opioid receptor agonist [D-Ala2, NMe-Phe4, Gly-ol5]-enkephalin (DAMGO) to suppress rhythmic activity in the preBötC of mice exposed to ROU suggests that this is likely due to changes in μ-opioid receptor expression or sensitivity. While these findings phenotype the development of tolerance to OIRD and begin to elucidate the central mechanisms that support it, they do not answer how susceptibility to OIRD and opioid overdose changes despite ROU, as Shepard Siegel demonstrated with The Heroin Overdose Mystery.

In The Heroin Overdose Mystery, Shepard Siegel demonstrated that opioid overdose susceptibility was altered depending on the environmental context of drug administration. This indicates that there are mechanisms of tolerance that develop with ROU that involve higher-order circuit-level adaptations to combat opioid overdose susceptibility. Chapter 2 will investigate the role of the Locus Coeruleus (LC) in the development of tolerance to OIRD. Furthermore, it will investigate how tolerance to OIRD changes depending on the environmental context of drug administration, and the involvement of the LC in this conditional and learned tolerance.

Methods

Animals

All animal protocols followed National Institution of Health guidelines for the appropriate care and use of animals and were approved by the Institutional of Animal Care and Use Committee at The University of Chicago. Experiments were performed in the light cycle. For fiber photometry studies, we used a transgenic mouse line where Cre-recombinase expression is driven by the norepinephrine (NE) transporter promoter and has high selectivity for NE cells in the Locus Coeruleus (LC) with low ectopic expression (*slc6a2*, mouse line: *Net-Cre*[1]). We used an additional transgenic mouse line for Cre-dependent expression of channelrhodopsin ChR2-tdTomato (strain number: 012567, The Jackson laboratory, mouse line: *Ai27D*[2]). For optogenetic experiments, *Net-cre* mice were crossed with *Ai27D* to selectively express ChR2 in the noradrenergic cells of the LC (LC^{NE}). Adult mice of both sexes (>9 weeks, 22-41g) on a *Net-Cre* background were used for simultaneous plethysmography and fiber photometry studies. Adult mice of both sexes (>9 weeks, 25-38g) on a *Net-Cre/Ai27D* background were used for simultaneous plethysmography and optogenetic studies. WT mice on a *C57BL6* background were used as sham controls for optogenetic experiments and for plethysmography-only experiments (>9 weeks, 20-40g). Mice were bred at the University of Chicago animal facilities. Mice used in this study were group housed with the same sex in AAALAC-approved facilities following a 12/12 h light/dark cycle and were given ad libitum access to food and water. All behavioral experiments occurred during their light cycle.

Surgery

Stereotaxic Surgical Procedures

All viral injections were done with a stereotaxic surgical device (Kopf Instruments) to position injections and implants correctly and sterile tools were used throughout to maintain a sterile surgical environment. Isoflurane (2-3% induction, 1-1.5% maintenance) was used to anesthetize the mice. Head hair was shaved using a trimmer, and the mice were head-fixed in the stereotaxic system. Sterile drapes were placed over a heating pad to maintain homeostatic body temperature, and ophthalmic lubricant was placed over the eyes. Betadine was applied on the scalp prior to any incision or injection. Bupivacaine (1 mg/kg, *s.c.*) was then injected into the scalp. Sterile tools were used to make an incision at the midline of the scalp. A micromotor drill attached to the stereotaxic apparatus was used to drill two small holes into opposite sides of the skull where two small screws were implanted. Cannula implantation for optogenetic experiments, and cannula implantations and viral injections for fiber photometry experiments followed (see below for details). At the end of the surgery, mice were injected with Meloxicam (5 mg/kg, s.c.) and saline (5 mL, s.c.) and returned to their cage. The cage was then placed on a heating tray until the mice recovered and regained normal mobility (about 1-3 days).

Viral injections and cannula implants for fiber photometry

A Hamilton syringe was attached to the stereotaxic apparatus for viral injections and slowly lowered to the Locus Coeruleus. A syringe pump was used to control the viral injection volume to 400 nL and flow rate to 100 nL/min. The needle was held in place for a total of 10 minutes to allow for sufficient viral infusion and was then slowly removed.

To selectively monitor the activity of the noradrenergic cells in LC (LC^{NE}), we injected a *Cre*-dependent genetically encoded Ca^{2+} indicator (GCaMP) virus (pGP-AAC-CAG-FLEX-jGCaMP8s-WPRE, Addgene: 162380) into the LC. *Net-Cre* transgenic mice were used for selective expression of GCaMP in LC^{NE} neurons. Fiber optic cannulas (MFC_400/430-0.66_6mm_MF1.25_FL, Doric) were implanted using a cannula holder attached to the stereotaxic system. Dental cement was attached to the screws, skull, and cannula to create a head cap to hold and protect the fiber optic cannula. Experimenters waited at least 3 weeks for the virus to fully express before checking the fluorescent signal.

LC coordinates relative to Bregman for cannula placement were AP: -5.4, ML: 0.85, DV: -3.75. Two DV viral injections were done dorsal and ventral to the coordinate at -3.9 and -3.6. DV cannula placement was at -3.75 (verified using Paxinos and Franklin's Mouse Brain Atlas, 2001).

Cannula implants for optogenetics

Fiber optic cannulas (MFC_200/250-0.66_6mm_MF1.25_FL, Doric) were implanted using a cannula holder attached to the stereotaxic system. *Net-cre*/*Ai27D* transgenic mice were used for selective expression of Channelrhodopsin2 (ChR2) in LC^{NE}. Dental cement was attached to the screws, skull, and cannula to create a head cap to hold and protect the cannula. Experimenters waited at least 2 weeks before beginning habituation and experimental protocols. LC coordinates relative to Bregma for cannula placement were AP: -5.4, ML: 0.85, DV: -3.75 (Paxinos and Franklin, 2001).

Behavioral Protocols

Repeat Opioid Use Protocol with Context-Pairing

Both breathing with plethysmography and LC^{NE} activity with fiber photometry were measured during this protocol. The duration of the Repeat Opioid Use protocol was seven days and consisted of two phases. Phase One consisted of context-pairing with either fentanyl or saline for five consecutive days. Adult mice expressing GCaMP in LC^{NE} were administered fentanyl (0.7 mg/kg, *i.p.*) daily in a distinctive environmental context (Fentanyl-Paired context). The same mice were also administered saline (0.2-0.3 mL, depending on mouse weight, *i.p.*) daily in another distinctive environmental context (Saline-Paired context). To make the environments distinctive, each had visual, tactile, audio, and olfactory cues associated with them. Because mice needed to remain in the plethysmography chamber to gather breathing data, the chamber became part of the environmental context. See-through chambers were placed into an opaque box to prevent mice from seeing experimenters. The box had visual cues on the walls and around the chamber, and an audio that was played outside of the chamber. Scents for olfactory cues were mixed with the Room Air and flowed directly into the chamber, floor bottoms of the chamber were textured and acted as the tactile cue. Context one: green box with triangle taped on one side, four 3-D blue or purple shapes, floor bottom with small circular holes in it, white noise audio, and vanilla scent. Context two: white box with square and circle taped on two walls, four 3-D orange shapes, floor bottom made of mesh wiring, 80 BPM metronome audio, and almond scent. Which context was Fentanyl Paired and which was Saline Paired was counterbalanced across all of the subjects. Previous experiments demonstrated that there was no difference in the degree of respiratory depression depending on time of day of administration (e.g. morning or afternoon). To avoid any lingering effects of fentanyl carrying over into saline sessions, mice

were injected with saline and placed in their Saline-Paired context each morning, and injected with fentanyl and placed in their Fentanyl-Paired context each afternoon. There was an average of 3-4 hours between the morning and afternoon sessions. Sessions consisted of a 15-minute baseline recording prior to any injection, and then a 15-minute recording after the injection of either fentanyl or saline. Phase Two consisted of a two-day protocol directly following Phase One. During Phase Two, there was only one session a day and mice only received fentanyl injections. Sessions again consisted of a 15-minute baseline recording prior to injection, and a 15-minute post-fentanyl injection recording. On one day of the protocol, mice again received fentanyl in the Fentanyl Paired context, on the other day they received fentanyl in the Saline Paired context. Which context came first during Phase two was counterbalanced across the subjects.

Hypercapnic Ventilatory Response after Repeat Opioid Use with Context-Pairing

In an additional set of subjects (n=4), we slightly modified the Repeat Opioid Use with Context-Pairing protocol and only measured breathing. During this protocol, there was an initial day prior to the beginning of Day 1 where we measured subjects' Hypercapnic Ventilatory Response (HVCR) in a plethysmography chamber without any contextual cues associated with it. Mice then went through Phase One of the protocol. Phase Two again consisted of two days but instead of fentanyl administration, the HCVR was tested in the Fentanyl Paired and Saline Paired contexts. The HCVR protocol consisted of the following: Baseline breathing was initially measured in room air for 10 minutes (5 min, FiO_2 = 21%, $FiCO_2$ = 0%, balanced N_2; 5min duration) and then switched to a hypercapnic gas mixture (i.e., hypercapnia, FiO_2 = 21%, $FiCO_2$ = 5% CO_2, balanced N_2; 7 min duration).

Acute Opioid Use Protocol

Only breathing was measured during this protocol, and optogenetic manipulation of LC^{NE} or sham stimulation was conducted. The Acute Opioid Use protocol consisted of one day and was only one session. Mice were placed in a plethysmography chamber inside of a silver box to prevent them from seeing the experimenters during the protocol. There were no cues or salient features about the box or plethysmography chamber. Mice were placed in the chamber and baseline breathing was recorded for 5 minutes. The light was turned on (for specifics see optogenetics section) and breathing prior to fentanyl injection with optogenetic stimulation was recorded for 5 minutes. The mouse was then injected with fentanyl and 15-minutes of breathing post-fentanyl injection with optogenetic stimulation was recorded. Importantly, this was the first time any subject had received fentanyl.

Simultaneous Whole Body Plethysmography and Fiber Photometry

Whole Body Plethysmography

Respiration was measured daily during the ROU protocol using unrestrained whole-body plethysmography in a custom-constructed chamber (500mL) connected to a strain gauge pressure transducer. To conduct simultaneous fiber photometry recordings, the fiber optic patchcord was fed through a hole in the top of the chamber and attached to the mouse's fiber optic cannula. An air-tight environment inside of the chamber was maintained by sealing the hole with modeling clay. Transducer signals were amplified via a Max II amplifier (BUXCO, CITY) and recorded using Synapse (TDT) software. Room air (19-21% O_2, balanced N_2) continuously flowed through the system at 0.6 liters per minute.

Chamber temperature (22-27 °C) was recorded each day of the ROU with context protocol prior to mouse placement in the plethysmography chamber. Barometric pressure was assessed across experimental sessions by using a website that provided the average barometric pressure (timeanddate.com) for the Hyde Park, IL for each experimental day. Body weight and temperature (35.7-37.3 °C) were recorded for V_T calculation, and mice were placed in the chamber and tethered to the fiber optic cable to record baseline breathing and LC^{NE} activity (15 minutes). At the end of the control period, calibrations for baseline V_T were taken, the mouse was removed from the chamber and administered fentanyl (0.7 mg/kg, i.p.) or saline (0.2-0.3 mL, depending on animal weight) before being promptly returned to the chamber and retethered to the fiber optic cable to record drug-affected breathing and LC^{NE} activity (15 minutes). Post-injection calibration measurements for V_T calculations were done prior to the removal of the mouse from the chamber at the end of the 15-minute fentanyl or saline recording. Once the animal was removed, body temperature measurements were again recorded (36.1-37.8 °C). Prior to the experimental protocol, mice were habituated to tethering, handling, i.p. injections (saline, 0.2-0.3 mL, depending on mouse weight) and a plethysmography chamber of a slightly different shape that would not be used in the protocol for 5 consecutive days.

Fiber Photometry

Fiber photometry was conducted using the TDT RZ10X system with a lock-in amplifier for signal demodulation, in conjunction with a Doric 6-port fluorescent mini cube (FMC6_IE(400-410)_E1(460-490)_F1(500-540)_E2(555-570)_F2(580-680)_S, Doric). The mini cube was equipped with 415 nm (isosbestic control) and 465 nm (GCaMP) excitation and 525 nm emission filters suitable for our fluorophores of interest. 465 nm (GCaMP) was

modulated at 330 Hz and 415 nm (isosbestic control) was modulated at 210 Hz. The signal was sampled at 1017.3 Hz. Output power levels were matched between isosbestic and GCaMP signals and were kept consistent throughout the 7 days of the protocol. A Doric Mono Fiberoptic Patchcord (MFP_400/430/1100-0.57_2m_FCM-MF1.25_LAF) was tethered to the fiber optic cannula on the animal's head through a hole in the top of the plethysmography chamber. Mice were habituated to tethering during the 5-day habituation prior to any experimentation. TDT Synapse software was utilized to record and process fluorescent signals, track power levels, and simultaneously capture breathing signals. Photometry sessions lasted 30 minutes on average, including both baseline and fentanyl/saline sessions.

Post hoc Analysis of Simultaneous Whole-Body Plethysmography and Fiber Photometry

Fiber photometry and breathing data collected through the TDT system were analyzed in MATLAB using the *TDTbin2mat* function. LC^{NE} activity and breathing was analyzed using a combination of MATLAB and custom scripts. The last 5 minutes of baseline were analyzed. The 15 minutes of fentanyl data were analyzed in 5-minute bins (minutes 0-5, 5-10, 10-15), to ensure proper fitting of 415 nm to 465 nm. Raw GCaMP data was corrected for motion artifact and baseline fluctuations by fitting the 415 isosbestic signal to the 465 GCaMP signal with the *polyfit* function. We then subtracted the 415 fit from the 465 signal and divided the difference by the 415 fit ($\Delta F/F$ (=[F465-$Ffit_{415}$]/ $Ffit_{415}$)). A Z-score of $\Delta F/F$ was used to compare across mice and across days. For both baseline and fentanyl/saline sessions, we used the mean and standard deviation from the baseline session of that day to calculate the Z-score. The *findpeaks* function was used to locate LC^{NE} fiber photometry events. The threshold for an event to be counted was set at a Z-score of 2 for all days, sessions, and animals. This is to ensure with 95% confidence

that the events being counted were significantly different from the mean fluorescent signal. Various metrics were obtained about each LC^{NE} event (amplitude, width, area under the curve) and the breathing during that LC^{NE} event (widths, amplitude, instantaneous frequency, acceleration).

The *findpeaks* function was used to identify breaths. Respiratory rate (RR, breath*min^{-1}) was calculated by multiplying the average instantaneous frequency by 60 seconds. Tidal volume (V_T, μL*$breath^{-1}$*g^{-1}) was calculated using the amplitude of breaths as described in Lim R et al. (2014)[3] and was normalized to weight. Baseline periods used baseline calibrations and body temperature recordings for V_T measurements, and post-injection (fentanyl or saline) periods used post-injection calibrations and body temperature recordings for V_T measurements. Minute ventilation (V_e = mL*min^{-}1*kg^{-1}) was calculated as the product of tidal volume (V_T, μL*$breath^{-1}$*g^{-1}) and respiratory rate (RR, breath*min^{-1}). Breathing during the last five minutes of the 15-minute baseline period was analyzed and used as a baseline reference. Breathing was analyzed for the duration of the 15-minute post-injection period.

Definition of Tolerance with Repeat Opioid Use: Two comparisons of V_e during OIRD were made between: (1) Day 1 and Day 5 in the Fentanyl Paired context; and, (2) in the Fentanyl Paired and Saline Paired contexts following ROU. Tolerance is defined as a "diminished response to a substance that occurs with frequent use" [4]. Thus, we defined the development of tolerance to Opioid-Induced Respiratory depression with Repeat Opioid Use as a smaller decrease in V_e after fentanyl administration compared to V_e prior to fentanyl administration. Tolerance between days was assessed by comparing V_e during the first five minutes after fentanyl injection normalized to baseline V_e, (averaged over the last five minutes of the baseline period). Comparisons between Day 1 and Day 5 included all 9 animals. Only animals who

developed tolerance during the protocol were included for comparisons between Fentanyl Paired and Saline Paired (n=7/9). Mice were considered to not develop tolerance and excluded from the Fentanyl Paired/Saline Paired analysis if: 1) Day 1 normalized V_e during the first five minutes after fentanyl administration was greater than 2 of the 3 final days of the protocol (Day 5, Fentanyl Paired, Saline Paired), and 2) Day 1 normalized V_e throughout the 15-minute fentanyl recording was greater than 2 of the 3 final days of the protocol (Day 5, Fentanyl Paired, Saline Paired).

The *findpeaks* function was used to find periods of high-frequency breathing, designated High Frequency Respiratory Transients (HFRT), that occurred both prior to fentanyl and after fentanyl administration. Prior to fentanyl, HFRT was defined as a breathing frequency > 8 Hz[5]. During fentanyl breathing, HFRTs were defined as 1) an instantaneous breathing frequency 20% higher than the mean instantaneous frequency during respiratory depression and 2) one standard deviation above the instantaneous frequency of the previous breath. To identify where HFRTs occurred in the breathing signal after fentanyl administration, a vector containing consecutive instantaneous frequencies of breaths during each 5-minute bin of analysis was generated. Time stamps of the HFRTs were used to average the LC^{NE} signal dynamics during the HFRT. The Matlab code used for this analysis is available upon request.

Simultaneous Whole Body Plethysmography and Optogenetics

Whole Body Plethysmography

Respiration was measured daily during the Acute Opioid Use protocol using unrestrained whole-body plethysmography in a custom-constructed chamber (500mL) connected to a strain gauge pressure transducer that allowed for simultaneous measurements of breathing and

optogenetic manipulation. The fiber optic cable was fed through a hole in the top of the chamber and attached to the mouse's fiber optic cannula. An air-tight environment inside of the chamber was maintained by sealing the hole with modeling clay. Transducer signals were amplified via a Max II amplifier (BUXCO, CITY) and recorded using Axoscope (Molecular Devices) software. Room air (19-21% O_2, balanced N_2) continuously flowed through the system at 0.6 liters per minute.

Chamber temperature (21- 24 °C) was recorded prior to the Acute Repeat Opioid Use Protocol and mouse placement in the plethysmography chamber. Barometric pressure was assessed across experimental sessions by using a website that provided the average barometric pressure (timeanddate.com) for the Hyde Park, IL for each experimental day. Body weight and temperature (35.8-36.6 °C) were recorded for V_T calculation, and mice were placed in the chamber and tethered to a ThorLabs Mono Fiberoptic Patchcord (RJPFL4, ThorLabs). Breathing was recorded for 5 minutes, then, optogenetic stimulation was initiated and remained on for the next 5 minutes while breathing continued to be recorded. At the end of this initial 10-minute period, calibrations for baseline V_T were taken, the mouse was removed from the chamber and administered fentanyl (0.7 mg/kg, i.p.) before being promptly returned to record drug-affected breathing. Optogenetic stimulation was again turned on when the subject was placed back in the chamber and remained on for the next 15 minutes. Post-injection calibration measurements for V_T calculations were done prior to the removal of the mouse from the chamber at the end of the 15-minute fentanyl recording. Once the animal was removed, body temperature measurements were again recorded (34.9-36.3 °C). Prior to the experimental protocol, mice were habituated to tethering, handling, i.p. injections (saline, 0.2-0.3 mL, depending on mouse weight), and a plethysmography chamber.

Optogenetics

Pulses of blue light (473 nm) were used to activate ChR2 using a DPSS laser system generated by a Master-9 Pulse Stimulator. Brief pulses of light at a frequency of 20 Hz (10 ms duration during 50 ms intervals) were used as the stimulation pattern to try to induce phasic LC activity. 20 Hz firing pattern was chosen to broadly simulate LC activity during periods of high arousal and physiological LC responses to salient stimuli[6,7]. A power meter was used to measure and confirm light power of ~5 mW prior to tethering the animal. Mice were at least 2 -3 weeks post-op prior to experimentation and were habituated to the plethysmography chamber, tethering, handling, and i.p. injections for 5 days prior to any experimentation.

Post hoc Analysis of Simultaneous Whole-Body Plethysmography and Optogenetics

Breathing data was analyzed with Clampfit 11 (Molecular Devices). (RR, breath*min^{-1}) was calculated by multiplying the average instantaneous frequency by 60 seconds. Tidal volume (V_T, μL*breath^{-1}*g^{-1}) was calculated using the amplitude of breaths as described in Lim R et al. (2014)[3] and was normalized to weight. Baseline periods used baseline calibrations and body temperature recordings for V_T measurements, and post-fentanyl injection periods used post-injection calibrations and body temperature recordings for V_T measurements. Minute ventilation (V_e = mL*min-1*kg^{-1}) was calculated as the product of tidal volume (V_T, mL*breath^{-1}*g^{-1}) and respiratory rate (RR, breath*min^{-1}). Breathing during the first five-minute period of baseline (no optogenetic stimulation) was used as a baseline reference. Breathing was sampled from 10-second window bins of quiescent breathing (no movement artifact) for each minute bin of the protocol.

Post hoc Analysis for Hypercapnic Ventilatory Response Protocol

Breathing data was analyzed with Clampfit 11 (Molecular Devices). (RR, breath*min^{-1}) was calculated by multiplying the average instantaneous frequency by 60 seconds. Tidal volume (V_T, μL*breath^{-1}*g^{-1}) was calculated using the amplitude of breaths as described in Lim R et al. (2014)[3] and was normalized to weight. Minute ventilation (V_e = mL*min^{-}1*kg^{-1}) was calculated as the product of tidal volume (V_T, μL *breath^{-1}*g^{-1}) and respiratory rate (RR, breath*min^{-1}). Breathing was sampled from 10-second window bins of quiescent breathing (no movement artifact) for each minute bin of the protocol.

Statistical Analysis and Figures

Receiver Operating Characteristic (ROC) analyses were performed using custom code in R (available upon request). All other statistical analyses were performed using Origin (OriginLab Corporation, Northampton, MA). Statistical significance was defined as $p < 0.05$. Unless otherwise stated, values are reported as a mean ± SEM. Biorender was used to make experimental protocol and method schematics.

Histology

Immunohistochemistry and viral placement

Mice were anesthetized with isoflurane. Standard protocols were used for perfusion procedures. Mice were perfused with 20 mL chilled PBS, followed by 20 mL chilled 4% paraformaldehyde in PBS. Brains were removed and placed in falcon tubes filled with PFA for ~24 hours. Brains were removed and placed in a falcon tube filled with a 30% sucrose solution. Once brain sunk to the bottom of the tube (~1-3 days), they were frozen in OCT blocks. Slicing

was done on a Leica Cryostat and 40 μm bilateral coronal slices were taken of the LC and direct rostral and caudal areas. Slices were kept in cryoprotectant solution after slicing until ready to immunohistochemical processing.

Immunofluorescent staining was performed on all sections from a single series, at room temperature and with agitation, unless otherwise noted. Tissue was rinsed in 1X phosphate buffered saline (PBS, pH 7.4) 3 times for 10 minutes each to remove cryoprotectant. Tissue was then washed in PBS supplemented with 0.5% Tween-20 (PBS-T) twice for 5 minutes each, and placed in a blocking buffer for 30 minutes (50mM glycine, 0.1% (v/v) TritonX-100, 0.1% (w/v) Bovine Serum Albumin, 0.05% (v/v) Tween20, and 2% (v/v) Normal Donkey Serum, in PBS). The primary antibodies rabbit anti-tyrosine hydroxylase (EMD Millipore #AB152) and chicken anti-GFP (Invitrogen #A10262) were diluted 1:500 and 1:200, respectively, in antibody buffer (PBS supplemented with 0.1% TritonX-100, 0.05% Tween2, 0.1% (v/v) hydrogen peroxide, and 10mM glycine), which was applied to the tissue overnight at 4°C. The next day, tissue was washed 3 times for 5 minutes each in 0.5% PBS-T, then incubated for 2 hours with secondary antibody solution, containing 1:1000 each donkey anti-chicken IgY (H+L) Alexa Fluor 488 (Invitrogen #A78948) and donkey anti-rabbit IgG (H+L) Alexa Fluor PLUS 647 (Invitrogen #A32795) in 0.1% PBS-T. Afterwards, tissue was washed three times for 5 minutes each in PBS, mounted on glass slices, and cover slipped with Prolong Gold with DAPI (Invitrogen #P36935).

Images were captured on a Zeiss Axio Imager.M2 upright epi-fluorescence microscope using a 10x N-Achroplan 0.25 numerical aperture (NA) objective. All sections were imaged with identical collection parameters. Image files were first captured as z-stacks with a step-size of 1 μm, and then flattened using the two-dimensional maximum intensity projection algorithm in ImageJ (NIH) before quantification. Total cell counts within LC were made by hand for TH-

positive or GFP-positive cells from the individual fluorescent channel images. Dual-labeled cells were quantified by using the Image Calculator function in ImageJ to create a co-localization mask based on fluorescent intensity overlap, and the output was similarly counted by hand. Solely single-labeled cell counts (e.g., TH-positive but GFP-negative) were calculated by subtracting the colocalized cell count from the total cell count within each section. All measurements were done first within single sections per subject, then averaged for all sections within a subject before further plotting and statistical analyses.

Results

Repeat Opioid Use leads to changes in Locus Coeruleus activity that coincides with changes in breathing.

I. Fentanyl has differential effects on aggregate Locus Coeruleus activity following Repeat Opioid Use

To determine the underlying neural mechanisms that contribute to the development of tolerance to Opioid-Induced Respiratory Depression (OIRD) with Repeat Opioid Use (ROU), we used whole-body plethysmography and fiber photometry in freely behaving *Net-Cre* mice expressing GCaMP8s in the noradrenergic cells of the Locus Coeruleus (LC^{NE}) (**Fig 14A**). On average across subjects, GCaMP8s was expressed in 38% of Tyrosine Hydroxylase^{+} (TH^{+}) cells in the LC (**Supp Fig 1**). This allowed for simultaneous measurements of breathing and intracellular Ca^{2+} activity in LC^{NE}. Mice underwent a repeat opioid use (ROU) protocol that consisted of five consecutive days of fentanyl administration in a distinct context (i.e., the Fentanyl Paired context) and saline administration in a different distinct context (i.e., the Saline Paired context) (**Fig 14B**). No differences in the number of LC events were observed prior to

injection in either the Fentanyl Paired context or the Saline Paired context when comparing Day 1 (*i.e.*, when mice are naïve to fentanyl exposure) to Day 5 (i.e., when mice have been exposed to repeated fentanyl exposure) of the ROU protocol (**Supp Fig 2**). While aggregate LC^{NE} activity increased in response to fentanyl administration on Day 1 (**Fig 14C**), changes in aggregate LC^{NE} activity were not evident after fentanyl administration on Day 5 (**Fig 14D**). Moreover, aggregate LC^{NE} activity was unaffected by saline injection on either day of ROU (**Supp Fig 3**). As these analyses suggested that ROU leads to changes in the LC^{NE} response to fentanyl administration, we next assessed how ROU alters breathing in response to fentanyl.

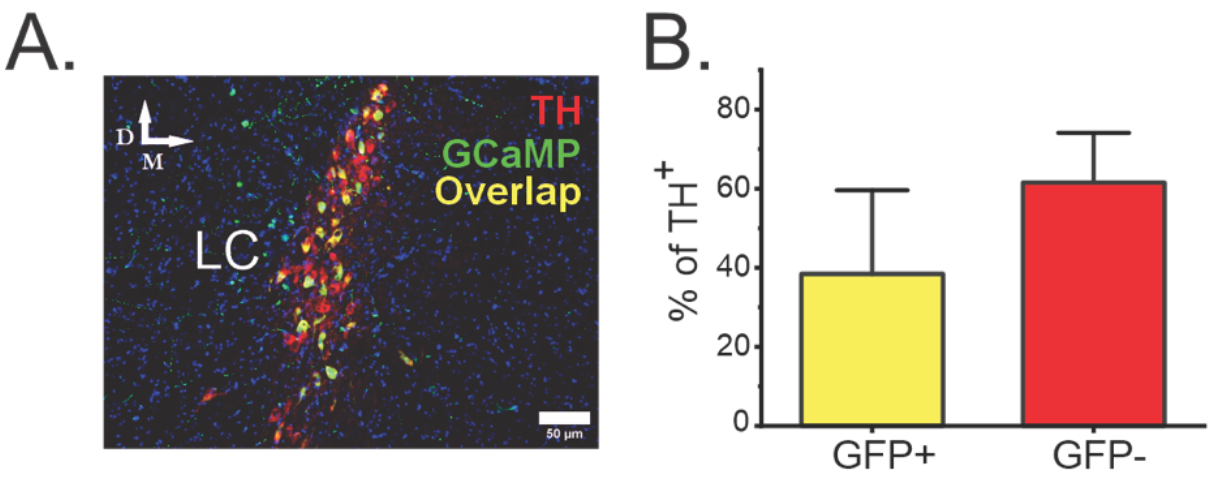

Supplemental Figure 1. Verification of GCaMP expression in LC^{NE} neurons

A) Example image showing expression of GCaMP in TH+ cells.
B) Quantification of GCaMP expression within the TH+ cells.

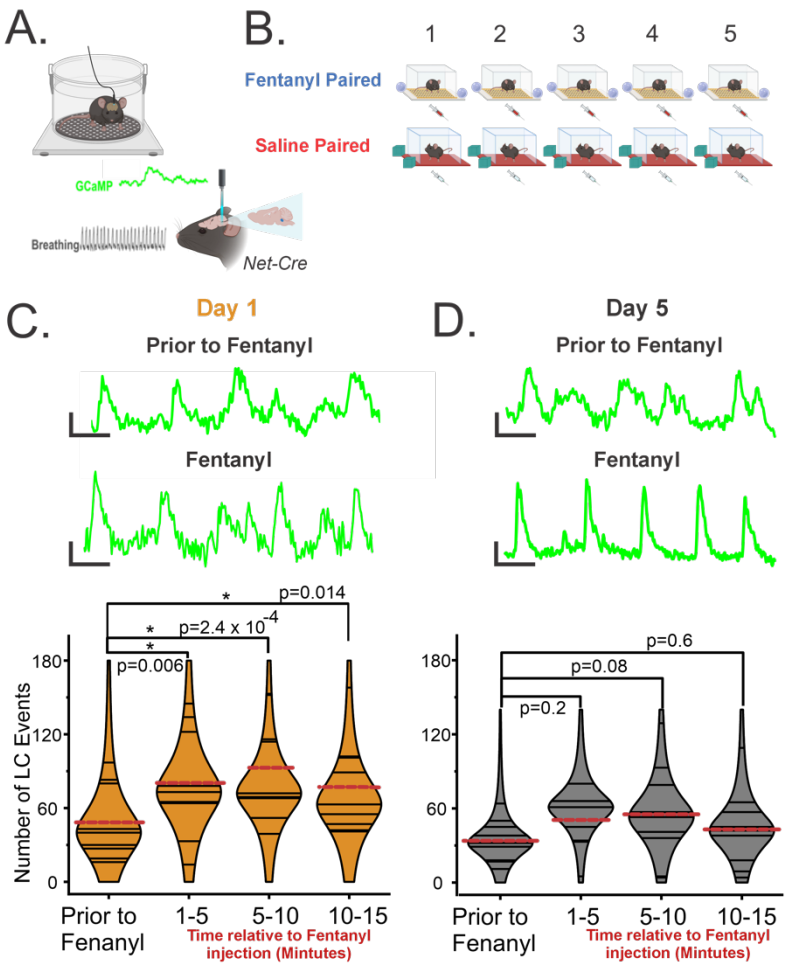

Figure 14. Fentanyl has differential effects on aggregate LC^{NE} activity following Repeat Opioid Use

A) Schematic showing simultaneous fiber photometry and plethysmography experimental set up with viral GCaMP8s and cannula placement in the LC in *Net-Cre* mice.

B) Schematic of the 5-day experimental ROU protocol. Top: Daily fentanyl injection in the Fentanyl Paired context. Bottom: Daily saline injection in the Saline Paired context.

C) Day 1 of ROU protocol: Top: Example traces of fluorescent LC^{NE} signals prior to fentanyl and after fentanyl injection. Scale bars: 2.5 sec x 1 z-score. Bottom: Mean Number of LC Events prior to, and 0-5, 5-10, and 10-15 minutes after fentanyl administration. RM One-Way ANOVA $p<0.0001$, *Post hoc:* Dunnett's pairwise comparison, control=prior to fentanyl, n=9. Red dotted line indicates group mean.

D) Day 5 of ROU protocol: Top: Example traces of fluorescent LC^{NE} signals prior to fentanyl and after fentanyl injection. Scale bars: 2.5 sec x 1 z-score. Bottom: Mean Number of LC Events prior to, and 0-5, 5-10, and 10-15 minutes after fentanyl administration. RM One-Way ANOVA $p=0.14$, *Post hoc:* Dunnett's pairwise comparison, control=prior to fentanyl, n=9. Red dotted line indicates group mean.

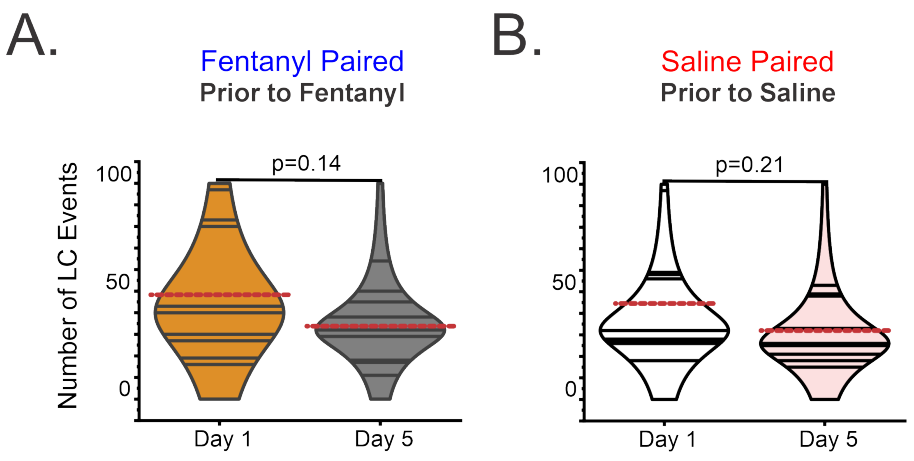

Supplemental Figure 2. Repeat Opioid Use does not alter LC^{NE} activity prior to Fentanyl and Saline injection in the Fentanyl Paired or Saline Paired contexts, respectively

A) Mean Number of LC Events prior to fentanyl injection on Day 1 and Day 5 in the Fentanyl Paired context. Paired t-test (p=0.14). Red dotted line indicates group mean.
B) Mean Number of LC Events prior to saline injection on Day 1 and Day 5 in the Saline Paired context. Paired t-test (p=0.21). Red dotted line indicates group mean.

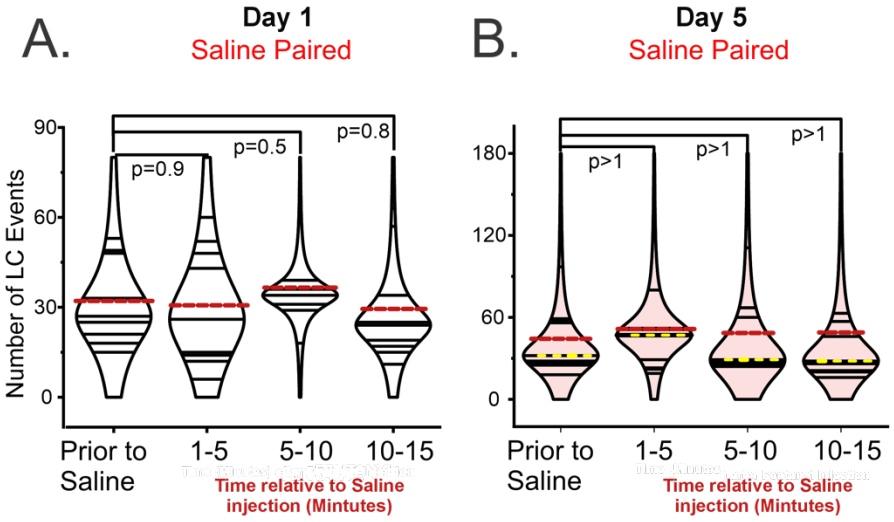

Supplemental Figure 3. LC^{NE} activity is not altered by Saline injection

A) Day 1 of ROU protocol: Mean Number of LC Events prior to, and 0-5, 5-10, and 10-15 minutes after saline administration. RM One-Way ANOVA p=0.7, *Post hoc:* Dunnett's pairwise comparison, control=prior to fentanyl, n=9. Red dotted line indicates group mean.
B) Day 5 of ROU protocol: Mean Number of LC Events prior to, and 0-5, 5-10, and 10-15 minutes after saline administration. Friedman ANOVA p=0.27, *Post hoc:* Dunn's pairwise

comparison, n=9. Red dotted line indicates group mean. Yellow dotted line indicates group median.

II. Repeat Opioid Use results in a distinct pattern of Opioid-Induced Respiratory Depression after fentanyl administration

Respiratory rate (RR, *i.e.* the number of breaths per minute), tidal volume (V_T, *i.e.* the volume of air breathed in per breath), and minute ventilation (V_e, *i.e.* the amount of air breathed within a minute) were measured prior and following injections on Day 1 and Day 5 of ROU in the Fentanyl Paired and Saline Paired contexts. Breathing in the Fentanyl Paired context prior to fentanyl administration was similar on Day 1 and Day 5, as no differences in RR, V_T, or V_e were evident between days. V_e in the Saline Paired context prior to saline injection was decreased on Day 5 as compared to Day 1, driven by a decrease in RR, as there was no change in V_T (**Supp Table 2**). While breathing was unaffected by saline injection on Days 1 and 5 of the ROU protocol (**Table 5**), fentanyl administration caused respiratory depression when subjects were naïve to fentanyl (Day 1) as well as after the ROU protocol (Day 5) (**Fig 15A**). During the initial 5 minutes after fentanyl injection, breathing decreased in RR, V_T, and V_e on Day 1 following fentanyl administration. On Day 5, RR and V_e were decreased after fentanyl, but not V_T (**Table 6**). While respiratory depression occurred on both Day 1 and Day 5, differences were observed between the two days (**Fig 15B**). Fitting a model to the data sets from each day revealed distinct patterns of respiratory depression on Day 5 compared to Day 1 in RR, V_T, and V_e with subjects experiencing overall less respiratory depression by Day 5 (**Fig 15C**). Importantly, while the majority of subjects developed tolerance (n=7/9, 77%) throughout the ROU protocol, n=2/9 (23%) did not (see methods for tolerance definition).

Context	Metric	Day 1		Day 5		P-value	Test
Fentanyl Paired		Mean	Median	Mean	Median		
	RR (bpm)	257.42 ± 19.43		222.96 ± 17.12		0.19	Paired t-test
	TV (µL/*breath/g)	3.14 ± 0.22		2.78 ± 0.38		0.35	Paired t-test
	MV (mL/min/g)	0.85 ± 0.11	0.81	0.7 ± 0.14	0.48	0.3	Wilcoxon Signed Ranks
Saline Paired		Mean	Median	Mean	Median		
	RR (bpm)	290.92 ± 13.24		211.62 ± 20.73		0.008	Paired t-test
	TV (µL/*breath/g)	3.24 ± 0.57	2.61	2.64 ± 0.26	2.27	0.43	Wilcoxon Signed Ranks
	MV (mL/min/g)	1 ± 0.19	0.86	0.6 ± 0.09	0.54	0.02	Wilcoxon Signed Ranks

Supplemental Table 2. Respiratory metrics prior to fentanyl administration on Day 1 and Day 5

Day	Metric	Baseline		Saline		P-value	Test
Day 1		Mean	Median	Mean	Median		
	RR (bpm)	290.92 ± 13.24		270.61 ± 10.52		0.09	Paired t-test
	TV (µL/*breath/g)	3.24 ± 0.57	2.61	3.06 ± 0.4	2.43	0.73	Wilcoxon Signed Ranks
	MV (mL/min/g)	1 ± 0.2	0.86	0.9 ± 0.14	0.71	0.55	Wilcoxon Signed Ranks
Day 5		Mean	Median	Mean	Median		
	RR (bpm)	211.72 ± 20.73		225.73 ± 16.79		0.14	Paired t-test
	TV (µL /*breath/g)	2.64 ± 0.26		2.76 ± 0.22		0.55	Paired t-test
	MV (mL/min/g)	0.59 ± 0.09		0.65 ± -.05		0.32	Paired t-test

Table 5. Respiratory metrics after saline administration on Day 1 and Day 5

Day	Metric	Baseline		Fentanyl		P-value	Test
Day 1		Mean	Median	Mean	Median		
	RR (bpm)	257.4 ± 19.4		157.1 ± 10.9		0.002	Paired t-test
	TV µL/*breath/g)	3.14 ± 0.22		2.44 ± 0.13		0.014	Paired t-test
	MV (mL/min/g)	0.85 ± 0.11	0.81	0.4 ± 0.04	0.36	0.004	Wilcoxon Signed Ranks
Day 5		Mean	Median	Mean	Median		
	RR (bpm)	223.96 ± 17.12		162.8 ± 10.02		0.004	Paired t-test
	TV (µL/*breath/g)	2.78 ± 0.38		2.48 ± 0.21		0.35	Paired t-test
	MV (mL/min/g)	0.7 ± 0.14	0.48	0.41 ± 0.03	0.43	0.012	Wilcoxon Signed Ranks

Table 6. Respiratory metrics after fentanyl administration on Day 1 and Day 5

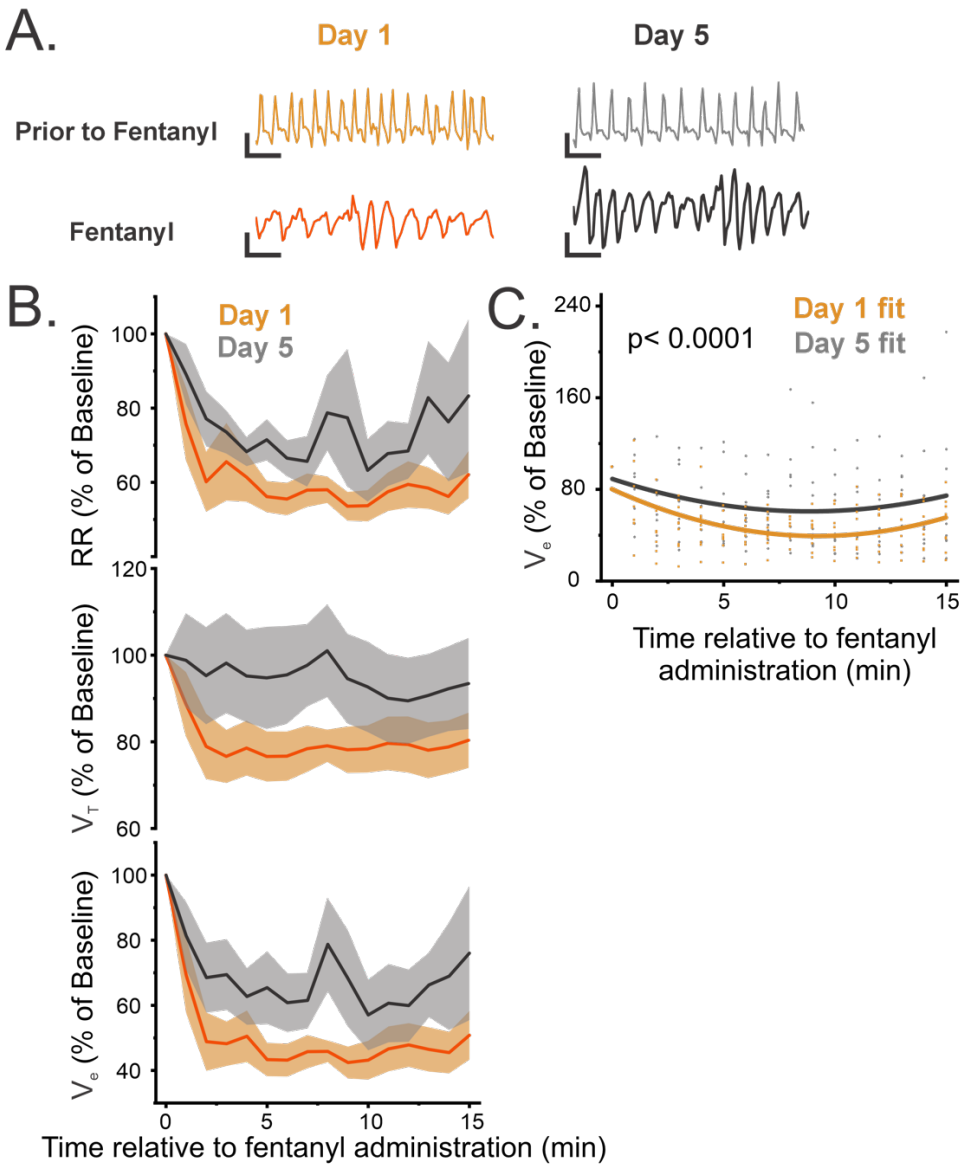

Figure 15. Repeat Opioid Use results in a distinct pattern of breathing after fentanyl administration and less overall respiratory depression

A) Representative breathing traces on Day 1 (yellow) and Day 5 (gray), prior to fentanyl (top), and after fentanyl administration (bottom). Scale Bars: 1 sec x 3 µL.

B) Time course of mean RR top), V_T (middle), and V_e (bottom) during OIRD on Day 1 (yellow) and Day 5 (gray) during OIRD. The shaded region represents the SEM (n=9).

C) Polynomial fits of V_e during OIRD breathing in the Day (yellow) and Day 5 (gray) data sets. RR (*data not shown)* (F-test, $p<0.0001$, D1: $R^2=0.23$, D5: $R^2=0.06$), V_T (*data not shown*) (F-test, $p<0.0001$, D1: $R^2=0.07$, D5: $R^2=0.007$), and V_e (F-test, $p<0.0001$, D1: $R^2=0.26$, D5: $R^2=0.05$) fit comparisons were also different from Day 1 to Day 5. Raw data points for each animal (n=9) are plotted behind the V_e fits.

III. Coupling between Locus Coeruleus activity and breathing is increased during respiratory depression after ROU

Because of these changes to both LC^{NE} activity and the degree of Opioid-Induced Respiratory Depression (OIRD) following ROU, we next sought to determine how ROU impacted the relationship between LC^{NE} activity and breathing after fentanyl administration. On both Day 1 and Day 5 of ROU, we observed that LC events coincided with bouts of High-Frequency Respiratory Transients (HFRTs) both prior to (**Fig 16A**) and during exposure to fentanyl (**Fig 16B**). These were apparent by increases in V_T as well as RR. Prior to fentanyl administration, the percentage of LC^{NE} events that corresponded with HFRTs (RR ranged from 8 to 16 Hz during HFRT) did not change from Day 1 (20% ± 7.2) to Day 5 (21% ± 7.2). After fentanyl administration, HFRTs were defined as an increase in RR by 20% greater than the mean RR during respiratory depression. The percentage of LC^{NE} events that corresponded with HFRTs (HFRT-LC^{NE} events) during the initial five minutes post fentanyl injection increased from 60% ± 3.9 on Day 1 to 78% ± 6 on Day 5 (**Fig 16C)**. Furthermore, the increase in breathing during HFRT-LC^{NE} events is greater on Day 5 as compared to Day 1 and is evident throughout the 15-minute protocol in RR, V_T, and V_e (**Fig 16D**). We next sought to determine if there were any differences in the waveform of HFRT-LC^{NE} that coincided with the breathing changes we saw by Day 5 of ROU. To look at the average waveform of HFRT-LC^{NE} events, we aligned LC^{NE} activity based on the start time of corresponding HFRTs, similar to an event-triggered average analysis. This indicated that following fentanyl administration, the initiation of LC^{NE} activity preceded the start of the HFRT on both Day 1 and Day 5, suggesting LC^{NE} is upstream of the motor output of respiratory activity (**Fig 16E**). However, ROC AUC analysis revealed chance ability (54%) of model predictions to distinguish between the distributions of HFRT-LC^{NE} event

amplitudes on Day 1 and Day 5 indicated by no departure from the unity line (**Supp Fig 4**). This demonstrates no change in LC^{NE} event amplitude between Day 1 and Day 5.

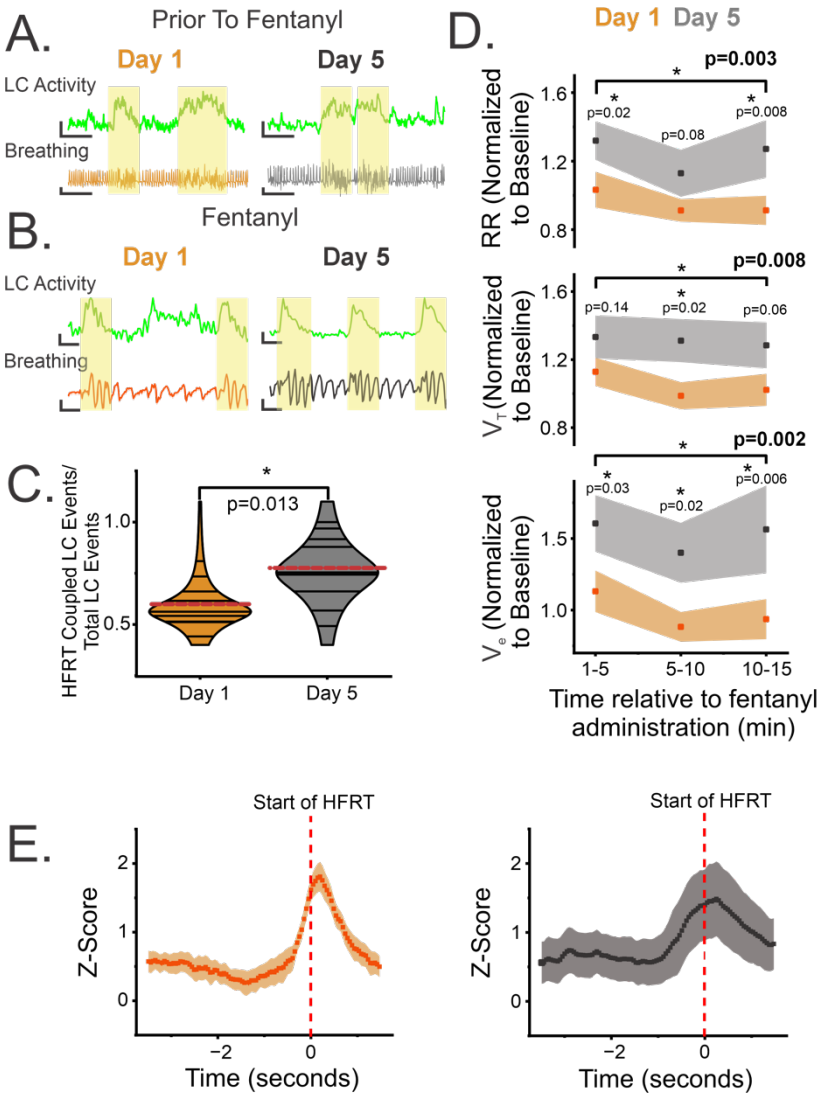

Figure 16. Repeat Opioid Use leads to a stronger coupling between LC^{NE} activity and breathing during respiratory depression

A) Representative traces of simultaneous fluorescent LC activity and breathing prior to fentanyl injection on Day 1 (left) and Day 5 (right). LC activity with corresponding HFRTs (HFRT-LC^{NE}) are highlighted in yellow. Scale bars: top: 2 z-score x 5 sec, bottom: 2 µL x 5 sec.

B) Representative traces of simultaneous fluorescent LC activity and breathing after fentanyl injection on Day 1 (left) and Day 5 (right). HFRT-LC^{NE} events are highlighted in yellow. Scale bars: top: 1 z-score, 1 sec, bottom: 2 µL x 1 sec.

C) Mean Proportion of HFRT coupled LC events out of the total Number of LC events on Day 1 (yellow) and Day 5 (gray) during OIRD. Paired t-test (p=0.013), (n=9). Red dotted line indicates group mean.

D) Mean RR (top), V_T (middle), and V_e (bottom) during HFRT-LC^{NE} events during minutes 0-5, 5-10, and 10-15 after fentanyl administration on Day 1 (yellow) and Day 5 (gray). RR, V_T, V_e: RM Two-Way ANOVA p<0.001. *Post hoc:* Tukey pairwise comparison (n=9). Significant interactions of Day 1 and Day 5 within time bins (min 0-5, 5-10, 10-15) are indicated.

E) Mean LC activity during HFRTs on Day 1 (yellow, left) and Day 5 (gray, right). The start of the HFRTs were aligned to the red dotted line at time 0. LC activity for 3 seconds prior and 2 seconds after the start of the HFRT was averaged across all events and all animals (n=9).

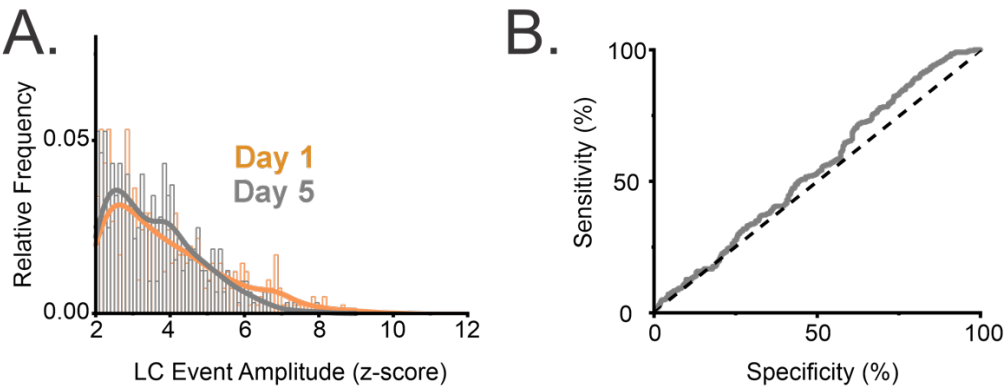

Supplemental Figure 4. Repeat Opioid Use does not alter HFRT-LC^{NE} event amplitude after fentanyl injection

A) Overlap of the frequency distribution of HFRT-LC^{NE} event amplitude on Day 1 (yellow) and Day 5 (gray).

B) ROC analysis of A. AUC of 54% reveals chance levels of model predictions distinguishing Day 1 from Day 5 distributions.

Adaptations in Locus Coeruleus activity that develops alongside tolerance to Opioid-Induced Respiratory Depression from Repeat Opioid Use is conditional

I. The context of fentanyl administration results in differences in tolerance to Opioid-Induced Respiratory Depression during the initial period after fentanyl administration

It is well established that tolerance to opioid overdose susceptibility and the analgesic effects of opioids are dependent on the environmental context of drug administration[8–18], a phenomenon called context-dependent tolerance. To test if tolerance to the respiratory depressive effects of opioids is also dependent on context, two additional days were added to the ROU protocol, where mice received fentanyl in the Fentanyl Paired context on one day, and fentanyl in the Saline Paired context on the other day. Only mice who developed tolerance during the first five days of the ROU protocol were included in this analysis (n=7/9). Breathing was compared between the two contexts. Prior to fentanyl administration, there were no differences in breathing when subjects were in the Fentanyl Paired and Saline Paired contexts, as demonstrated by similar RR, V_T, and V_e (**Supp Table 3**). During the initial five minutes after fentanyl injection, there was no decrease in breathing when subjects were in the Fentanyl Paired context, as evidenced by no change in RR, V_T, and V_e from prior to fentanyl. In the Saline Paired context, there was an initial decrease in V_e, which was driven by a decreased RR, as there was no change in V_T during the initial five minutes after fentanyl injection (**Table 7**). However, subjects do eventually reach equivalent steady state respiratory depression in both the Fentanyl Paired and Saline Paired contexts after this initial period (**Fig 17D)**. This suggests a difference in the onset of depression between contexts. Fitting a model to the data sets from each day revealed distinct patterns of

respiratory depression in the Fentanyl Paired context compared to the Saline Paired context in RR, V_T, and V_e (**Fig 17D,E**).

Metric	**Fentanyl Paired**		**Saline Paired**		**P-value**	**Test**
	Mean	Median	Mean	Median		
RR (bpm)	227 ± 23		242.1 ± 18.6		0.5	Paired t-test
TV (µL/*breath/g)	2.57 ± 0.28	2.3	2.78 ± 0.17	2.84	0.56	Wilcoxon Signed Ranks
MV (mL/min/g)	0.62 ± 0.1		0.73 ± 0.08		0.32	Paired t-test

Supplemental Table 3. Respiratory metrics prior to fentanyl administration in the Fentanyl Paired and Saline Paired contexts after ROU

Context	Metric	Baseline		Fentanyl		P-value	Test
Fentanyl Paired		Mean	Median	Mean	Median		
	RR (bpm)	227 ± 23		199.77 ± 17.34		0.06	Paired t-test
	TV (µL/*breath/g)	2.57 ± 0.28	2.3	2.66 ± 0.24	2.58	0.47	Wilcoxon Signed Ranks
	MV (mL/min/g)	0.62 ± 0.1		0.53 ± 0.06		0.15	Paired t-test
Saline Paired		Mean	Median	Mean	Median		
	RR (bpm)	242.11 ± 18.62		170.35 ± 14.5		0.0017	Paired t-test
	TV (µL/*breath/g)	2.78 ± 0.17		2.51 ± 0.14		0.16	Paired t-test
	MV (mL/min/g)	0.73 ± 0.08		0.45 ± 0.06		0.008	Paired t-test

Table 7. Respiratory metrics after fentanyl administration in the Fentanyl Paired and Saline Paired contexts after ROU

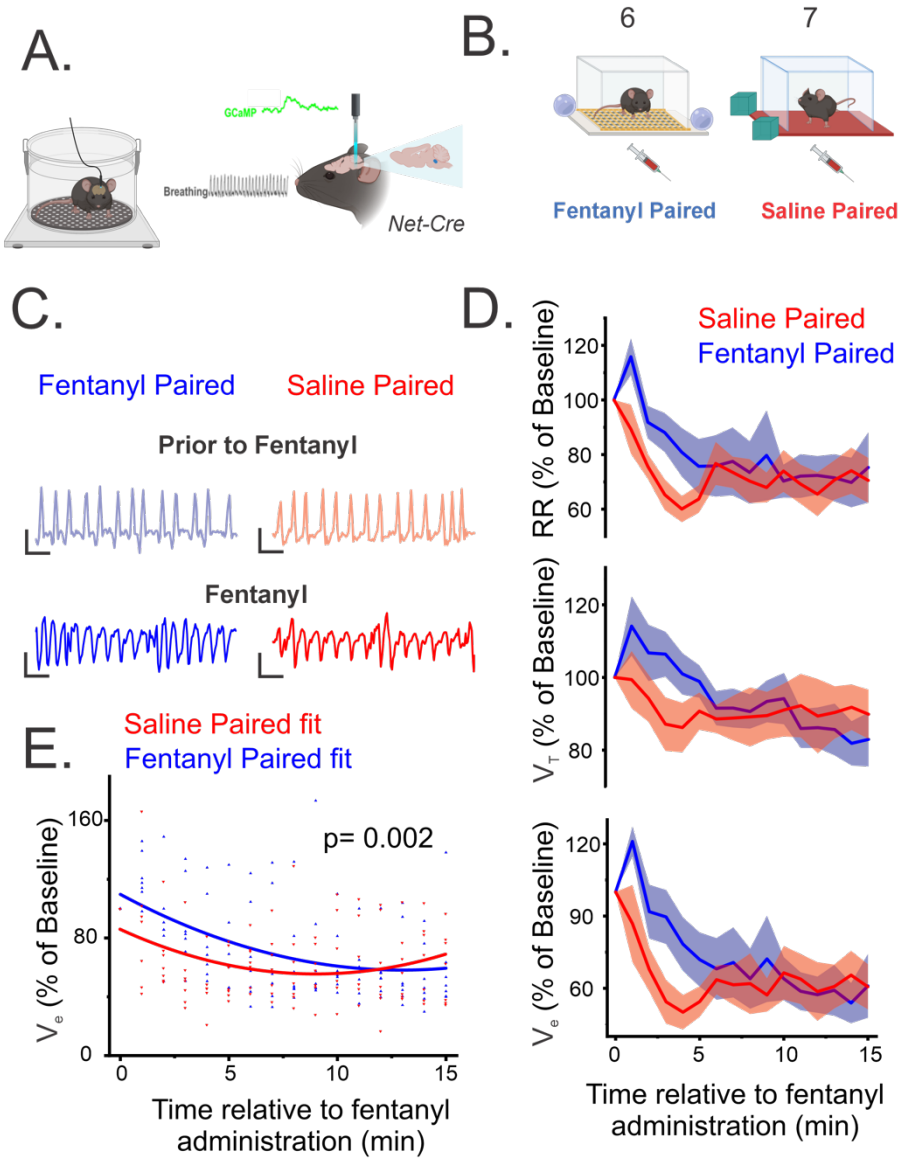

Figure 17. The context of fentanyl administration results in differences in the degree of Opioid-Induced Respiratory Depression during the initial period after fentanyl administration

A) Schematic showing simultaneous fiber photometry and plethysmography experimental setup with viral GCaMp8s and cannula placement in the LC in *Net-Cre* mice.

B) Schematic of days 6 and 7, after the 5-day ROU protocol. Mice receive fentanyl injection in the Fentanyl Paired context on one day and fentanyl in the Saline Paired context on the other

C) Representative breathing traces when in the Fentanyl Paired (blue) and Saline Paired (red), prior to fentanyl (top), and after fentanyl administration (bottom). Scale Bars: 1 sec x 3 µL.

D) Time course of mean RR (top), V_T (middle), and V_e (bottom) during OIRD in the Fentanyl Paired (blue) and Saline Paired (red) during OIRD. The shaded region represents the SEM (n=7).

E) Polynomial fits of V_e during OIRD breathing in the Fentanyl Paired (blue) and Saline Paired (red) data sets. RR (*data not shown*) (F-test, p=0.01, FP: R^2=0.17, SP: R^2=0.12), V_T (*data not shown*) (F-test, p=0.007, FP: R^2=0.22, SP: R^2=0.03), and V_e (F-test, p=0.002, FP: R^2=0.26, SP: R^2=0.11) fit comparisons were also different between Fentanyl Paired and Saline Paired. Raw data points for each animal (n=7) are plotted behind the V_e fits.

II. Coupling of Locus Coeruleus activity and breathing are attenuated when the location of fentanyl administration is altered

Because of the initial difference in respiratory depression between the Fentanyl Paired and Saline Paired contexts, we next sought to determine how the relationship between HFRTs and LC^{NE} activity changed during this initial period of depression depending on the context of fentanyl administration. We again see HFRT-LC^{NE} events prior to fentanyl, as well as during respiratory depression (**Fig 18A**). However, there are no differences in the percentage of HFRT-LC^{NE} events prior to fentanyl and after fentanyl administration between the two contexts. In the Fentanyl Paired context, there was no change in the percentage of HFRT-LC^{NE} events prior to fentanyl compared to after fentanyl injection (53% ± 13.2 and 71% ± 8.2, respectively). However, in the Saline-Paired context, the percentage of HFRT-LC^{NE} events increased from 25% ± 5.9% prior to fentanyl injection to 83% ± 5.2 after fentanyl injection (**Fig 18B**). Furthermore, during this initial period of depression, the degree of the increase in breathing during HFRT-LC^{NE} events was greater in the Fentanyl Paired context as compared to Day 1 of the ROU protocol (similar to results comparing Day 1 and Day 5). This was evident in V_e and driven by RR, as there was no change in V_T. This increase was not evident when the subjects were in the Saline-Paired context (**Fig 18C**). Direct comparison of the frequency distributions of V_e during HFRT-LC^{NE} events in the Fentanyl Paired and Saline Paired contexts reveals a rightward shift in the distribution curve, demonstrating that breathing during HFRT-LC^{NE} events is greater in the Fentanyl Paired context as compared to the Saline Paired. ROC AUC analysis

revealed greater than chance ability (68%) of model predictions to distinguish between the distributions of V_e during HFRT-LC^{NE} events in Fentanyl Paired vs. Saline Paired contexts (**Fig 18D**). This difference in the distributions suggests that OIRD V_e during HFRT-LC^{NE} is distinct based on the context of drug administration, and greater in the Fentanyl Paired context. Event-triggered average analysis again indicated that following fentanyl administration, the initiation of LC^{NE} activity preceded the start of the HFRT, again supporting LC^{NE} modulation being upstream of the motor output of respiratory activity (**Fig 18E**). ROC AUC analysis revealed chance ability (52%) of model predictions to distinguish between the distributions of HFRT-LC^{NE} event amplitudes between Fentanyl-Paired and Saline-Paired contexts indicated by no departure from the unity line (**Supp Fig 5**). This demonstrates no change in LC^{NE} event amplitude between Fentanyl Paired and Saline Paired contexts.

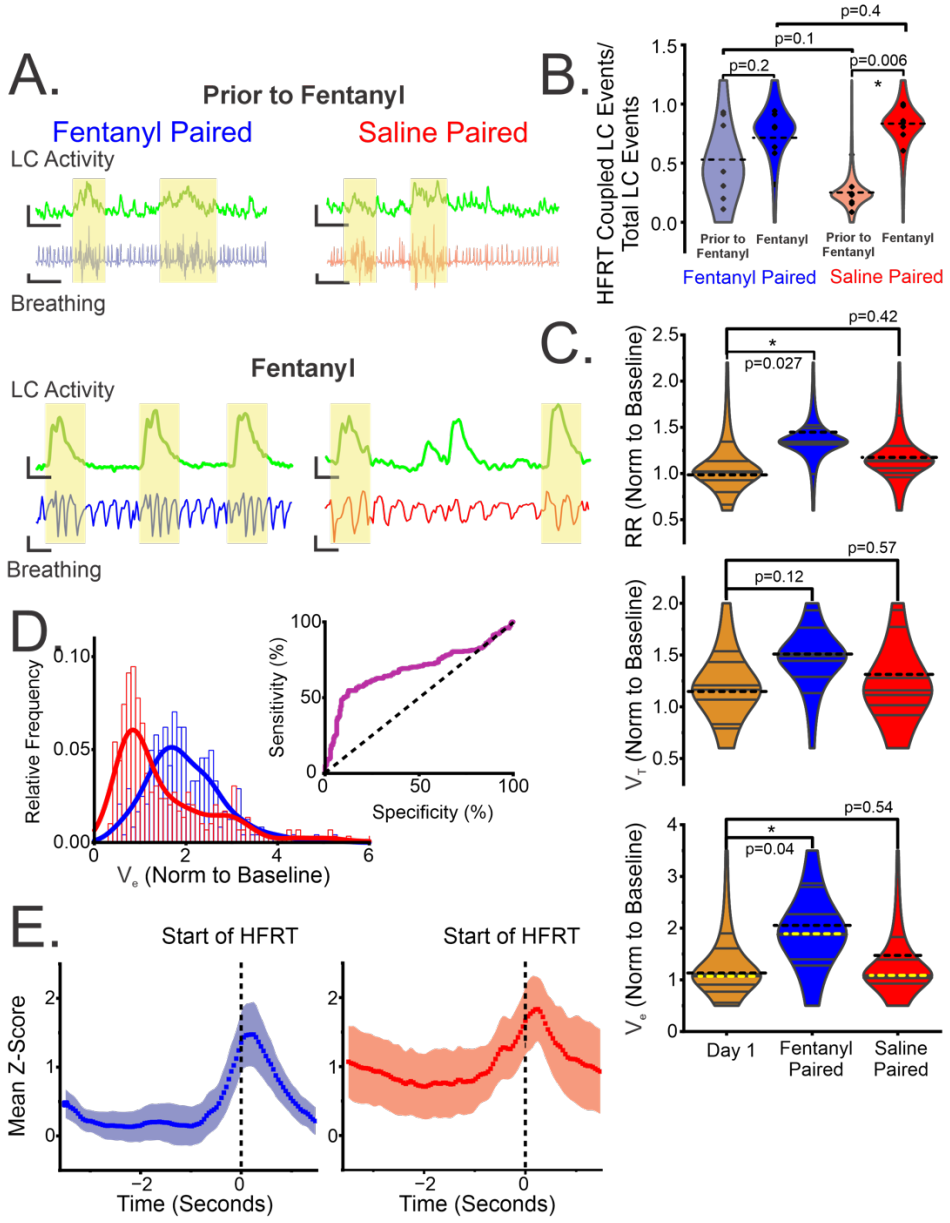

Figure 18. HFRT-LC^{NE} coupling is lost when the context of fentanyl administration is changed from the Fentanyl Paired to Saline Paired context

A) Top: Representative traces of simultaneous fluorescent LC activity and breathing prior to fentanyl injection in the Fentanyl Paired (left) and Saline Paired (right). LC activity with corresponding HFRTs (HFRT-LC^{NE}) are highlighted in yellow. Scale bars: top: 3 sec x 2 z-score, bottom: 3 sec x 2 µL. Bottom: Representative traces of simultaneous fluorescent LC activity and breathing after fentanyl injection in the Fentanyl Paired (left) and Saline Paired (right) contexts. HFRT-LC^{NE} events are highlighted in yellow. Scale bars: 1 sec x 1 z-score, bottom: 1 sec x 2 µL.

B) Mean Proportion of HFRT coupled LC events out of the total Number of LC events in the Fentanyl Paired (blue) and Saline Paired (red) contexts, both prior to fentanyl and during OIRD (minutes 0-5). RM Two-Way ANOVA $p<0.0001$. *Post hoc:* Tukey's pairwise comparison, n=7. Red dotted line indicates group mean.

C) Mean RR (top), V_T (middle), and V_e (bottom) during HFRT-LC^{NE} events during OIRD (minutes 0-5) on Day 1 (yellow), in Fentanyl Paired (blue), and Saline Paired (red). RR and V_T: RM One-Way ANOVA $p<0.0001$. *Post hoc:* Dunnett's pairwise comparison, control=Day 1. V_e: Friedman ANOVA $p<0.049$, *Post hoc:* Dunn's pairwise comparison. n=7. Red dotted line indicates group mean. Yellow dotted line indicates group median.

D) Frequency distribution of V_e during HFRT-LC^{NE} Events in the Fentanyl Paired (blue) and Saline Paired (red) contexts. Inset: ROC analysis of the frequency distribution. AUC of 68% reveals the model predictions distinguishing between the two distributions.

E) Mean LC activity during HFRTs in Fentanyl Paired (blue, left) and Saline Paired (red, right) contexts. The start of the HFRTs were aligned to the black dotted line at time 0. LC activity for 3 seconds prior and 2 seconds after the start of the HFRT was averaged across all events and all animals (n=7).

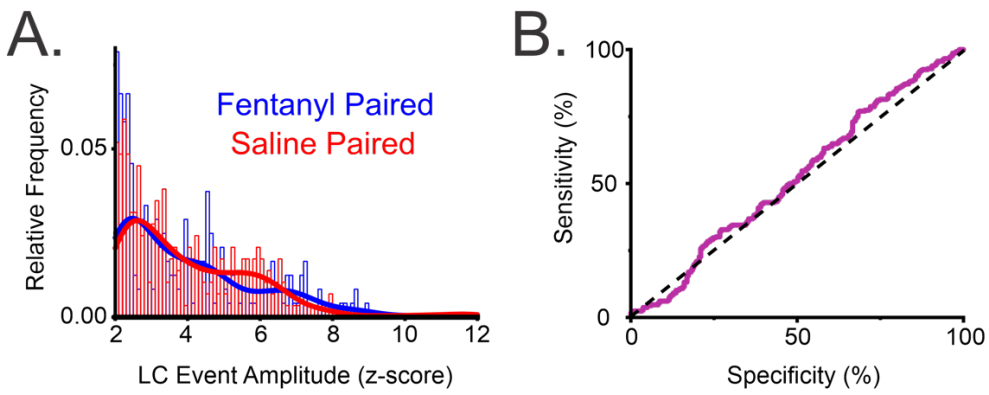

Supplemental Figure 5. The context of drug administration does not alter HFRT-LC^{NE} event amplitude after fentanyl injection

A) Overlap of the frequency distribution of HFRT-LC^{NE} event amplitude in Fentanyl Paired (blue) and Saline Paired (red).

B) ROC analysis of A. AUC of 52% reveals chance levels of model predictions distinguishing Fentanyl Paired and Saline Paired distributions.

III. The Hypercapnic Ventilatory Response is conserved in the Fentanyl Paired but not the Saline Paired context

OIRD leads to elevated CO_2 and decreased O_2. These changes in blood gases will initiate chemoreflex responses to stimulate breathing and return blood gases to normal levels. To determine potential mechanisms behind the context-dependent difference in OIRD and HFRT-LC^{NE} activity that was observed in the initial phase after fentanyl administration, we next sought to determine if context altered the Hypercapnic Ventilatory Response (HCVR), the chemoreflex resulting from elevated CO_2. An additional group of C57*BL6* mice underwent the five-day ROU protocol with context pairing. Whole-body plethysmography was used to measure their breathing throughout the protocol. On the two final days of the protocol, mice did not receive fentanyl but instead underwent an HCVR challenge in the Fentanyl Paired and Saline Paired contexts, and their breathing in response was measured (**Fig 19B**). This was compared to an initial HCVR response measured prior to the ROU protocol (Habituation). There was no difference in the HCVR response in the Fentanyl Paired context as compared to Habituation, evidenced by no change in V_e. This was due to an enhanced RR during HCVR in the Fentanyl Paired context. However, there was a decrease in the HCVR when subjects were in the Saline Paired context as compared to Habituation, demonstrated by a decrease in V_e. This reveals that a conserved HCVR only occurs when in the Fentanyl Paired context and corresponds to increased tolerance to OIRD (**Fig 19D**).

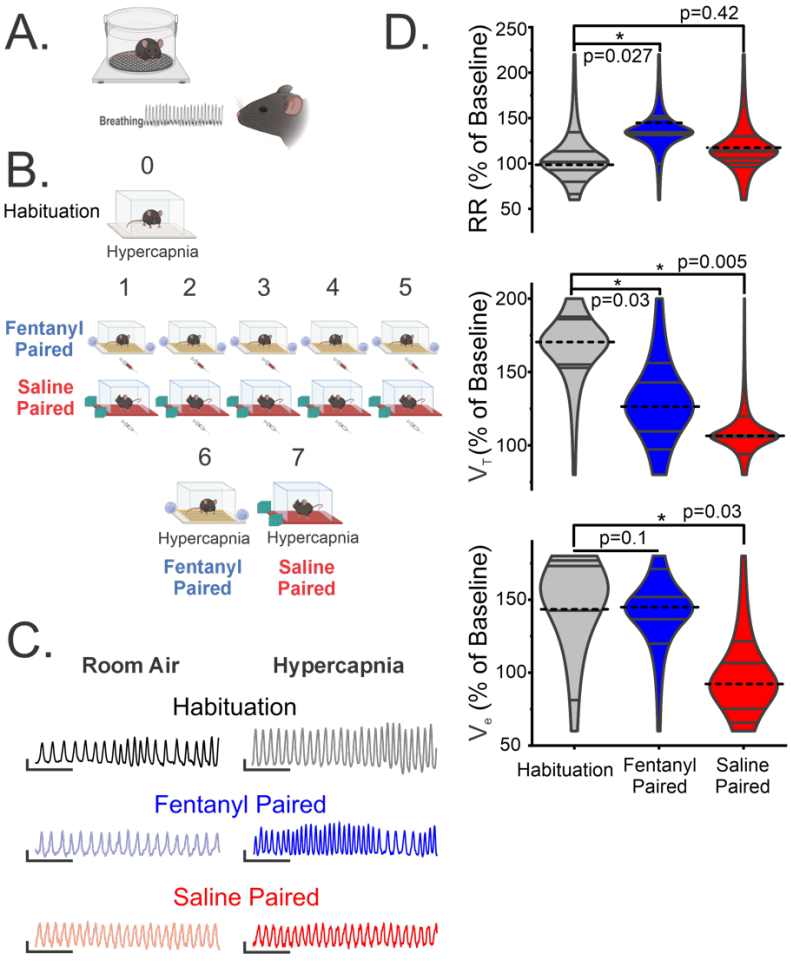

Figure 19. The Hypercapnic Ventilatory Response is conserved in the Fentanyl Paired, but not Saline Paired context

A) Schematic showing plethysmography only experimental setup in C57*BL6* mice.

B) Schematic of the 8-day experimental ROU protocol with hypercapnia testing. Top: prior to the ROU protocol, baseline HCVR is measured (Day 0, Habituation). Middle: Days 1-5, ROU protocol, e.g. daily fentanyl injection in the Fentanyl Paired context and daily saline injection in the Saline Paired context. Bottom: Days 6-7, HCVR is measured in the Fentanyl Paired and Saline Paired contexts.

C) Representative breathing traces during Room Air (left) and Hypercapnic (right) conditions on Habituation Day (top), in the Fentanyl Paired context (middle) and in the Saline Paired context (bottom). Scale bars: 1 sec x 3 µL.

D) Mean RR (top), V_T (middle), and V_e (bottom) on Habituation (gray), in Fentanyl Paired (blue) and Saline Paired (red) contexts. RR: RM One-Way ANOVA $p<0.002$, V_T: RM One-Way ANOVA $p<0.0002$, V_e: RM One-Way ANOVA $p<0.002$, *Post hoc:* Dunnett's pairwise comparison, control=Habituation, n=4. Red dotted line indicates group mean.

Enhanced Locus Coeruleus activity is sufficient for improving Opioid-Induced Respiratory Depression

I. *Optogenetic stimulation of the Noradrenergic cells of the Locus Coeruleus results in less respiratory depression during acute fentanyl administration*

Trials in the ROU protocol where subjects spontaneously overdosed revealed that overdose consisted of a cessation of HFRT- LC^{NE} events, suggesting their role in combating severe respiratory depression and subsequent overdose (**Supp Fig 6**). Because we observed increased HFRT-LC^{NE} events as well as enhanced breathing during these events with the development of tolerance to OIRD after ROU, we next sought to determine whether increasing LC^{NE} activity reduced respiratory depression after acute fentanyl administration. We used *Net-Cre/Ai27D* mice for selective expression of ChR2 in LC^{NE} neurons ($ChR2^{+/+}$) and C57*BL6* as sham controls ($ChR2^{fl/fl}$). Simultaneous plethysmography and optogenetics were used to measure breathing while stimulating LC^{NE}. While both groups experienced respiratory depression, stimulation of LC^{NE} resulted in less respiratory depression after acute fentanyl administration. This difference was seen in RR and V_e, but not V_T (**Fig 20C,D**). These results suggest that adaptations in V_T with ROU are due to other pharmacodynamic mechanisms outside of enhanced LC^{NE} activity.

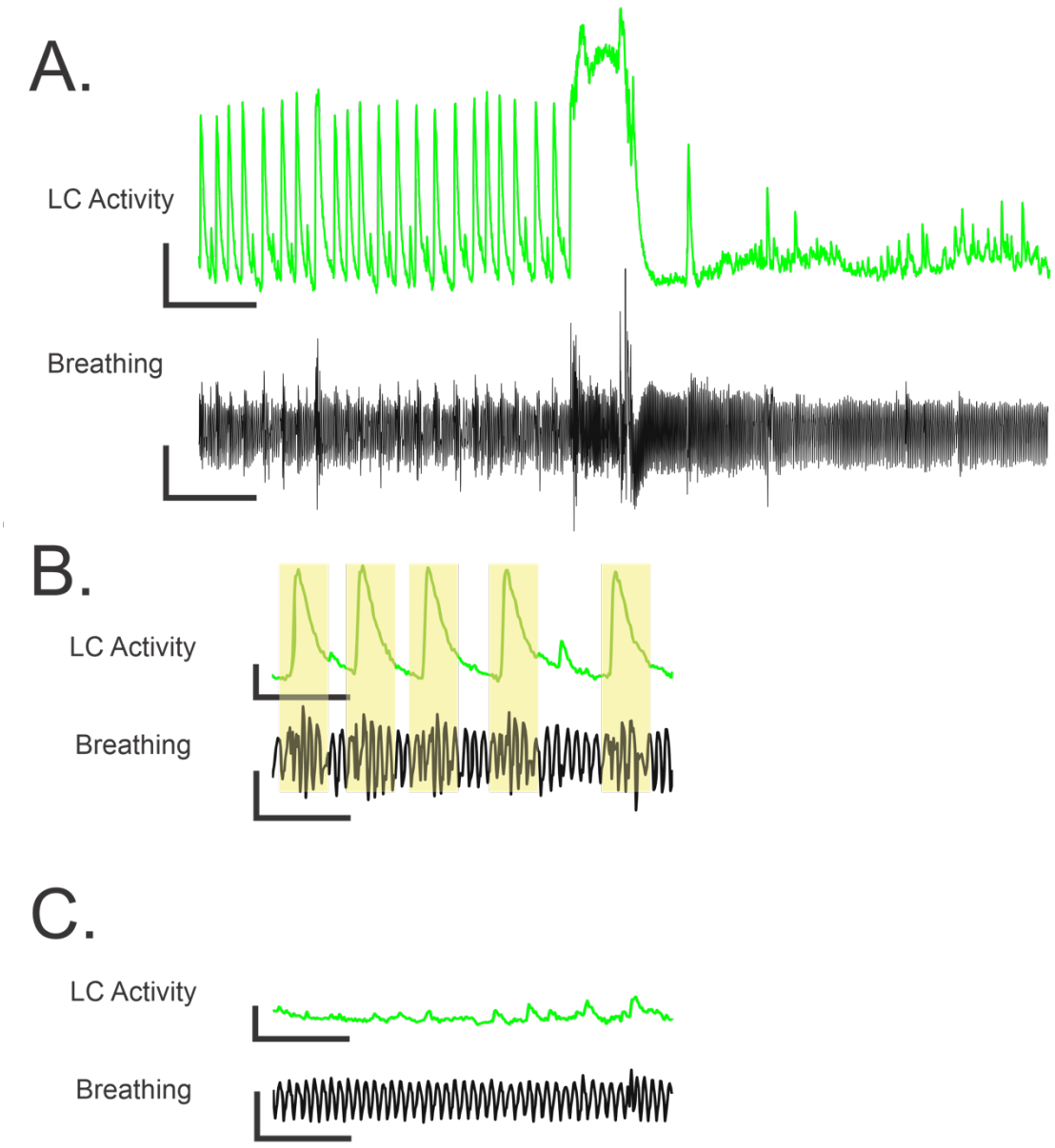

Supplemental Figure 6. HFRT-LC^{NE} activity ceases during fentanyl-induced overdose

A) Representative traces of simultaneous LC^{NE} activity and breathing before and during fentanyl-induced overdose. Scale Bars: (top) 25 sec x 2 z-score, (bottom) 25 sec x 3 µL.

B) Zoomed in representative trace prior to overdose showing simultaneous LC^{NE} activity and breathing consisting of HFRT-LC^{NE} events (highlighted in yellow). Scale Bars: (top) 5 sec x 2 z-score, (bottom) 5 sec x 3 µL.

C) Zoomed in representative trace after overdose showing cessation of both LC^{NE} activity and HFRT breathing. Scale Bars: (top) 5 sec x 2 z-score, (bottom) 5 sec x 3 µL.

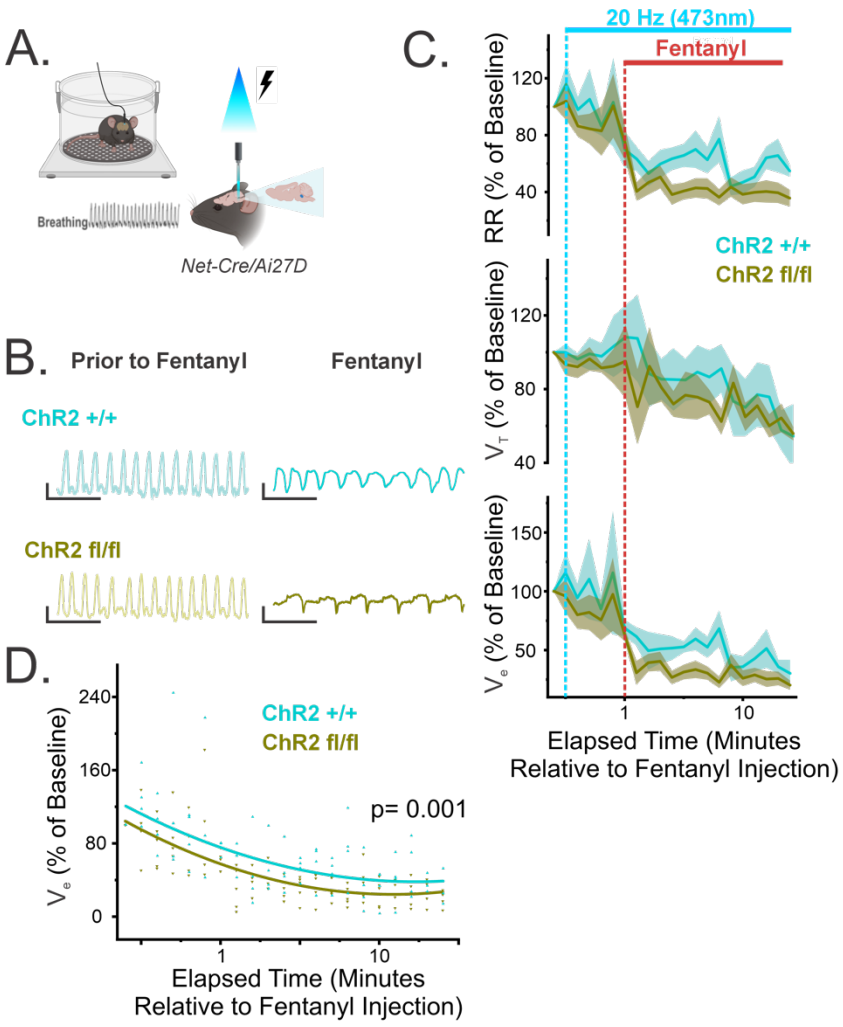

Figure 20. Optogenetic stimulation of LC^{NE} results in less respiratory depression during acute fentanyl administration

A) Schematic showing simultaneous optogenetics and plethysmography experimental set up with cannula placement in the LC in *Net-Cre/Ai27D* mice.

B) Representative breathing traces in the ChR2$^{+/+}$ (experimental, light blue) mice and in ChR2$^{fl/fl}$ (sham, green) mice. Scale bars: 1 sec x 2 µL.

C) Time course of mean RR (top), V_T (middle), and V_e (bottom) with 20 Hz stimulation (minutes -5 to 0), and during OIRD after fentanyl administration at time 0, with concurrent 20 Hz stimulation (minutes 0-15) in ChR2$^{+/+}$ (light blue n=5) and ChR2$^{fl/fl}$ (green, n=5).

D) Polynomial fits of V_e during OIRD breathing in ChR2$^{+/+}$ (light blue) and ChR2$^{fl/fl}$ (green) data sets. RR (*data not shown*) (F-test, p<0.0001, ChR2$^{+/+}$: R^2=0.35, ChR2$^{fl/fl}$: R^2=0.56) and V_e (F-test, p=0.001, ChR2$^{+/+}$: R^2=0.42, ChR2$^{fl/fl}$: R^2=0.57) fit comparisons were different between ChR2$^{+/+}$ and ChR2$^{fl/fl}$ groups. V_T (*data not shown*) (F-test, p=0., ChR2$^{+/+}$: R^2=0.16, ChR2$^{fl/fl}$: R^2=0.25) was not different. Raw data points for each animal (n=5 per group) are plotted behind the V_e fits.

Discussion

Summary of Major Findings

Despite the development of tolerance to the effects of opioids with Repeat Opioid Use (ROU), repeat users are driving the opioid epidemic and overdose deaths[19]. Respiratory depression is a hallmark of opioid overdose, yet the neural mechanisms of how tolerance to respiratory depression develops with ROU are not well understood. In Chapter 1, we find that five days of ROU results in tolerance to Opioid-Induced Respiratory Depression (OIRD) (i.e. progressively less respiratory depression after fentanyl administration throughout the 5 days) in the majority of animals. We demonstrated a neural correlate of this tolerance by showing that ROU resulted in less suppression of the preBötC by opioid neuromodulation. However, it still remained unanswered how susceptibility to OIRD and opioid overdose changes despite ROU. In this study, we demonstrate a novel neural mechanism of tolerance to OIRD with ROU.

In this study, we find that tolerance to OIRD following ROU is associated with an enhancement of LC^{NE} activity that is coordinated with High-Frequency Respiratory Transients (HFRT-LC^{NE}). Furthermore, this coordinated LC^{NE} activity correlates with a greater stimulation of breathing after ROU. Importantly, we determine that enhanced HFRT-LC^{NE} activity is conditional and dependent upon the environmental context of drug administration. Despite having repeatedly received fentanyl and developed a tolerance to OIRD, the administration of fentanyl in the Saline Paired context (i.e. a context not previously associated with the drug) attenuates tolerance to OIRD and the degree to which breathing is increased during HFRT-LC^{NE} activity. The difference in the degree of depression is most prominent in the initial period after fentanyl administration. Furthermore, the Hypercapnic Ventilatory Response (HCVR) is conserved when subjects are in the Fentanyl Paired context, but not the Saline Paired, suggesting

that chemosensory responses of the respiratory network are not solely reflexive, but can be influenced by higher-order brain areas. Finally, we show that excitation of LC^{NE} neurons is sufficient to attenuate the degree of respiratory depression after acute fentanyl administration. Not only do these results implicate LC^{NE} in a novel mechanism of tolerance to OIRD, but they highlight the labile nature of drug tolerance and how susceptibility to OIRD and subsequent overdose is dynamic and dependent upon exteroceptive stimuli. Together these results suggest that failure to establish associations of drug effects and drug cues or removing drug cues prior to drug taking increases OIRD and overdose susceptibility.

Acute Opioid Administration effects on LC^{NE} activity and LCNE adaptations following Repeat Opioid Use

This is the first study to investigate the effects of acute fentanyl administration on LC^{NE} activity in awake, freely behaving mice. Both *in vivo and in vitro* work have previously shown that application of opioids to the LC results in decreased neurotransmitter release, hyperpolarization, and decreases in spontaneous firing rate from opioid-mediated mechanisms of increase GIRK channel conductance and voltage-gated Ca^{2+} channel inhibition[20,21]. Contrary to these findings, we find that in intact, awake mice, acute fentanyl administration results in an overall increase in LC^{NE} activity as compared to LC^{NE} activity prior to fentanyl administration. The disagreement between our results and previous findings could stem from our use of a systemic injection of fentanyl as compared to the direct application of an opioid onto the LC. μ-opioid receptors (μ-OR) are expressed throughout the brain, and the increased activity in the LC that we observe could be the result of enhanced activity in brain areas, such as the Ventral Tegmental Area (VTA), that the LC receives input from. Additionally, it could be due to

increased activity in peripheral oxygen sensing areas, such as the Carotid Bodies, which sense fentanyl-induced hypoxia and relay this information to the central nervous via the Nucleus Tractus Solitarius (NTS), which projects to the LC. Furthermore, previous *in vivo* studies were performed under anesthesia, which induces a decreased arousal state, that corresponds to deceased tonic LC activity, potentially confounding the effect of opioids on LC[22,23].

We do not find that the increase in LC activity in response to fentanyl is sustained with ROU. Our data shows that as tolerance to OIRD develops with repeat use, the fentanyl-induced increase in LC activity during respiratory depression ceases. The increase in overall LC^{NE} activity during initial fentanyl administration could be in response to severe respiratory depression, which causes deviations in blood gases (i.e. increases in CO_2 and decreases in O_2). Increased CO_2 will stimulate the LC activity to improve breathing and resolve blood gas deviations[24–26]. LC stimulation can enhance inspiratory network activity when the network is in a lower excitatory state[27], further supporting increased LC activity during acute opioid administration as a mitigation effort to combat respiratory depression. Our results show that on Day 1 of the ROU protocol, LC^{NE} activity precedes HFRT initiation, suggesting that LC^{NE} mechanisms could be involved with stimulating breathing in response to respiratory depression. This finding is consistently seen throughout the final three days of the ROU protocol (Day 5, Fentanyl Paired and Saline Paired), but we find that HFRT-LC^{NE} activity is enhanced after ROU as compared to Day 1. In Chapter 1, we found acute fentanyl administration inhibited the normally positive relationship between minute ventilation (V_e) and oxygen consumption (VO_2). After ROU, fentanyl no longer inhibits this positive relationship. The increased overall LC activity on Day 1 paired with the mismatch between V_e and VO_2 suggests that the recovery of this positive relationship by Day 5 may be a function of decreased metabolic demand from a lack

of fentanyl-induced increases of uncoordinated LC^{NE} activity. The adaptation of decreased metabolic demand is particularly important during hypoxic conditions, such as OIRD.

A challenge in treating fentanyl-induced overdose is wooden chest syndrome, which is defined by increased rigidity in the diaphragm, chest wall, and upper airways[28]. Enhanced muscle rigidity on Day 1 could contribute to the mismatch observed between V_e and VO_2. Wooden chest syndrome is fentanyl- or fentanyl-analog-induced respiratory depression and does not occur with morphine, heroin, and other naturally derived opioids[28]. Lesion of the LC or blocking α_1 adrenergic receptors will attenuate fentanyl-induced muscle rigidity, suggesting a role of noradrenergic release from the LC in the generation of wooden chest syndrome (Liu 1989). Importantly, naloxone does not reverse it. Integrating enhanced LC activity and the mismatch between V_e and VO_2 with what is known about wooden chest syndrome could suggest that the enhanced overall LC^{NE} activity on Day 1 results in a greater degree of wooden chest syndrome as compared to Day 5. We postulate that HFRTs represent a cyclical pattern of breaking wooden chest syndrome. Results from Chapter 1 show that tolerance to opioid inhibition develops with ROU at the level of the preBötC, suggesting enhanced inspiratory drive during respiratory depression after ROU. A conservation of the HCVR was demonstrated in the Fentanyl-Paired context, as well as the difference in the initial degree of respiratory depression. We hypothesize that ROU increases inspiratory drive and primes the respiratory network to respond to increased CO_2, resulting in the start of the HFRT. As breathing increases during the HFRT, CO_2 decreases, and respiratory drive decreases with it, resulting in wooden chest syndrome overcoming respiratory drive again. The functional organization of LC^{NE} neurons is proposed to be composed of neuronal ensembles that have distinct inputs and outputs and promote different behavioral outputs and functions. This raises the potential that coordinated

HFRTT-LC^{NE} events may be a part of a distinct functional ensemble that provides inspiratory drive, while LC^{NE} activity that is not correlated with changes in breathing could contribute to wooden chest syndrome. A future direction to validate these hypotheses is to measure muscle activity in conjunction with breathing and LC^{NE} activity to confirm when wooden chest syndrome is present.

Repeat Opioid Use impacts breathing and tolerance to Opioid-Induced Respiratory Depression

Our results demonstrate that after ROU and the development of tolerance to OIRD, fentanyl no longer significantly decreases Tidal Volume (V_T). We find that this maintenance of V_T after fentanyl administration occurs whether the subject is in the Fentanyl Paired or Saline Paired context. This tolerance to fentanyl reflected in the V_T of breathing is also demonstrated at the level of the preBötC. In Chapter 1, our investigations revealed that ROU increases the tolerance of preBötC suppression by opioids in both the frequency and amplitude of the inspiratory burst, but that while increasing dosages of the μOR agonist DAMGO will cause a decrease in frequency, the amplitude is not affected, even at high dosages. While some neuronal subpopulations of preBötC neurons are involved in both rhythm (frequency) and pattern (amplitude) generation, other subpopulations only impact either rhythm or pattern generation[29]. Future investigations are needed to resolve the development of pharmacodynamic tolerance in the subpopulations of preBötC neurons responsible for rhythm versus pattern generation of inspiratory rhythmogenesis. We find that the degree of depression in Respiratory Rate (RR) is differentially affected by the context of drug administration, while V_T is not. This suggests an additional mechanism of tolerance outside of increased inspiratory drive from the preBötC that leads to greater RR after fentanyl administration. Furthermore, our optogenetic experiments

support the hypothesis of enhanced LC^{NE} activity having a greater effect on maintaining RR after fentanyl administration than V_T. We find that stimulating LC^{NE} prior to and during fentanyl administration improves RR during OIRD, but does not change V_T. These data suggest the importance of enhanced LC^{NE} activity as a mechanism to increase RR during respiratory depression, while mechanisms that support V_T enhancement appear at the level of the preBötC.

Locus Coeruleus activity coupled with breathing minimizes Opioid-Induced Respiratory Depression

Despite the generalized reduction in LC^{NE} activity in response to fentanyl administration after five days of ROU, the proportion of LC^{NE} activity that correlates with HFRTs increases by Day 5 as compared to Day 1. The increase of this coordinated HFRT-LC^{NE} activity occurs with the development of tolerance to OIRD, suggesting an adaptive role of LC^{NE} and its coupling with breathing in mitigating respiratory depression. It is well known that acute opioid use causes suppression of activity in areas of the brainstem that are important for breathing, such as the PreBötzinger Complex (preBötC) and Kolliker Fuse Nucleus (KF)[30,31]. Repeat opioid use does not lead to tolerance at the level of the KF[32] and the correlation between its activity and breathing that exists under room air ceases during OIRD[33]. While the KF does not develop tolerance, our data from Chapter 1 demonstrates that network activity in the preBötC does develop tolerance to opioid neuromodulation with ROU.

The LC has been shown to develop cellular tolerance to opioid neuromodulation[20]. We show that LC^{NE} activity correlates with breathing during respiratory depression on first fentanyl exposure as well as after repeat use. Additionally, we observed that when subjects overdosed, there was a complete cessation of LC^{NE} activity as well as corresponding HFRTs. This example

further elucidates the importance of LC^{NE} in maintaining breathing during OIRD. In Chapter 1 we used the μ-OR specific agonist DAMGO to show that μ-OR specific tolerance develops with ROU at the level of the preBötC. Switching the context of drug administration to the Saline Paired context results in less tolerance to OIRD. This suggests that the development of tolerance at the level of the preBötC is not sufficient to prevent respiratory depression, and that there are additional mechanisms of tolerance that involve enhanced coordinated LC activity and breathing. There are known projections from LC to preBötC[33]. Future studies should explore if these direct projections are active during the HFRT-LC^{NE} activity we observed and if this alters inspiratory drive through a NE-dependent mechanism or if it is through another neurotransmitter, such as glutamate.

Locus Coeruleus activity and Noradrenergic tone stimulate breathing

The LC is not a canonical central respiratory control center but it is well-documented that LC activity can stimulate breathing and will increase its activity in response to elevated CO_2 to stimulate breathing and return blood gases to homeostatic levels[24–26]. The LC is the primary source of adrenergic drive in the brain and projects to the preBötC and throughout the respiratory network[34,35]. It has been well-established that NE impacts intrinsic bursting properties of preBötC neurons to enhance both the amplitude and frequency of inspiratory rhythmogenesis by recruiting more cells as pacemaker neurons, leading to a reconfiguration of the network towards facilitation into a state more difficult to perturb[27]. Blocking α_1 receptors in the isolated preBötC slice will remove NE-mediated inspiratory facilitation. Unpublished data from our lab suggests that NE enhances synaptic properties by increasing inspiratory drive potential via a NMDAr mediated mechanism. These data demonstrate the possibility of the enhancement of HFRT-LC^{NE}

activity to be the result of direct NE projections from LC to the preBötC to enhance inspiratory drive and in turn, reduce susceptibility to opioid inhibition. Future studies should examine the release of NE in preBötC and other areas of the respiratory network, such as the KF, or RTN, after fentanyl administration and assess whether this NE release correlates with the HFRT-LC^{NE} activity observed. Using retrograde GCaMP viral techniques to selectively monitor activity in LC projections to preBötC, KF, or RTN would also further elucidate the circuit mechanism behind these findings.

Network state and the order of neuromodulation matters to maintain stable breathing during Opioid-Induced Respiratory depression

The LC is involved with other behavioral states relevant to repeat drug use, such as cue-reward processing [36]. Similarly to dopaminergic activity in the VTA, repeated association of a cue with a subsequent reward results in an increase of LC^{NE} activity with the presentation of the cue and the initiation of movement towards the reward, but prior to the receipt of the reward[36,37]. Our results show that with the development of tolerance to OIRD, there is enhanced HFRT-LC^{NE} activity. If this is a result of enhanced noradrenergic drive in the respiratory network directly from LC, we hypothesize that it begins to occur prior to fentanyl administration if the subjects are in the Fentanyl-Paired context, but does not if they are in the Saline Paired context. This is interpreted from acute fentanyl administration leading to an increase in LC activity after fentanyl administration, as well as the increase in the proportion of HFRT-LC^{NE} events in the Saline Paired context after fentanyl injection but no increase in the Fentanyl Paired context. Our results display a shift towards a network state where LC^{NE} activity is more tightly coupled to autonomic control, as evidenced by the greater stimulation of breathing during HFRT-LC^{NE} events when

subjects are in the Fentanyl-Paired context. Burgraff et al. previously showed that increased synchronization in the preBötC minimizes opioid-induced depression of the network[38]. Because NE stimulates rhythmogenesis[27], increased NE tone prior to opioid modulation could mimic an increased synchronized state in preBötC that results in decreased susceptibility to inhibition by opioids. Indeed, unpublished data from the lab shows when adrenergic tone precedes the addition of DAMGO to the isolated preBötC slice, opioid neuromodulation has less of a destabilizing effect on rhythmogenesis. This idea is supported *in vivo* with our optogenetic studies that stimulate LC^{NE} activity both prior to and during fentanyl to mitigate OIRD in subjects. Additional studies should combine optogenetic and fiber photometry approaches to generate the same pattern of LC activity observed in our fiber photometry experiments to more specifically test whether this pattern of activity is sufficient to mitigate respiratory depression and whether this specific pattern is necessary before fentanyl administration and subsequent respiratory depression occurs.

The importance of context-pairing in the maintenance of tolerance to Opioid-Induced Respiratory Depression

Previous work has identified exteroceptive cues, such as the context of drug administration, as an important factor in the maintenance of tolerance to the effects of opioids. While these previous studies have focused on analgesic effects and overdose susceptibility, this study demonstrates how tolerance to OIRD is likewise contingent upon the context of drug administration. Unlike our comparisons of Day 1 and Day 5 of the ROU protocol where we see differences in OIRD that extend throughout the 15-minute fentanyl protocol, when comparing OIRD between Fentanyl-Paired and Saline-Paired contexts, the difference observed is the degree

of OIRD during the initial five minutes after fentanyl administration. The increase in the proportion of HFRT-LC^{NE} events in the Saline-Paired context *after* fentanyl administration could be interpreted as the loss of a pre-emptive, compensatory role of LC^{NE} activity that occurs prior to fentanyl administration to combat subsequent OIRD. This is not observed in the Fentanyl Paired context. The LC is chemosensitive and will increase its activity to stimulate breathing in response to elevated CO_2. We find that subjects have a conserved Hypercapnic Ventilatory Response (HCVR) after the ROU protocol when they are in the Fentanyl Paired context, but an attenuated HCVR when in the Saline Paired context. One could extrapolate these results to suggest that when in the Fentanyl Paired context, there is heightened LC^{NE} activity prior to drug administration, facilitating a stronger HCVR in response to fentanyl-inducing respiratory depression and elevated blood gas levels of CO_2. This enhanced HCVR could reflect the hypothesized shift in the state of the respiratory network by LC^{NE}, which increases the stabilization and synchronization of the respiratory network in preparation for fentanyl perturbation. Again, using retrograde GCaMP viral techniques to measure activity in LC to RTN projections will help answer the mechanism behind the conserved HCVR in the Fentanyl Paired context.

We do not see any direct differences in breathing prior to fentanyl administration between the Fentanyl Paired and Saline Paired contexts on Day 6 and Day 7 of the protocol. We also see no differences in breathing prior to fentanyl on Day 1 and Day 5 when mice are in the Fentanyl Paired context. However, we see that V_e is decreased in the Saline Paired context on Day 5 as compared to Day 1, driven by a decrease in RR as V_T is unchanged. Day 1 is the first time mice are in both the Fentanyl Paired and Saline Paired contexts. As a result of each context being novel on this first day, we would expect enhanced arousal and increased breathing. Similar

breathing between Day 1 and Day 5 in the Fentanyl Paired context could indicate that by Day 5, the Fentanyl Paired context remains a salient stimulus, not because it is novel as it is on Day 1, but because it predicts the subsequent receipt of fentanyl reward. This conserved enhancement in breathing could suggest a conditioned compensatory response to combat OIRD that occurs when mice are in the Fentanyl Paired context. Thus, the decrease in RR and V_e seen in the Saline Paired context on Day 5 could reflect habituation to the Saline Paired context because it is no longer a salient novel stimulus, nor does not predict a drug reward.

While the difference in the pattern of OIRD between the Fentanyl Paired and Saline Paired contexts is only evident in the initial five-minute period after fentanyl administration, this period of depression is clinically relevant in reducing overdose risk. Fentanyl induces a much more rapid decline in ventilation than morphine or heroin[39,40], shortening the naloxone intervention window in fentanyl-induced overdose. However, our data suggests the ability context of drug administration to increase tolerance during the initial period of respiratory depression, potentially extending the window of intervention or preventing the initial rapid decline in ventilation until fentanyl has begun to metabolize into its inactive form[40].

The role of HFRT-LC^{NE} activity

The LC is not a homogeneous population of neurons as was once thought. Recent work has suggested that LC neurons form functional ensembles depending on their projection sites and the distinct behaviors they mediate[41,42]. Gap junction-mediated rhythmic, synchronous oscillations of activity have been reported in the LC[41]. The results from this study reflect both of these hypotheses. We see at least two distinct types of LC^{NE} activity, 1) those that are correlated with HFRTs (HFRT-LC^{NE}) and 2) those that are not. HFRT-LC^{NE} activity appears to be in a

rhythmic oscillation. With the development of tolerance to fentanyl from ROU, we see the proportion of the HFRT-LC^{NE} events increase and a stronger degree of increased breathing during those LC^{NE} events. While we do not have proof of causation, these results suggest that there is a subpopulation of LC^{NE} neurons that could be a part of the circuitry mediating the HFRTs during fentanyl to maintain breathing and that the synaptic strength in this connection is increased with ROU. This could happen by 1) a reconfiguration of the LC^{NE} network that increases the number of neurons responsible for stimulating breathing, 2) by increasing the number of action potentials from this population of LC^{NE} neurons, and 3) LC^{NE}-mediated synaptic plasticity occurring at post-synaptic sites, such as the preBötC. However, we see no difference in the amplitude of HFRT-LC^{NE} events on the first day of fentanyl administration (Day 1) or after ROU (Day 5). We also see no difference in the amplitude depending on the context of drug administration (Fentanyl-Paired, Saline-Paired). This indicates that this strengthening seen between breathing and HFRT-LC^{NE} events with ROU does not occur based on presynaptic changes in the LC. We hypothesize the possibility of a direct pathway from LC to preBötC and that the rhythmic activity of HFRT-LC^{NE} is phasic bursting, leading to the co-release of NE and glutamate in the preBötC. ROU and continued co-release potentiate the synaptic connections between LC^{NE} and glutamatergic inspiratory neurons in the preBötC. Thus, neurotransmitter release from the LC in preBötC increases inspiratory drive to a greater degree after ROU, leading to the larger increases in breathing during HFRT-LC^{NE} events that we see by Day 5. Future studies should aim to investigate if these HFRT-LC^{NE} events lead to the release of NE in the preBötC and how undergoing the ROU protocol alters the postsynaptic response of inspiratory neurons to NE.

The Locus Coeruleus may be driving microarousals to combat opioid overdose

The LC is also important for arousal, another important brain state relevant to opioid use[43]. Breathing is enhanced during behavioral states of vigilance, arousal, and drug-seeking behaviors[44,45]. One possible explanation for HFRT-LC^{NE} activity is that these are microarousals that, for a short period of time, lead to a stimulation of breathing, which in turn results in enough ventilation in the lungs to prevent further respiratory depression and overdose. Arousal during altered states of consciousness, such as sleep, occurs in response to changes in blood gases[46] and may also occur during overdose. There is a subset of neurons in the preBötC that are not required for inspiratory rhythmogenesis but project to and increase activity in the LC and contribute to arousal behaviors[44]. These preBötC to LC projections communicate the state of the respiratory network, which the LC then relays throughout the brain, including to cortical areas that support arousal. Future studies should investigate the potential of microarousals during fentanyl by measuring norepinephrine release or EEG activity in brain areas of vigilance, such as the Prefrontal Cortex (PFC), and their correlation to LC^{NE} rhythmic activity seen during respiratory depression. Retrograde viral techniques could again be employed to specifically investigate the activity LC projections to PFC during OIRD and its relationship to HFRTs.

Circuit Hypotheses for Context-Dependent Tolerance to Opioid-Induced Respiratory Depression

While Chapter 1 uncovers one mechanism of pharmacodynamic tolerance with ROU, the present study demonstrates that there are circuit-based central mechanisms that support tolerance to OIRD with ROU. The development of context-dependent tolerance to fentanyl involves changes in LC activity and its relationship with breathing, but other areas of the brain are certainly involved in this phenomenon.

Fentanyl is a rewarding stimulus and will lead to an increase in VTA activity. Context-dependent tolerance is a learned mechanism of tolerance and will involve activation of the hippocampus. It has been shown that simultaneous activation of VTA terminals in the hippocampus and glutamatergic Schaffer collaterals resulted in LTP, and aided in contextual learning[47]. Both the VTA and the LC project to the hippocampus and increased LC activity from acute fentanyl administration could facilitate LTP in the hippocampus and subsequent associative learning of the environmental context with the opioid drug reward. This may lead to increased VTA and hippocampal activity when the animals are in the Fentanyl Paired context that then relays this contextual information to the LC, which in turn projects to respiratory circuitry and results in context-dependent tolerance to OIRD. Based on our findings from this study, we present two potential circuits that contribute to the phenomenon of context-dependent tolerance to OIRD.

The first is a descending pathway that projects directly from LC to areas in the respiratory network that are responsible for pattern and rhythm generation, such as the preBötC, and sensory input, such as the RTN. As mentioned, it is well described in the literature that LC is the primary source of NE to the preBötC[33,34] and that NE in the preBötC increases the robustness of the inspiratory rhythm[27]. Suppression by opioids of preBötC is critical to inducing respiratory depression[30], thus increasing adrenergic drive in preBötC could attenuate OIRD. We observe a conserved HCVR in the Fentanyl Paired context, therefore the descending pathway could involve areas in the respiratory network that are responsible for the HCVR, such as the RTN. Enhanced RTN activity prior to fentanyl administration would increase the HCVR that occurs when fentanyl induces respiratory depression and subsequent deviations in blood gases, leading to a greater excitatory drive from RTN to preBötC and other inspiratory areas.

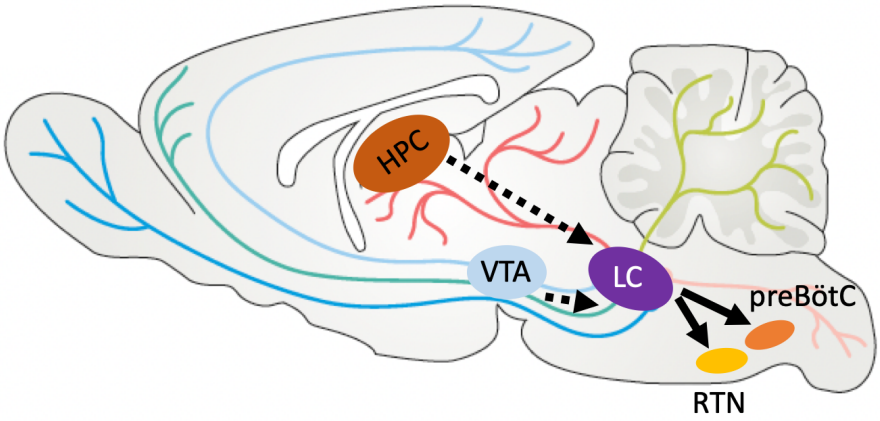

Figure 21. Schematic of the proposed descending pathway

HPC: Hippocampus, LC: Locus Coeruleus, VTA: Ventral Tegmental Area, preBötC: PreBötzinger Complex, RTN: Retrotrapezoid Nucleus

A second circuit mechanism could involve an ascending pathway that provides top-down control of respiratory circuitry. This study demonstrates that the autonomic control of breathing can be influenced by environment and is a behavior based on experiential learning, which suggests higher-order areas could be involved. LC is known to project to the PFC, which in turn could modulate activity in the respiratory network. Projections from PFC to respiratory centers exist[48] and top-down control of breathing is well-established[49]. The PFC contains μ-ORs and acute fentanyl administration will suppress cortical excitability. If tolerance to opioid neuromodulation develops at the level of the PFC with ROU, then HFRT-LC^{NE} activity could lead to enhanced excitatory drive from the PFC to respiratory nuclei. This circuit could support the hypothesis of HFRTs being microarousals that temporarily increase breathing.

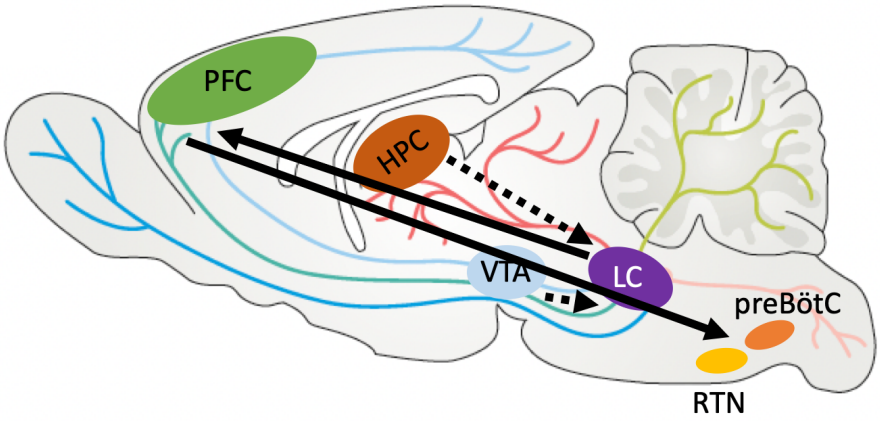

Figure 22. Schematic of the proposed ascending pathway

HPC: Hippocampus, LC: Locus Coeruleus, VTA: Ventral Tegmental Area, preBötC: PreBötzinger Complex, PFC: Prefrontal Cortex, RTN: Retrotrapezoid Nucleus.

While these circuit proposals are merely speculative, future studies should investigate their feasibility with retrograde viral approaches to selectively stimulate LC projections in different regions and observe whether this improves OIRD. Simultaneously monitoring neurotransmitter release would elucidate whether this is an NE-dependent mechanism or if fast synaptic transmission from glutamate release is also involved.

Translational potential of this study

This work has both translational as well as interventional potential. This study demonstrates that the degree of respiratory depression is affected by the context of drug administration. Extrapolating this data with Siegel's work on context-dependent overdose susceptibility indicates that respiratory depression, the initial stage in the progression towards opioid overdose, can be mitigated by drug administration occurring in an environmental context where the user has received the drug before. Educating users on this easy way to protect against harmful respiratory effects could reduce the risk of opioid overdose for this population. This

could be of particular importance if the user increased the risk of their behavior, for example, if they received drugs from a new source.

This work also demonstrated the role of LC^{NE} in the development of tolerance to OIRD, as well as the ability of LC^{NE} excitation to mitigate OIRD. Fentanyl-induced overdose leads to cardiorespiratory arrest faster than heroin or morphine-induced overdose, and Naloxone is unable to reverse overdose after cardiorespiratory collapse. Because epinephrine is typically used to reverse cardiorespiratory collapse, a future direction of investigation is the use of epinephrine in combination with naloxone to reverse fentanyl overdose.

Study Limitations

While our evidence supports these theories, our study is not without its limitations. Outside of the optogenetic experiments, the data in this study is correlational. While we use *Net-cre* mice and a cre-dependent GCaMP virus to selectively monitor LC^{NE} cells, our methods do not confirm whether it is enhanced noradrenergic tone that leads to tolerance to OIRD. All neurons in the core of LC are noradrenergic, but they also release other neurotransmitters and neuromodulators[41], including glutamate, which drives synchronization and stability within the respiratory network. Thus, one limitation of this study is that it lacks a direct measurement of NE release from the LC to decipher whether it is enhanced adrenergic drive during HFRT-LC^{NE} events that leads to changes in breathing. Injection of the fluorescent NE sensor (GRAB NE) into LC projection areas we hypothesize are involved in OIRD tolerance (preBötC, KF, RTN, PFC) would help resolve whether it is specifically enhancement of adrenergic drive that is facilitating a stabilized respiratory network state. Following this up with selective adrenergic receptor blockers will help elucidate which adrenergic receptors are involved.

Another study limitation is that we did not monitor muscle activity during respiratory depression. Skeletal muscle and upper airway rigidity, also known as wooden chest syndrome, occur with fentanyl administration and, in addition to the suppression of the respiratory network, is a major contributor to the inability of users to breathe. While we suspect that there are changes in the degree of wooden chest syndrome with ROU, it is essential to monitor muscle activity in order to conclude this. Furthermore, because LC activity and α_1 activation by fentanyl have been implicated in the development of wooden chest syndrome, it is important to ensure that the enhanced HFRT-LC^{NE} activity observed with ROU and the development of tolerance to OIRD is not LC activity that is associated with muscle rigidity.

Finally, while whole-body plethysmography is an accepted method to measure respiratory rate, tidal volume, and calculate minute ventilation, tidal volume measurements may be overestimated as a result of the fentanyl exposure, which increases airway rigidity. Other methods that directly measure the movement of the diaphragm, or using a head-in plethysmogrphy would estimate tidal volume better. However, these techniques severely limit the mobility of the animal, interrupt its ability to interact with the environment and make an association between the context and cue.

Concluding Remarks

This study provides mechanistic insight into central changes that occur with ROU that correlate with the development of tolerance to OIRD. The practical application of this work is that it informs what influences the conditional nature of OIRD and overdose susceptibility in ROU. The demonstrated adaptability of the respiratory network to protect against opioid perturbations, and ways in which this protective mechanism is lost, are crucial in understanding

the driving force behind overdose deaths and improving overdose outcomes. Moreover, this study exemplifies how the autonomic behavior of breathing can become a learned response through experience. These results suggest that breathing is in part a learned behavior and that it is possible to train people to breathe better in states of dysregulated breathing to improve respiratory outcomes. Whether useful for diseased states or during instances where respiratory physiology is challenged, such as mountain climbing or extreme exercise, the results of this study suggest that a conditioned cue could engage learned mechanisms of respiratory control that alter aspects of the autonomic control of breathing to protect against network perturbations. Breathing is a neurobiological behavior shaped by many different brain regions, both a part of and distinct from the respiratory network. Identifying the ability of these areas to alter breathing with higher-order processes may help us to uncover novel solutions to treat abnormal breathing. In this study, we identified the correlative role of the LC in a learned mechanism of tolerance to OIRD, resulting in improved respiratory outcomes after fentanyl administration. These results are pivotal in furthering our understanding of how one might alter breathing beyond the canonical respiratory network.

References

1. Wissing, C. *et al.* Targeting Norepinephrine Neurons of the Locus Coeruleus: A Comparison of Model Systems and Strategies. Preprint at https://doi.org/10.1101/2022.01.22.477348 (2022).
2. Madisen, L. *et al.* A toolbox of Cre-dependent optogenetic transgenic mice for light-induced activation and silencing. *Nat. Neurosci.* **15**, 793–802 (2012).
3. Lim, R. *et al.* Measuring respiratory function in mice using unrestrained whole-body plethysmography. *J. Vis. Exp. JoVE* e51755 (2014) doi:10.3791/51755.
4. Lyden, J. & Binswanger, I. A. The United States opioid epidemic. *Semin. Perinatol.* **43**, 123 (2019).
5. Kepecs, A., Uchida, N. & Mainen, Z. F. The Sniff as a Unit of Olfactory Processing. *Chem. Senses* **31**, 167–179 (2006).

6. Devilbiss, D. M. & Waterhouse, B. D. Phasic and Tonic Patterns of Locus Coeruleus Output Differentially Modulate Sensory Network Function in the Awake Rat. *J. Neurophysiol.* **105**, 69–87 (2011).
7. Grimm, C. *et al.* Tonic and burst-like locus coeruleus stimulation distinctly shift network activity across the cortical hierarchy. *Nat. Neurosci.* 1–11 (2024) doi:10.1038/s41593-024-01755-8.
8. Tiffany, S. T. & Maude-Griffin, P. M. Tolerance to Morphine in the Rat: Associative and Nonassociative Effects.
9. Tiffany, S. T., Maude-Griffin, P. M. & Drobes, D. J. Effect of Interdose Interval on the Development of Associative Tolerance to Morphine in the Rat: A Dose-Response Analysis.
10. Tiffany, S. T., Drobes, D. J. & Cepeda-Benito, A. Contribution of associative and nonassociative processes to the development of morphine tolerance. *Psychopharmacology (Berl.)* **109**, 185–190 (1992).
11. Baker, T. B. & Tiffany, S. T. Morphine Tolerance as Habituation.
12. Cepeda-Benito, A. & Tiffany, S. T. Effect of number of conditioning trials on the development of associative tolerance to morphine. *Psychopharmacology (Berl.)* **109**, 172–176 (1992).
13. Cepeda-Benito, A. & Tiffany, S. T. Role of drug-administration cues in the associative control of morphine tolerance in the rat. *Psychopharmacology (Berl.)* **122**, 312–316 (1995).
14. Siegel, S. Evidence from Rats That Morphine Tolerance Is a Learned Response.
15. Siegel, S. The Heroin Overdose Mystery.
16. Siegel, S. Pavlovian conditioning and drug overdose: When tolerance fails. *Addict. Res. Theory* **9**, 503–513 (2001).
17. Siegel, S., Baptista, M. A. S., Kim, J. A., McDonald, R. V. & Weise-Kelly, L. Pavlovian psychopharmacology: The associative basis of tolerance. *Exp. Clin. Psychopharmacol.* **8**, 276–293 (2000).
18. Siegel, S., Hinson, R. E., Krank, M. D. & McCully, J. Heroin 'Overdose' Death: Contribution of Drug-Associated Environmental Cues. *Science* **216**, 436–437 (1982).
19. Webster, L. R. Risk Factors for Opioid-Use Disorder and Overdose. *Anesth. Analg.* **125**, 1741–1748 (2017).
20. Levitt, E. S. & Williams, J. T. Morphine Desensitization and Cellular Tolerance Are Distinguished in Rat Locus Ceruleus Neurons. *Mol. Pharmacol.* **82**, 983–992 (2012).
21. Duggan, A. W. & North, R. A. Electrophysiology of opioids. *Pharmacol. Rev.* **35**, 219–281 (1983).
22. Hayat, H. *et al.* Locus coeruleus norepinephrine activity mediates sensory-evoked awakenings from sleep. *Sci. Adv.* (2020) doi:10.1126/sciadv.aaz4232.
23. Kjaerby, C. *et al.* Memory-enhancing properties of sleep depend on the oscillatory amplitude of norepinephrine. *Nat. Neurosci.* **25**, 1059–1070 (2022).
24. Gargaglioni, L. H., Hartzler, L. K. & Putnam, R. W. The locus coeruleus and central chemosensitivity. *Respir. Physiol. Neurobiol.* **173**, 264–273 (2010).
25. Quintero, M. C., Putnam, R. W. & Cordovez, J. M. Theoretical perspectives on central chemosensitivity: CO2/H+-sensitive neurons in the locus coeruleus. *PLOS Comput. Biol.* **13**, e1005853 (2017).
26. Biancardi, V., Bícego, K. C., Almeida, M. C. & Gargaglioni, L. H. Locus coeruleus noradrenergic neurons and CO2 drive to breathing. *Pflüg. Arch. - Eur. J. Physiol.* **455**, 1119–1128 (2008).

27. Viemari, J.-C. & Ramirez, J.-M. Norepinephrine Differentially Modulates Different Types of Respiratory Pacemaker and Nonpacemaker Neurons. *J. Neurophysiol.* **95**, 2070–2082 (2006).
28. Torralva, R. & Janowsky, A. Noradrenergic Mechanisms in Fentanyl-Mediated Rapid Death Explain Failure of Naloxone in the Opioid Crisis. *J. Pharmacol. Exp. Ther.* **371**, 453–475 (2019).
29. Cui, Y. *et al.* Defining preBötzinger Complex rhythm and pattern generating neural microcircuits in vivo. *Neuron* **91**, 602–614 (2016).
30. Bachmutsky, I., Wei, X. P., Kish, E. & Yackle, K. Opioids depress breathing through two small brainstem sites. *eLife* **9**, e52694 (2020).
31. Varga, A. G., Reid, B. T., Kieffer, B. L. & Levitt, E. S. Differential impact of two critical respiratory centres in opioid-induced respiratory depression in awake mice. *J. Physiol.* **598**, 189–205 (2020).
32. Levitt, E. S. & Williams, J. T. Desensitization and Tolerance of Mu Opioid Receptors on Pontine Kölliker-Fuse Neurons. *Mol. Pharmacol.* **93**, 8–13 (2018).
33. Liu, N. *et al.* Respiratory Control by Phox2b-expressing Neurons in a Locus Coeruleus–preBötzinger Complex Circuit. *Neurosci. Bull.* **37**, 31–44 (2021).
34. Doi, A. & Ramirez, J.-M. State-Dependent Interactions between Excitatory Neuromodulators in the Neuronal Control of Breathing. *J. Neurosci.* **30**, 8251–8262 (2010).
35. Krohn, F. *et al.* The integrated brain network that controls respiration. *eLife* **12**, e83654 (2023).
36. Bouret, S. & Sara, S. J. Reward expectation, orientation of attention and locus coeruleus-medial frontal cortex interplay during learning. *Eur. J. Neurosci.* **20**, 791–802 (2004).
37. Heer, C. M. & Sheffield, M. E. J. Distinct catecholaminergic pathways projecting to hippocampal CA1 transmit contrasting signals during behavior and learning. 2023.11.29.569214 Preprint at https://doi.org/10.1101/2023.11.29.569214 (2023).
38. Burgraff, N. J., Bush, N. E., Ramirez, J. M. & Baertsch, N. A. Dynamic Rhythmogenic Network States Drive Differential Opioid Responses in the In Vitro Respiratory Network.
39. Hill, R., Santhakumar, R., Dewey, W., Kelly, E. & Henderson, G. Fentanyl depression of respiration: Comparison with heroin and morphine. *Br. J. Pharmacol.* **177**, 254–265 (2020).
40. Torralva, R. *et al.* Fentanyl but not Morphine Interacts with Nonopioid Recombinant Human Neurotransmitter Receptors and Transporters. *J. Pharmacol. Exp. Ther.* **374**, 376–391 (2020).
41. Poe, G. R. *et al.* Locus coeruleus: a new look at the blue spot. *Nat. Rev. Neurosci.* **21**, 644–659 (2020).
42. Noei, S., Zouridis, I. S., Logothetis, N. K., Panzeri, S. & Totah, N. K. Distinct ensembles in the noradrenergic locus coeruleus are associated with diverse cortical states. *Proc. Natl. Acad. Sci.* **119**, e2116507119 (2022).
43. Sara, S. J. & Bouret, S. Orienting and Reorienting: The Locus Coeruleus Mediates Cognition through Arousal. *Neuron* **76**, 130–141 (2012).
44. Yackle, K. *et al.* Breathing control center neurons that promote arousal in mice. *Science* **355**, 1411–1415 (2017).
45. Price, J. L. *et al.* Effects of arousal modulation via resonance breathing on craving and affect in women with substance use disorder. *Addict. Behav.* **127**, 107207 (2022).
46. Ramirez, J.-M., Ramirez, S. C. & Anderson, T. M. Sudden Infant Death Syndrome, Sleep, and the Physiology and Pathophysiology of the Respiratory Network. in *SIDS Sudden*

Infant and Early Childhood Death: The Past, the Present and the Future (eds. Duncan, J. R. & Byard, R. W.) (University of Adelaide Press, Adelaide (AU), 2018).
47. Sayegh, F. J. P. *et al.* Ventral tegmental area dopamine projections to the hippocampus trigger long-term potentiation and contextual learning. *Nat. Commun.* **15**, 4100 (2024).
48. Gabbott, P. L. A., Warner, T. A., Jays, P. R. L., Salway, P. & Busby, S. J. Prefrontal cortex in the rat: projections to subcortical autonomic, motor, and limbic centers. *J. Comp. Neurol.* **492**, 145–177 (2005).
49. Hassan, S. F., Cornish, J. L. & Goodchild, A. K. Respiratory, metabolic and cardiac functions are altered by disinhibition of subregions of the medial prefrontal cortex. *J. Physiol.* **591**, 6069–6088 (2013).